Performance Analysis of IEEE 802.11 DCF Power Save Mode in IBSS

Pravati Swain

Performance Analysis of IEEE 802.11 DCF Power Save Mode in IBSS

Thesis submitted in partial fulfillment of the requirements for the degree of

Doctor of Philosophy

by

Pravati Swain

Under the supervision of

Prof. Sukumar Nandi

and

Dr. Purandar Bhaduri

Department of Computer Science and Engineering

INDIAN INSTITUTE OF TECHNOLOGY GUWAHATI

Guwahati 781039, India

March, 2014

To

My Parents

Whose blessings, constant inspiration and love
paved my path of success

Declaration

I certify that

a. The work contained in this thesis is original and has been done by myself and the general supervision of my supervisor.

b. The work has not been submitted to any other Institute for any degree or diploma.

c. Whenever I have used materials (data, theoretical analysis, results) from other sources, I have given due credit to them by citing them in the text of the thesis and giving their details in the references.

d. Whenever I have quoted written materials from other sources, I have put them under quotation marks and given due credit to the sources by citing them and giving required details in the references.

Place: IIT Guwahati
Date:

Pravati Swain
Research Scholar
Department of CSE,
Indian Institute of Technology Guwahati,
Guwahati, INDIA 781039

Acknowledgements

It is a real pleasure for me to thank all the people who have supported me to materialize this thesis. First and foremost, I thank my supervisors, Professor Sukumar Nandi and Dr. Purandar Bhaduri, for their great work in supervising, guiding and mentoring me in a very friendly and cooperative way throughout the work with this thesis. I am grateful to them for their careful guidance and encouragement during my thesis work. I am deeply indebted to them for transforming me in an analysis and critical thinker. I have learnt a lot of things from them staring from academic to non academic matters.

I am grateful to members of doctoral committee (DC), Dr. J. Deka, Dr. H. K. Kapoor, Dr. S. Biswas and Prof. R. Bhattacharya for their valuable comments. I would like to thank Prof. S. B. Nair, the Head of the Department of Computer Science and Engineering and other faculty members for their support and help.

I would like to acknowledge the support from Human Resource Development Group and Council of Scientific & Industrial Research (CSIR), India during the period of research. I am thankful to Prof. S. K. Bose, faculty, EEE, IIT Guwahti and Prof. S. Raju, faculty, MNC, IIT Guwahati for their help and encouragement at the initial phase of my thesis work.

My sincere thanks go to all office staffs Bhrigu, Raktajit and Nanu for helping me in many occasions. I am also thankful to Prabin for providing me different resources at various time whenever required.

I would to like to express my heartiest thanks to my fellow research scholar Sandip Chakraborty, with whom I spent time discussing technical matters. I would like to express my sincere thanks to Dr. Nityananda

Sarma for his help and encouragement at the initial phase of my thesis work. I am thankful to Dr. Arup Bhattacharya who helped me in many ways.

I am thankful to my friends Srinivasa Naika (Sir), Shashi Shekhar Jha (Jha), Mamata Samal (Apa). We used to discuss many issues some technical, some non technical. I am indebted to them for their kind help and suggestions which made me more stronger and confident in all aspects. My thanks to Nilkanta (Nilu), Shirshendu, Mayank, Satish, Sibaji, Shilpa and Debanjan. We used to discuss many topics during evening tea break. This discussion helped me to get refreshed time to time. I am thankful to my friends Namita, Bharti and Anu apa who made my stay at IIT Guwahati pleasant. I would like to thank to my friends Smita Das, Smita Panda, Nutan, Sankar, Jitu who always encourage me to think big.

Finally, I would like to mention someone for whom I am able to finish my Ph.D. work. My parents for their endless encouragements. They always encourage me to think big. I am also thankful to my brother (bhai) and sister-in-law (Bhauja), uncle (dadu), Grandmother (Maa), Baba, Mama for their love and encouragement.

Place: IIT Guwahati

Date: **Pravati Swain**

Abstract

The IEEE 802.11 standard defines a power management algorithm for wireless LAN. In the power management for Independent Basic Service Set (IBSS), time is divided into Beacon Intervals (BIs) and each BI is divided into an Announcement Traffic Indication Message (ATIM) window and a data window. The stations that have successfully transmitted an ATIM frame within the ATIM window compete to transmit data frames in the rest of the BI. This work analyzes the performance of the IEEE 802.11 Power Save Mode (PSM) in single hop ad hoc networks using a discrete-time Markov chain for a data frame transmission together with the corresponding ATIM frame transmission. We present an analytical model to compute the throughput, average delay and power consumption in IEEE 802.11 DCF PSM in IBSS under ideal channel and saturated traffic condition. The impact of network size and beacon interval size on the throughput, delay and power consumption of the IEEE 802.11 DCF in Power Save Mode is also analyzed.

An unsaturated traffic model is also considered where data is transmitted in a burst. An analytical model of IEEE 802.11 DCF PSM in IBSS under unsaturated traffic is then presented. The impact of data arrival rate, network size and size of the BI on the performance of the IEEE 802.11 DCF in PSM is also analyzed. This can be used to find an efficient scheme that can maximize the network throughput while saving power consumption for resource constrained ad hoc wireless networks. The analytical work for both saturated and unsaturated traffic condition is validated with simulation results obtained from Qualnet 5.0.1 network simulator.

Contents

List of Figures

List of Tables

List of Algorithms

Abbreviation

AP	Access Point
ACK	Acknowledgement
AIFS	Arbitration Interframe Space
ATIM	Announcement Traffic Indication Message
BEB	Binary Exponential Backoff
BI	Beacon Interval
BSS	Basic Service Set
CCA	Clear Channel Assessment
CFP	Contention Free Period
CSMA/CA	Carrier Sense Multiple Access/Collision Avoidance
CSMA/CD	Carrier Sense Multiple Access/Collision Detection
CTS	Clear To Send
CW	Contention Window
DCF	Distributed Coordination Function
DIFS	DCF Interframe Space
DS	Distributed System
DSSS	Direct Sequence Spread Spectrum
DTMC	Discrete Time Markov Chain
EIFS	Extended Interframe Space
ESS	Extended Service Station

ABBREVIATION

FHSS	Frequency Hopping Spread Spectrum
FSM	Finite State Machine
HR/DSSS	High Rate Direct Sequence
HCF	Hybrid Coordination Function
IBSS	Independent Basic Service Set
IFS	Interframe Space
MAC	Medium Access Control
MANET	Mobile Ad hoc Network
NAV	Network Allocation Vector
PC	Point Coordinator
PCF	Point Coordination Function
PSC	Physical Carrier Sensing
PHY	Physical layer
PIFS	PCF Interframe Space
PSM	Power Save Mode
QoS	Quality of Service
RTS	Request To Send
SIFS	Short Interframe Space
slrc	station long retry count
ssrc	station short retry count
TIM	Traffic Indication Map
TSF	Time Synchronization Function
VCS	Virtual Carrier Sensing
WLAN	Wireless Local Area Network
WPSM	Without Power Save Mode

Chapter 1

Introduction

Wireless communication is a key technology to design today's smarter world. A recent report [5] published in 2011 has identified wireless devices and technologies as the fundamental backbone of the future network communication. Wireless Fidelity, better known as 'WiFi' [6], is the most popular technology in the domain of wireless communication, that allows an electronic device to exchange data or connect to the Internet through wireless media using radio waves. The WiFi Alliance [7] defines WiFi as any *Wireless Local Area Network* (WLAN) product that is based on the Institute of Electrical and Electronics Engineers (IEEE) 802.11 standards [2].

The IEEE 802.11 standard [2] provides specifications for both medium access control (MAC) and physical (PHY) layers for a WLAN device. The standard was published in 1997 and elucidated in 1999. A number of IEEE 802.11 task groups (assigned as 'a', 'b', 'd', 'e', 'g', 'h', etc.) have been created to amend the standard in many aspects such as high data rates [8], quality of service (QoS) [9, 10], etc. In IEEE 802.11 WLAN, different coordination functions are introduced for accessing the shared wireless medium. Among others, the distributed coordination function (DCF) is a contention based MAC protocol on the basis of the conventional carrier sense multiple access/collision avoidance (CSMA/CA) mechanism [11, 12]. Another contention free MAC protocol, called the point coordination function (PCF) is built on the top of the DCF. A network can use the hybrid coordination function (HCF) which is an amalgam of DCF and PCF, for the quality service between the two extremes. WLAN supports two operating modes for wireless stations, infrastructure basic service set [13] and independent basic service set (IBSS) [14], as presented in

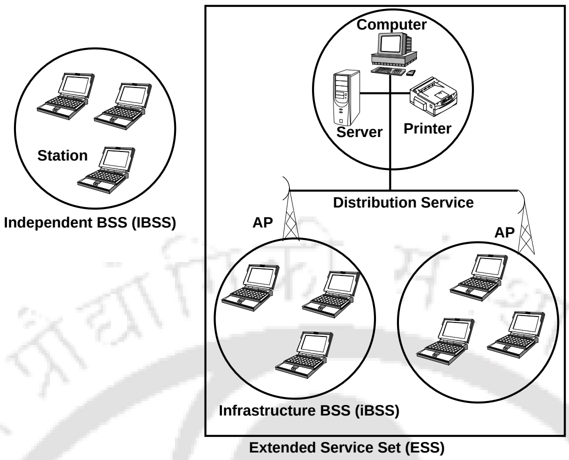

Figure 1.1: IEEE 802.11 WLAN Networks

Figure 1.1. In the infrastructure network, the wireless stations communicate through a central coordinator, called an access point (AP). The APs are connected to the internet through a wired distribution system (DS). The IEEE 802.11 WLAN network can be extended through interconnected APs and DS, called an extended service set (ESS). IBSS is another communication mode of IEEE 802.11 WLAN network, where the stations create ad hoc connections among themselves, without any centralized control, and communicate with each other through the contention based channel access mechanism.

Due to ease of deployment and maintenance for wireless communication media, low cost handheld devices equipped with wireless communication interfaces are widely used in the modern world, ranging from mobile phones, tablets, laptops, wireless sensors and personal gadgets. Different variations of wireless networks have emerged based on these small devices, like mobile ad-hoc networks (MANET) [15], sensor network [16], vehicular networks [17] and so on. One of the major problems in these networks is that the devices are battery operated, and therefore power constrained. Efficient protocols need to be designed that utilize minimum power during execution [18–20]. In wireless devices, maximum power is consumed during communication, that is the transmission and reception. Even when the wireless devices are not operating, i.e. they are not involved in active transmissions or receptions, they may operate in *promiscuous mode* [21] where the devices overhear the ongoing communications (also called *idle-listening*). This is a major source of unnecessary energy deviation from wireless interfaces. The IEEE 802.11 standard defines power save algorithms for both the infrastructure BSS and the IBSS networks, where a wireless station goes to the sleep mode when no data communication takes place. However, the power save algorithms for infrastructure BSS [22, 23] and IBSS [24–26] are different in nature. In infrastructure network, the AP acts as the central coordinator, and uses polling based functionality to instruct the wireless stations to go to the sleep mode when there is no active data communications. However, as there is no central coordinator in IBSS, the wireless stations should be synchronized for a sleep-wake up cycle.

Designing power saving algorithms for IBSS is more important, as most of the battery constrained networks, as mentioned earlier, operate in IBSS mode. The standard supports power save mode (PSM) operation along with distributed coordination function (DCF) for MAC layer channel access in the IBSS mode of operation. According to the PSM operation, if a station does not transmit or receive data in a time slot, then it should go to the sleep mode to save battery power that is wasted due to idle-listening. To enable this design, the standard divides the time into *beacon intervals* (BIs), and every BI is divided into an *announcement traffic indication message* (ATIM) window and a *data window*. A station that has data frames to send, is only allowed to do so, if it can successfully transmit an ATIM frame in the ATIM window. A station that neither transmits nor receives an ATIM frame in the ATIM window, goes to the sleep mode in the data window.

The performance of PSM in IBSS depends on several factors. Jung *et al.* [25] have shown that dynamic ATIM window size [1] may provide better network performance, in terms of overall network throughput, while conserving same amount of power. Further, the authors in [24] have proposed a scheme where an extra carrier sensing frame is transmitted before the ATIM frame transmission to save more battery power. This thesis models the standard IEEE 802.11 DCF PSM for IBSS in different network conditions to analyze the impact of different design parameters, such as ATIM and data window size, the network size, as well as the DCF parameters like the contention window (CW), over the performance metrics like network throughput, delay and power consumption.

[1] The standard defines fixed ATIM and data window size.

1.1 Motivation of the Research Work

Mathematical modeling of a communication protocol is important to analyze the impact of the design parameters over the performance metrics. In [1], Bianchi has presented a two dimensional Markov chain model of the IEEE 802.11 DCF to analyze the saturation throughput[2] of the network. From the analysis, the author has concluded that the throughput depends on the initial CW size, and the optimal value of initial CW depends on the number of contending stations in the network. Based on this analysis, a set of algorithms has been proposed in the literature to dynamically tune the minimum CW for IEEE 802.11 DCF [27–31] to optimize the network contention for providing better performance gain. A number of papers [3, 32–35] are built upon the original Bianchi's model for handling error-prone channels, non-ideal transmission channels and capture effects. However, all these analytical models do not consider the power save mode operations of the stations. Several analytical models are presented to analyze the performance of the IEEE 802.11 power save mode in infrastructure BSS [36–39]. As discussed earlier, modeling IEEE 802.11 DCF PSM in IBSS is essential for designing efficient power saving options for low energy battery powered wireless devices. As the PSM operation in IBSS significantly differs from the PSM of infrastructure BSS, a concrete mathematical model for IBSS PSM is required for analyzing the pros and cons of the standard algorithm.

Traffic characteristics play a crucial role in the design of any communication protocol. In a general purpose community wireless network, every station does not transmit or receive at all times. Further the traffic generation rate at every station varies with time, depending on the application demand. In general, a station gets saturated when it starts transmitting at the maximum supported data rate. Further, a network gets saturated when the total traffic generation rate from a set of contending stations overshoots the maximum network capacity. Most of the analytical models presented in the literature consider network saturation. Though modeling a protocol behavior in network saturation condition is necessary to visualize the protocol performance at extreme scenarios, it does not reflect

[2] A network is called saturated when the total transmission rate of the stations is more than the maximum network capacity.

the performance statistics of the protocol in different real world scenarios. The performance of a communication protocol may vary significantly in the unsaturated network conditions, when different stations transmit traffic at different data rates. For example, in a WLAN network which is based on IEEE 802.11 DCF, though TCP traffic shows fairness in network saturation, severe unfairness is observed when different stations have different number of TCP flows, and the network is unsaturated [40]. Although there exists analytical modeling for IEEE 802.11 DCF in unsaturated traffic conditions [41–43], the PSM is not analyzed till now in the literature, neither for saturated nor for unsaturated traffic condition in IBSS.

The discussion till now reveals the requirement for designing an analytical model for IEEE 802.11 DCF PSM in IBSS, for both saturated and unsaturated network conditions. The model at network saturation gives the performance overview of the protocol at the extreme scenario with the effect of network size over the performance metrics. On the other hand, the model at unsaturated traffic conditions helps to analyze the protocol performance in a real world scenario, with variable traffic arrival rates. The analytical models can be used to evaluate the effects of the design parameters over the network throughput, forwarding delay and power consumption. The analytical models can work as a basis for designing efficient power saving algorithms to maximize network performance, while minimizing the average power consumption as well as the deviation in power consumption, that can significantly increase the network lifetime.

1.2 Contributions of the Thesis

The objectives of this thesis are to design a mathematical model for IEEE 802.11 DCF PSM in IBSS under different traffic conditions, and analyze the results obtained from the model to evaluate the effect of the design parameters over the network performance. This analysis can serve as the basis for designing efficient algorithms to improve network lifetime for the networks with power constrained devices. For this purpose, the first contribution of this thesis models the IEEE 802.11 DCF PSM in IBSS in saturated traffic condition using a discrete time three dimensional Markov chain model to show the effect of the network size over performance metrics. In the next contribution of this thesis, the model is extended for unsaturated traffic conditions. The model is used to find out the impact of different performance parameters, such as data arrival rate, the ratio of ATIM and data window, CW etc., over the network throughput, average MAC delay, variation in delay, average power consumption, and the variation in power consumption. The thesis also compares the performance parameters between DCF with PSM and DCF without PSM. The following subsections give a brief description of the major contributions of this thesis.

1.2.1 Performance Analysis of IEEE 802.11 PSM in IBSS for Saturated Traffic

In this contribution, an analytical model is designed to analyze the performance of IEEE 802.11 DCF PSM in IBSS for saturated traffic conditions. For this purpose, a discrete time Markov model is introduced for a data frame transmission together with the corresponding ATIM frame transmission. The probability of successful transmission of an ATIM frame has significant impact on the data frame transmission. The model is used to calculate the probability that an ATIM frame and a data frame are transmitted successfully. The analytical model is validated by comparing the numerical results with simulation results, obtained from Qualnet 5.0.1 network simulator [44]. The throughput of the IEEE 802.11 DCF PSM in IBSS is analyzed using the analytical model of the ATIM frame and data frame transmissions. Further, the model is used for the analysis of delay and average power consumption during a data frame transmission. The effect of network size and the beacon interval over the network performance is also analyzed. Based on the results from the analytical model, the throughput-power trade-off in PSM is also discussed.

Based on this analytical model, a comparative study between IEEE 802.11 DCF with PSM and without PSM is reported for different beacon interval sizes. In IEEE 802.11 DCF without PSM, the performance metrics do not depend on the beacon interval size, whereas in PSM, the network throughput increases and the power consumption decreases as the size of the beacon interval increases. The model reveals that in IEEE 802.11 PSM, power saving comes at the cost of network throughput and delay. The contention among the stations is less in the data window for PSM, because some of the stations that fail to transmit ATIM frame in the ATIM window go to the sleep mode in the data window. This makes the data window throughput marginally higher. However, the ATIM transmission imposes an extra control message overhead that reduces overall channel throughput. This analysis gives the direction for designing an efficient power saving algorithm by dynamic tuning of the beacon interval size. Such an algorithm would provide maximum network performance while keeping the average power consumption constraint.

1.2.2 Performance Analysis of IEEE 802.11 PSM in IBSS for Unsaturated Traffic

As discussed earlier, data frames come in a burst from users in a wireless network that results in network unsaturation. In the first contribution of the thesis, the analytical model is designed considering the saturated traffic only, which shows the protocol performance at the extreme traffic load scenarios, and analyzes the impact of the network size over performance metrics. However, it can not capture the performance with different traffic arrival rates. For instance, when the network traffic comes in a burst, some stations may not participate in the ATIM handshaking procedure (if the station is neither a data transmitter nor a receiver), resulting in the reduction of the effective network size for the ATIM window. Therefore, it is important to extend the analytical model for unsaturated traffic condition.

In the next contribution of the thesis, a discrete time Markov model is presented for the ATIM and data frame transmissions in the IEEE 802.11 IBSS PSM for unsaturated traffic condition. The network throughput, delay and power consumption for IEEE 802.11 DCF PSM is analyzed in this work considering an unsaturated network. As earlier, the numerical results obtained from the proposed analytical model are compared with the simulation results to validate the proposed model. The effect of power saving over the network throughput, delay and power consumption for unsaturated traffic is analyzed for different network sizes and different beacon intervals. The performance of IEEE 802.11 IBSS PSM is also analyzed and compared with the standard IEEE 802.11 IBSS without PSM. From the results obtained through the analytical model of the unsaturated traffic condition, it is observed that in PSM, as the number of stations increases the average power consumption decreases. On the contrary, the average power consumption increases in IEEE 802.11 DCF without PSM. It is also observed from the analysis that the effect of the power consumption is more in the case of network unsaturation, compared to the saturated condition. The analysis for unsaturated traffic condition shows that there is a trade-off among throughput, MAC delay and average power consumption. Therefore, this contribution reveals that in a general community network, where network unsaturation is common, a dynamic and adaptive BI can provide better power saving with little compromise in delay and throughput.

1.3 Organization of the Thesis

This thesis is organized as follows.

Chapter 2 presents a brief overview of the IEEE 802.11 DCF with PSM in IBSS and the literature survey related to the analytical model of IEEE 802.11 DCF.

In **Chapter 3**, a discrete time Markov model is proposed to analyze the performance of the IEEE 802.11 PSM in IBSS for saturation traffic. The analytical model is used to compute the normalized throughput, average delay and power consumption under ideal channel condition for saturation traffic. The analytical model is validated through the simulation results, and the numerical results obtained from the model is used to evaluate the performance of the network under the PSM.

Chapter 4 presents an analytical model to compute the throughput, expected delay and expected power consumption in IEEE 802.11 PSM in IBSS for unsaturated traffic. The model is validated through the simulation results. The impact of the data arrival rate, network size and the size of the beacon interval on the performance of IEEE 802.11 DCF in PSM is also analyzed.

Finally, **Chapter 5** summarizes the overall contribution of this thesis, and presents some future research directions.

Chapter 2

Background and Literature Survey

The IEEE 802.11 standard provides the design specifications for the physical layer (PHY) and the medium access control (MAC) layer of a wireless local area network. For the specifications of PHY layer, it extends the support for different versions of physical layer technologies such as infrared, frequency hopping spread spectrum (FHSS) and direct sequence spread spectrum (DSSS). The 802.11a specification uses orthogonal frequency division multiplexing (OFDM), while 802.11b provides details for a high rate direct sequence spread spectrum layer (HR/DSSS). The MAC layer is responsible for controlling access to the wireless channel, where multiple users can transmit at the same time over the same channel. MAC protocols have been broadly grouped into two categories: distributed and centralized. In the centralized case, every wireless station communicates through an AP connected with the distribution system, whereas in the distributed case every station has the freedom to transmit or receive a frame without any centralized control, and the stations coordinates with each other for the decision of channel access.

The IEEE 802.11 standard [2] presents coordination functions that control medium access for a station. It presents polling and contention based medium access protocols know as point coordination function (PCF) and distributed coordination function (DCF) respectively. The PCF and the DCF can coexist within one station. The PCF interchanges between a contention free and a contention period in time, where as DCF is based on contention. In PCF, the contention period is used to give transmission facilities to new incoming stations to introduce themselves to the network. The PCF is known as optional access method which is implemented in infrastructure basic service set to present a contention free period (CFP). The AP acts as the point coordinator (PC) which eliminates the contention by polling the stations for frame transmission.

The DCF is used in an ad hoc network[1] to access the channel without any centralized coordination. The next section gives the detail design aspects of the DCF.

2.1 The IEEE 802.11 Distributed Coordination Function (DCF)

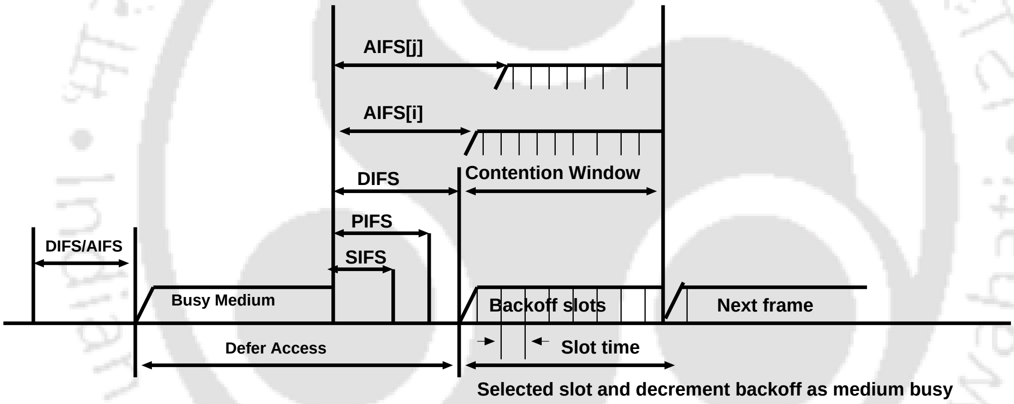

Figure 2.1: Inter Frame Spacing in IEEE 802.11

DCF is a contention based channel access protocol. In DCF, after a frame has been transmitted by a station, a certain amount of waiting time is required before any other station can further transmit another frame. This time interval is called the interframe space (IFS). IFS is classified into five types according to the specific purposes, as shown in Figure 2.1.

- **Short Interframe Space** (SIFS): The control frames are the highest priority frames in DCF. The SIFS is used for the highest priority frame transmissions. After the elapse of SIFS time interval, frame transmissions start.

[1]A wireless ad hoc network is a decentralized network where there is no AP to manage the network. Each station voluntarily participates in routing and forwarding of data frames from other stations.

- **PCF Interframe Space** (PIFS): PIFS is used during contention free operation. Stations start transmitting the frame after the elapse of the PIFS time interval[2].

- **DCF Interframe Space** (DIFS): A station starts to transmit data frames if the channel is idle for a time interval more than the DIFS. This is the minimal time in contention-based service.

- **Extended Interframe Space** (EIFS): This is not fixed in size and used when there is error in frame transmissions.

- **Arbitration Interframe Space** (AIFS): The AIFS is used by Quality of Service (QoS) stations to transmit the data and control frames.

DCF utilizes the carrier sense multiple access with collision avoidance (CSMA/CA) mechanism for channel access, with a binary exponential backoff for collision resolution. These have been discussed in the following subsections in details.

2.1.1 Carrier Sense Mechanism

In the DCF access mechanism, the carrier sensing mechanism is responsible for channel sensing and avoiding collisions. Both physical carrier sensing (PCS) and virtual carrier sensing (VCS) are used in DCF. The PCS is a mechanism in physical layer which notifies the MAC layer whether the medium is idle or not. The function used in physical layer for channel sensing is called the clear channel assessment (CCA). There is no literal sensing of the carrier in the VCS mechanism. Control frames are used to exchange information about the state (*idle* or *busy*) of the channel. These control frames are *'Request to Send'* (RTS) and *'Clear to Send'* (CTS) frames. The VCS mechanism sets the *'Network Allocation Vector'* (NAV) and updates it. The NAV is a timer that shows the amount of time the station should stay idle before the channel can be used. This NAV value counts down on a regular basis and when it becomes zero, it indicates that the channel is free.

[2]As mentioned earlier, PCF and DCF can coexist in a station. All the stations under PCF uses PIFS which is smaller than the DIFS. This implies that the point coordination traffic have priority to access the channel over the stations under the DCF access method.

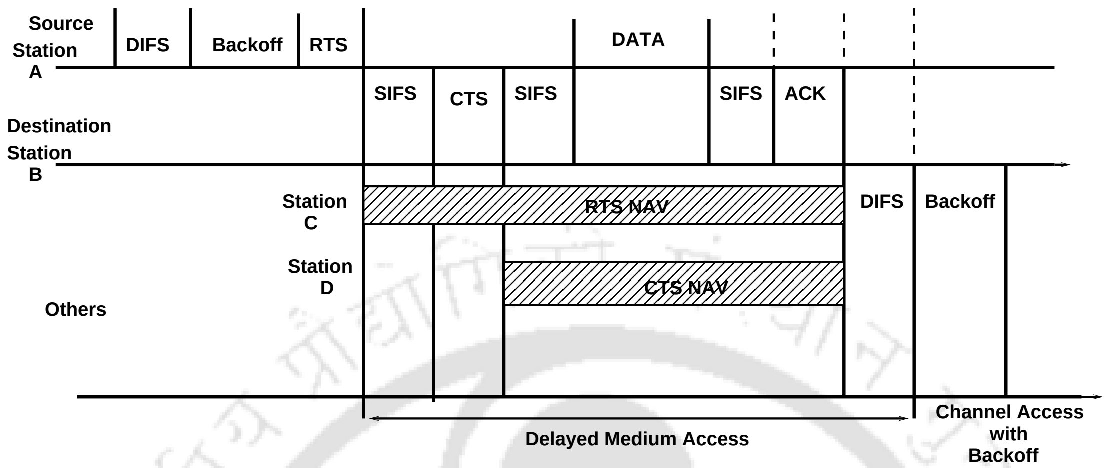

Figure 2.2: Virtual Carrier Sensing in IEEE 802.11

Figure 2.2 presents the virtual carrier sensing mechanism. Let us assume that station A and station B are in the same radio range. Station C is in the radio range of the station A, and station D is in the radio range of station B, but not within the radio range of station A. If station A wants to send a frame to station B, it sends an RTS frame to station B, to reserve the channel. After station B receives the RTS frame successfully, it sends a CTS frame to station A. Station C and station A are in same radio range. When station C receives the RTS for station A it sets a virtual channel busy for itself, as NAV. Similarly station D sets a NAV after receiving CTS from station B. After that, station A sends the data frames to station B and starts the Acknowledgement (ACK) timer. When station B receives the data frames it sends back an ACK to the station A.

Based on the PCS and VCS, DCF defines two access mechanisms for frame transmission: the default basic access mechanism which is a two-way handshake scheme based on PCS, and an optional four-way handshake scheme based on VCS. In the basic access mechanism which is depicted in Figure 2.3, before the frame transmission the station monitors the channel until the channel becomes idle for DIFS interval. To avoid channel capture, a station waits for a random backoff time between two consecutive new frame transmissions, even if the channel is sensed idle for DIFS time. A positive ACK is transmitted by the destination station after successful reception of the frame. An optional four-way handshaking technique (Figure 2.2) is know as RTS/CTS mechanism. Before transmitting a data frame,

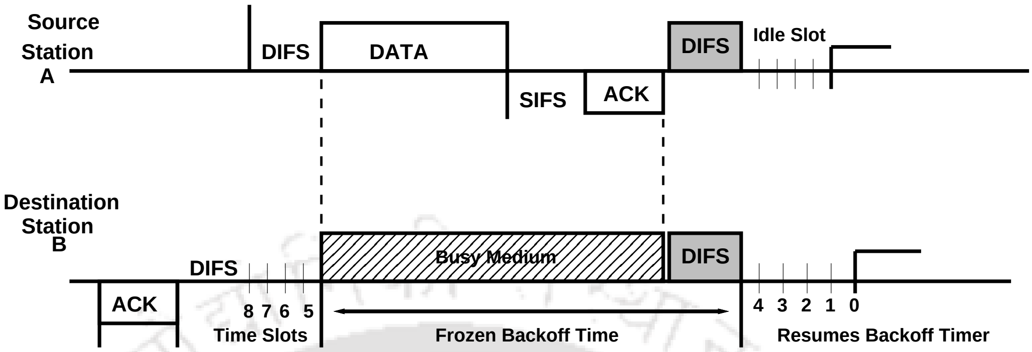

Figure 2.3: Basic Access Mechanism

the station sends an RTS frame to reserve the channel. The destination station acknowledges by a CTS frame after successful receipt of the RTS frame, after which the normal data frame transmission and ACK response occurs. This RTS/CTS mechanism is designed in the IEEE 802.11 protocol to avoid the hidden terminal problem [45] when pair of stations are in different radio ranges.

2.1.2 Binary Exponential Backoff

DCF uses the Binary Exponential Backoff (BEB) algorithm to avoid collision in the channel. If the channel is sensed busy, the station defers the channel access until the channel is sensed free. If the channel is idle, the data frame is forwarded according to the BEB algorithm. If the medium is sensed idle for an interval larger than DIFS period then the station starts to transmit frames; otherwise it defers the transmission until the medium is free. The backoff time is chosen as follows;

$$\text{Backoff Time} = \text{Random}() \times \text{Slot Time}$$

where the random value is uniformly distributed between $[0, \text{CW} - 1]$ where CW is the contention window size which satisfies $\text{CW}_{\min} \leq \text{CW} \leq \text{CW}_{\max}$. $CW_{\min}$ and $CW_{\max}$ are the minimum and maximum CW size. These values are based on the physical modulation characteristics. As long as the channel is sensed idle the backoff counter is decremented. The backoff value is frozen when the channel is sensed busy. After each unsuccessful transmission the value of CW is doubled up to $CW_{\max} = 2^m(CW_{\min})$. The constant m is called maximum backoff stage. For

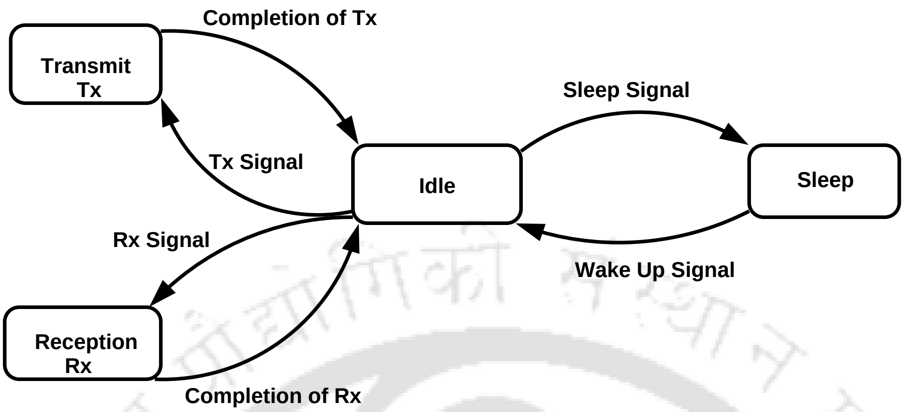

Figure 2.4: FSM for Communication Component

a successful transmission the CW is reset to $CW_{\min}$. At every slot, the CW is decreased by one. When the CW reaches zero, the station attempts to transmit the frame. If the transmission is successful, CW is set to its minimum value, otherwise, for every unsuccessful transmission attempts, CW is doubled. Once the frame transmission remains unsuccessful till the last backoff stage, the frame is dropped from the interface queue and the CW is set to its minimum value for a new frame transmission.

2.2 The IEEE 802.11 DCF in Power Save Mode (PSM)

In resource constrained wireless networks such as mobile ad hoc networks, sensor networks, vehicular networks, etc. power is an important resource to be managed. The design of energy efficient protocols for such networks is an important research area. The IEEE 802.11 standard defines power save algorithm for both infrastructure networks, where every wireless station communicates through an AP connected with the distribution system and IBSS, where the stations create ad hoc connections between themselves and communicate with each-other through a contention based channel access mechanism. During power management, a station is in one of these two states, namely, active mode (transmit, receive, idle) or sleep mode. A finite state machine (FSM) for communication component in power save mode is presented in Figure 2.4. During active mode, the station is in awake state and may transmit/receive frames at any time. At the time of power save mode, the station is in doze or sleep state hence is not able to transmit or receive and consumes very low power. A wireless station goes to sleep mode when no data communication takes place. However, the power save algorithm for infrastructure and IBSS networks are different in nature.

2.2.1 Power Management in Infrastructure Network

The IEEE 802.11 standard [2] has two different power modes, *power on* and *power save*. In power on mode a station transmits or receives frames at any time, whereas in power save mode a station goes to sleep state periodically to save battery power. In infrastructure networks, the AP acts as the central coordinator, and uses polling based functionality to facilitate the wireless stations to go to sleep mode when there is no data communication. In the power save mode, the AP informs the stations that frames are buffered. The AP periodically assembles a traffic indication map (TIM) and transmits it in beacon frames, which indicates whether the AP has any pending data frames destined to the station or not. If the AP broadcasts a beacon indicating the presence of a buffered packet for the station, the station stays in awake state and generates a PS-Poll frame to request the transmission of the packet until all the buffered packets are received. When multiple stations have buffered frames, all stations use the random backoff algorithm before transmitting the PS-Poll. If the AP broadcasts a beacon indicating that the AP has no buffered packet for the station, the station may enter the doze state immediately. The time interval after which a station periodically wakes up is called listen interval. The listen interval is a multiple of the beacon interval.

Figure 2.5 illustrates an example of the buffering and delivery process of frames when the station is in power save mode in an IEEE 802.11 infrastructure network. For every beacon interval, the AP transmits a beacon frame with a TIM information. As depicted in Figure 2.5, Station A has listen interval 2 while station B has listen interval 3. Station A wakes up every other beacon interval and station B wakes up every third to listen to the TIM. At the first beacon interval, there are frames for station A and no frame for station B thus station B immediately returns to

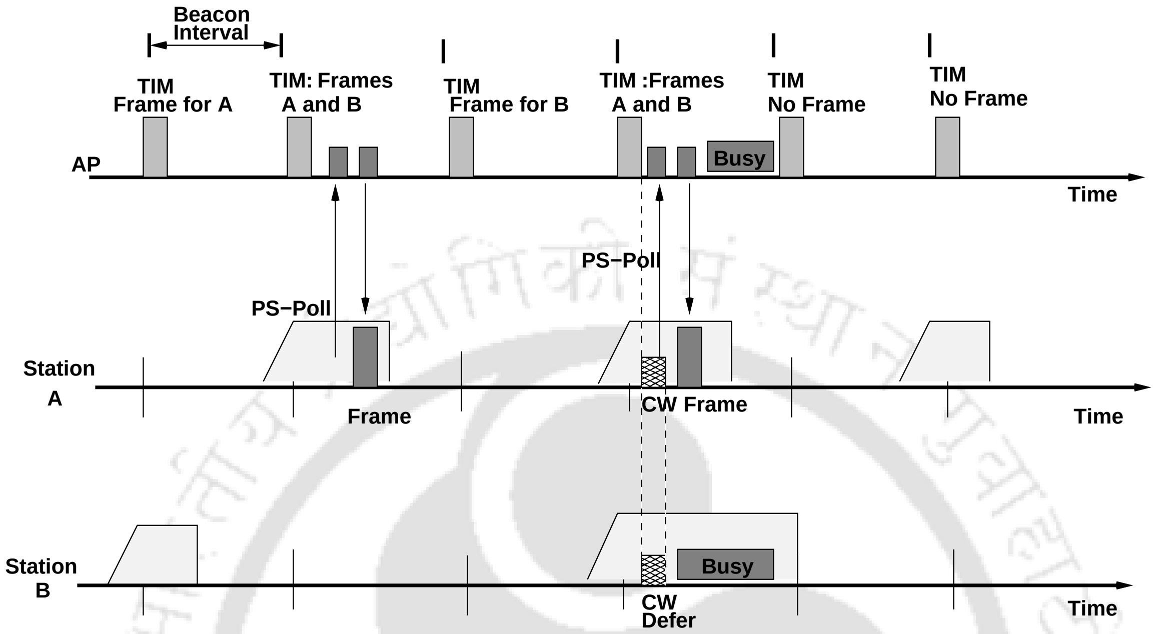

Figure 2.5: Power Management in Infrastructure Network [2]

doze state. In the second beacon interval, the TIM indicates that there are frames buffered for both station A and station B. Since station A is in awake state, it sends a PS-Poll without any contention, receives the buffered frame in response and returns to doze state. In the third beacon interval both the stations are in doze state. At the fourth beacon interval both stations wake up to listen to the TIM and there are frames buffered for both. Hence there is a contention to transmit the PS-Poll frames. Station A wins, issues a PS-Poll and receives its buffered frame. During the transmission, station B has to wait. If the AP discards the buffered frames for station B due to buffer overflow, the TIM at the fifth beacon indicates that no frames are buffered and station B can return to doze state.

2.2.2 Power Management in IBSS

In IEEE 802.11 DCF PSM for IBSS, time is divided into Beacon Intervals, and each beacon interval is divided into an ATIM window and a data window, as illustrated in Figure 2.6. If a station successfully transmits an ATIM frame in the ATIM window, then it is allowed to transmit a data frame in the data window. Otherwise it goes

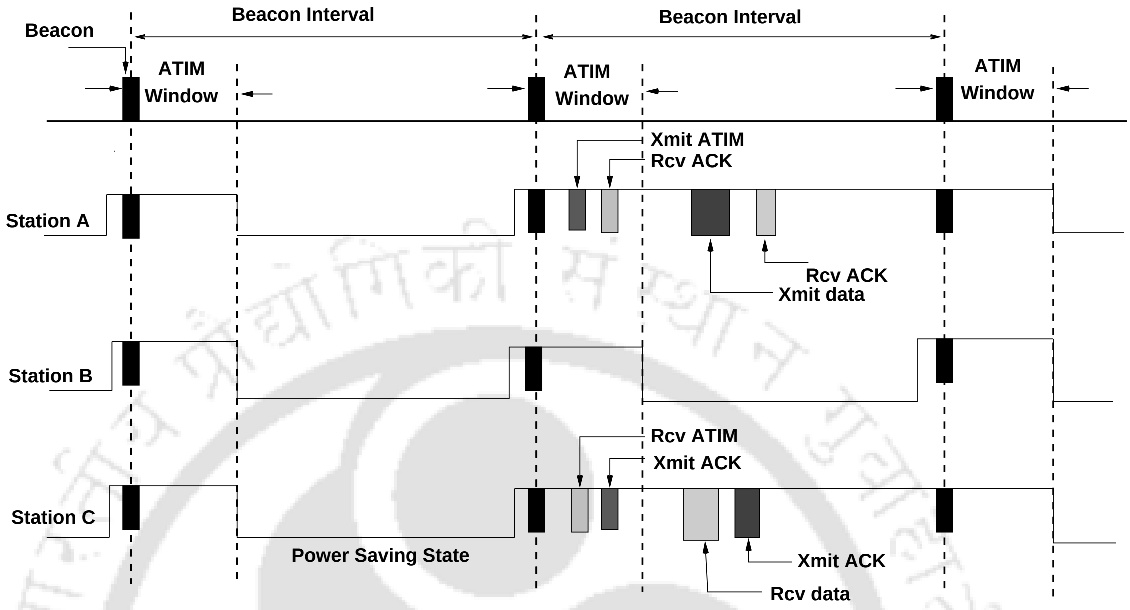

Figure 2.6: Power Save Mode in IBSS [2]

to sleep mode in the data window.

In an IBSS, the stations in PSM wake up to listen to beacon messages and stay awake for an ATIM window period. When the stations are in PSM, the transmitter buffers all the frames and announces them in the ATIM window through an ATIM frame. The ATIM frame is a control frame which is exchanged by the stations to determine whether to go for sleep mode or stay awake for data transmission after the end of the ATIM window. The transmission of ATIM frame and data frame are according to CSMA/CA DCF specified in the IEEE 802.11 [2]. If a station is unable to transmit an ATIM frame during the ATIM window, e.g., due to contention with another station or ending of the ATIM window, the data frame is rebuffered and an attempt is made to transmit an ATIM frame during the next ATIM window. A station may enter the power save state at the end of the ATIM window if it does not transmit or receive an ATIM frame successfully. The example of power save mode is illustrated in Figure 2.6. Station A announces a frame destined for station C by transmitting an ATIM frame during the ATIM window. Station C sends ATIM-ACK to station A and remains awake for the rest of the beacon interval. Station B goes to *power save* state at the end of the ATIM window, thus saving energy.

The stations that have successfully transmitted an ATIM frame within the

ATIM window compete to transmit a data frame in the rest of the beacon interval. If the station is unable to transmit the data frame in the beacon interval in which it was announced, e.g., due to contention with other stations or ending of the data window, the data frame is rebuffered and the station again transmits an ATIM frame during the next ATIM window. A station may discard data frames which are buffered for an excessive amount of time.

A number of works has been proposed in the literature to model the IEEE 802.11 DCF in different network conditions. The next section explores these works to give a brief overview of the analytical models proposed in the literature for performance analysis of wireless networks based on IEEE 802.11 standard.

2.3 Modeling of IEEE 802.11 DCF

There are a number of theoretical models that analyze the performance of the IEEE 802.11 DCF depending upon different network assumptions. Various mathematical techniques are used to analyze the performance of the IEEE 802.11 DCF such as queuing theory, Markov chain model and game theory. In IEEE 802.11 DCF, channel access by a station has an influence on its neighboring stations, and therefore game theory is an extremely useful tool to analyze such a network. In [46], the authors have proposed a game model to represent the IEEE 802.11 DCF mechanism and designed a simple Nash equilibrium backoff strategy for fairness. Several queuing models have been designed using the uniqueness of the fixed point to analyze the performance of the IEEE 802.11 DCF [41, 47–50, 50, 51]. In [52], authors have calculated the probability distribution of the MAC layer frame service time (i.e., the interval between the time the frame starts to contend for transmission and the time that the frame is either acknowledged for correct reception by the intended receiver or is dropped). Based on this distribution model of the MAC layer frame service time, they analyzed the queueing performance of the wireless LANs at different traffic load.

Bianchi [1] is the pioneer in the modeling of IEEE 802.11 DCF using discrete time Markov chain which is presented in Figure 2.7, assuming an ideal channel condition with saturation network traffic. He uses a two dimensional Markov chain to model the BEB mechanism and shows the effect of minimum CW over network

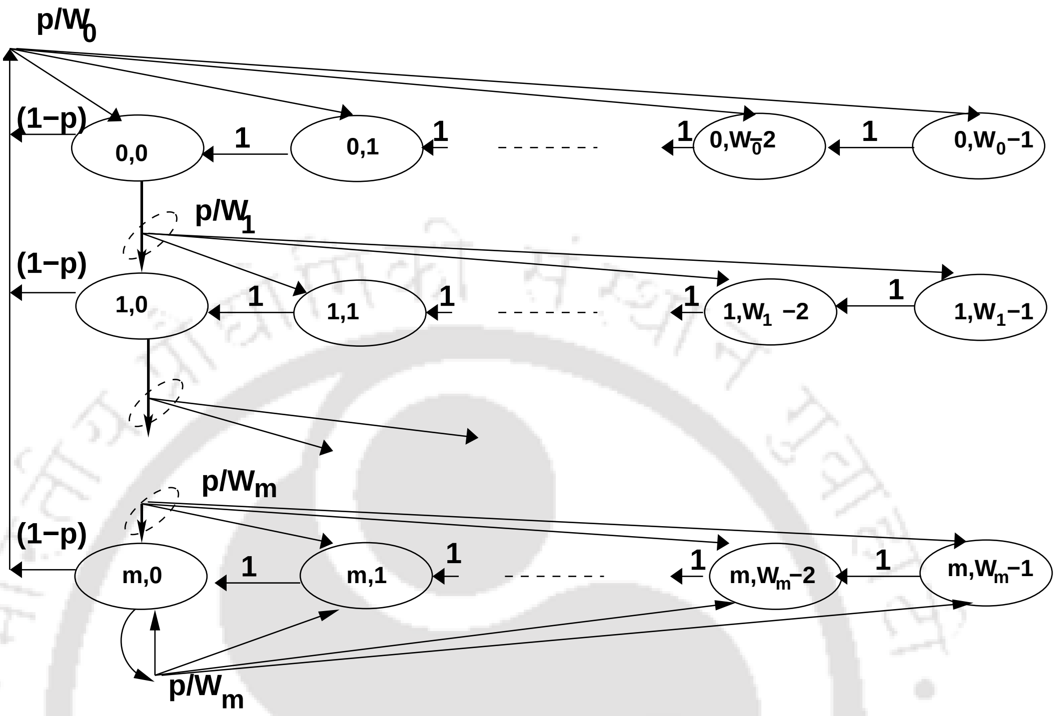

Figure 2.7: Markov model for data frame transmission in IEEE 802.11 DCF [1]

throughput. His analysis considers both CSMA/CA based basic access mechanism and RTS/CTS access mechanism for virtual carrier sensing. In CSMA/CA, the stations change their state depending upon the condition of the wireless channel. The wireless channel can either be in “busy” or “idle” state. The channel is considered idle when there is no transmission and busy if there is at least one transmission. If the channel is sensed busy then the station waits until the channel becomes idle. This implies that the total behavior of the network depends on the wireless channel condition. The probability p represents the collision probability that a packet is transmitted by a station. The probability p is assumed to be a constant and independent collision probability, irrespective of the number of retransmissions. The collision probability p can be expressed as a function of the probability τ (which indicates the probability that a station transmits in a randomly chosen slot), as follows:

$$p \;=\; 1-(1-\tau)^{(n-1)}.$$

Let P_{tr} be the probability that there is at least one data frame transmission in the considered slot time. The probability P_s that a data frame transmission is successful, is calculated in [1] as follows.

$$\begin{aligned} P_{tr} &= 1-(1-\tau)^n \\ P_s &= \frac{n\tau(1-\tau)^{(n-1)}}{P_{tr}}. \end{aligned}$$

As defined in [1], "throughput is the fraction of time the channel is used to successfully transmit payload bits". Let S denote the normalized system throughput which is expressed as:

$$\begin{aligned} S = \frac{E[payload\ info.\ transmitted\ in\ a\ slot\ time]}{E[length\ of\ a\ slot\ time]} \\ = \frac{P_s P_{tr} E[p]}{(1-P_{tr})\sigma + P_s P_{tr} T_s + (1-P_s) P_{tr} T_c} \end{aligned}$$

Let $E[P]$ be the average packet payload size (in terms of time unit, e.g., μs). It is assumed that all packets have the same size, so $E[p] = P$. Let T_s and T_c be the average time the channel is sensed busy because of a successful transmission or a collision respectively, and σ be the empty slot time. Let $H = PHY_{\text{hdr}} + MAC_{\text{hdr}}$ be the size of the packet header and δ the propagation delay. Then,

$$T_s = H + E[P] + SIFS + \delta + ACK + DIFS + \delta \tag{2.1}$$

$$T_c = H + E[P^*] + DIFS. \tag{2.2}$$

Here P* is the maximum length of packets that are involved in a collision.

Bianchi has given a closed form solution for the network throughput in an IEEE 802.11 DCF WLAN. Several works have extended Bianchi's analysis for IEEE 802.11 DCF for saturation condition, as discussed in the following subsection.

2.3.1 Extensions of Bianchi's [1] Model for Saturated Traffic Condition

The drawback of the work by Bianchi [1] is that, if there is a failure to transmit a frame there is no finite limit for the retransmission of the frame. In [53], the authors have presented a modified framework of the Bianchi's model, which introduces a fixed retry limit and analyzed the performance of Reliable Transport Protocol over IEEE 802.11 DCF. After the maximum limit if there is any collision, the frame will be dropped or the transmission will restart with a new backoff value. The backoff counter is decremented only during idle slots. This idea was first adopted in [54] and corrections of this paper have been addressed in [32]. According to [32], a slot is either an empty slot or a transmission slot and hence there is a self loop in each state, freezing the backoff counter with probability p when medium is busy; otherwise the backoff counter is decremented with probability $(1 - p)$. As the standard [2] describes, each station maintains two retry limits for each new frame, *station short retry count* (ssrc) and *station long retry count* (slrc). The maximum retry limit for a data frame is represented by slrc and the maximum retry limit for RTS frame transmission by ssrc. There is a three dimensional Markov model using ssrc and slrc to compute the IEEE 802.11 DCF performance [33]. In the paper [55], the authors have concluded that, under saturation conditions, the slot immediately following a successful transmission can be accessed only by the station that has successfully transmitted in the previous channel access. Moreover, due to the specific ACK timeout setting adopted in the standard [2], the slot immediately following a collision cannot be accessed by any station. Thus, the hypothesis of un-correlation between consecutive channel slots and statistical homogeneity is not generally true. This justifies why the backoff freezing model proposed in [54] does not provide accurate results.

Several other works exist that consider different network assumptions such as constant CW [56], slow decrease of CW [57], prioritized traffic [58], different packet length [59], finite load traffic [60–62], buffer size [63], etc. In [64], the authors have considered multiple frame transmission after successful channel contention and analyzed the performance of IEEE 802.11 DCF by calculating different conditional collision probabilities for multiple consecutive frame transmissions. In [65], the authors have modified the Bianchi's model [1] using a hybrid of the basic and the RTS/CTS access mechanisms with variable frame length. In a data rate switching mechanism, if a station has U $(U = 1)$ consecutive successful transmissions, it will increase its data rate until the highest data rate has been reached. If the station suffers D $(D = 1)$ consecutive unsuccessful transmissions, it will decrease its data

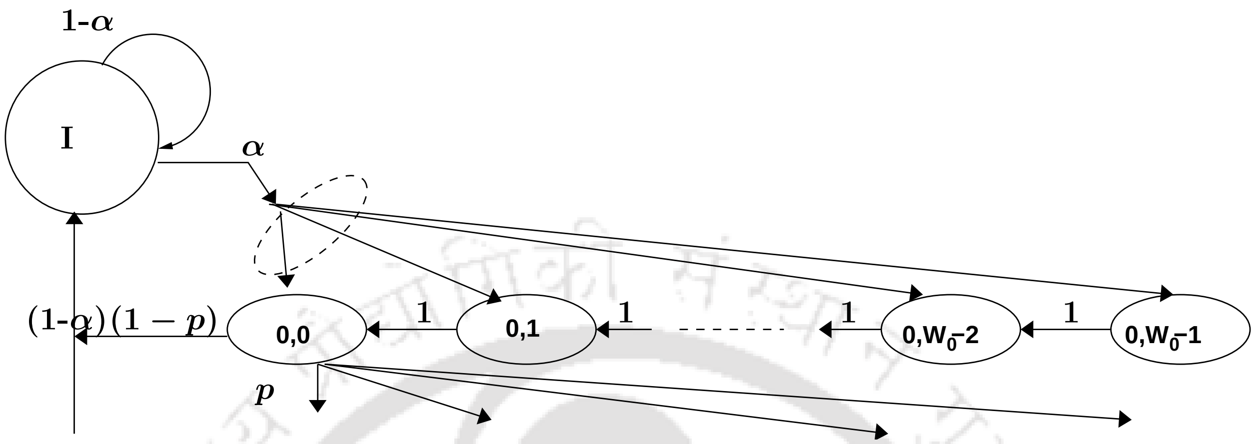

Figure 2.8: Markov model for data frame transmission in IEEE 802.11 DCF under unsaturated traffic [3]

rate to a lower data rate until the lowest data rate has been reached. This idea has been used in [66] to model the performance of IEEE 802.11 DCF. The paper [67] has formally studied the impact of the distance on the behavior of the IEEE 802.11 DCF and presented an analytical model that accounts for distance.

The models discussed till now have considered saturated traffic conditions only. However, as discussed in Chapter 1, modeling with saturated traffic conditions gives an overview of the network performance only at the extreme scenario, and may not always capture the real time traffic conditions. The next subsection discusses about the theoretical models proposed in the literature that explores the network performance in IEEE 802.11 DCF with variable traffic demands.

2.3.2 Performance Modeling of IEEE 802.11 DCF in Unsaturated Traffic Condition

Traffic in public wireless LANs follows self-similar characteristics [68] where data frames from users arrive in a burst. In such scenarios, only the stations that have frames to transmit contend for the channel access. Thus *network unsaturation* is common for practical wireless channel access scenarios. There are a few approaches for modeling IEEE 802.11 DCF in network unsaturation that provide characterizations of IEEE 802.11 DCF in the presence of bursty network traffic, such as error-prone channel condition [35], non ideal transmission channel and capture effect [3, 32], hidden terminals [34, 69, 70], fading channel effect [71–73], variable frame length [74], multi rate WLAN [75] and selfish station in the network [76]. The extended versions of the model in [1] have been presented in [77–81] under unsaturation condition for an error prone channel. Daneshgran *et al.* [3] have proposed a discrete time Markov chain model of IEEE 802.11 DCF under unsaturated traffic condition [3] which is presented in Figure 2.8. To represent the unsaturated traffic condition, the authors have introduced a new state called idle state which is labelled as I in Figure 2.8. There are two possible state transitions to the state I;

- After a successful frame transmission, the buffer of the transmitting station gets empty. This results in a transition to the state I with probability $(1-\alpha)(1-p)$. Here p is the collision probability of the frame transmission and α is the probability that a station has frame in the buffer for transmission.

- The station remains in the idle state with an empty buffer until a new packet arrives at the buffer for transmission. In Figure 2.8, this transition is expressed by a self loop in state I with probability $(1-\alpha)$.

Alshanyour *et al.* [42] have presented a four dimensional discrete time Markov chain that integrates the data and control frames retransmission limit, finite load and finite buffer capacity into one model. This model provides Quality of Service (QoS) performance and queuing behavior of the IEEE 802.11 DCF. Cao *et al.* [82] have proposed a discrete time Markov model considering both saturated and unsaturated system states. A system is saturated, if the MAC processing rate of the system (μ_1) is less than the total frame arrival rate (λ). Similarly, if the total frame arrival rate (λ) is less than the MAC process rate (μ_2) then the system is unsaturated. Whenever the traffic load satisfies the condition $\mu_1 < \lambda < \mu_2$ then system enters a dual state depending on the initial buffer condition. Hence, the throughput analysis depends on the initial buffer states even for the same traffic load which is considered in [82].

There are some literature that analyze the delay of IEEE 802.11 DCF in single hop network [83–87]. In [54], the authors have presented delay analysis of IEEE

[3] Extension of the Bianchi model [1]

802.11 protocol with no hidden terminals and of infinite retransmission attempts, derivation in the case of finite retry limits has been given in [88]. Wang *et al.* [56] have presented the access delay of DCF with constant contention window size. Xiao [58] has presented the saturation throughput, delay and frame dropping probabilities for IEEE 802.11e. To calculate the mean delay, Carvalho *et al.* [89] have found approximate formulae for both the mean and variance of the inter-departure time of frame by working with distributions. In [90], the authors have defined different types of delays such as the delay in successful frame transmission, frame drop and delay between two successful frame transmissions.

Researchers have tried to analyze the performance of IEEE 802.11 DCF in multihop network for both saturated and unsaturated traffic conditions [91–93]. Alizadeh *et al.* [94] have assumed RTS/CTS access mechanism (Section 2.2) with busy tone to eliminate the hidden terminal problem. In [95], only 3-node topology has been considered whereas the string topology has been considered in [96] to analyze the performance of IEEE 802.11 DCF in multihop network. Li *et al.* [97] have proposed a Markov chain model to analyze the per-node throughput by taking into consideration the important issues in multi hop networks, i.e., physical carrier sensing threshold, signal-to-interference plus noise ratio threshold and hidden terminal problems. In [98], the authors have presented a Parallel Space Time Markov Chain to model the IEEE 802.11 DCF in multihop ad hoc network using hidden terminal problem. Xiao textitet al. [99] have presented a four dimensional Markov chain model to evaluate the performance of the RTS/CTS scheme of the IEEE 802.11 protocol in multi hop ad hoc network. In [100], each station has been modeled as a discrete time $G/G/1$ queue. The end-to-end delay, delay jitter and the packet loss probability are derived from this model. Li *et al.* [101] have proposed a Markov chain model to analyze the IEEE 802.11 that exhibits substantial short-term unfairness in the presence of hidden terminals and concluded that the contention window (CW) improves the short-term fairness. Aydogdu *et al.* [102] have presented an analytical model of IEEE 802.11 DCF with hidden terminals and for various traffic loads in different multihop topologies.

2.4 Analytical Model of IEEE 802.11 DCF in PSM

A few researchers have designed analytical models to analyze the performance of the IEEE 802.11 Power Save Mode in infrastructure BSS [36–39, 103, 104] and in IBSS mode [105–107]. However the power save algorithm for infrastructure and IBSS networks are different in nature. This thesis focuses on IEEE 802.11 Power Save Mode in IBSS mode.

The IEEE 802.11 standard [2] defines the PSM scheme in IBSS to manage power by using the ATIM window in each beacon interval. However, several MAC protocols are designed for wireless LANs to further improve the power consumption over standard algorithms. Miller *et al.* [24] have proposed a scheme based on carrier sensing window which is shorter than the ATIM window. In [25], the authors have introduced a MAC protocol to improve power consumption in wireless LANs. The idea behind this protocol is that different stations use different ATIM window sizes and an adaptable ATIM window size is chosen dynamically. In [108], the authors have proposed to send a time synchronization function (TSF) beacon at the end of each ATIM window and add certain scheduling information in the beacon. This information ensures the data frame transmission to be contention free, which can help to achieve higher throughput and low energy consumption. Carvalho *et al.* [105] have proposed an analytical study of the IEEE 802.11 ad hoc networks by considering an active or passive state depending upon the channel state [4]. In the former a station may be in transmit or receive mode while in the latter the station is in idle mode. The analytical model assumes a station is always in the active state and not in sleep state. According to the paper [105], the total power consumption ξ_{total} is,

$$\xi_{\text{total}} = \xi_{\text{passive}} + \xi_{\text{active}}. \tag{2.3}$$

Here, ξ_{passive} and ξ_{active} denote the energy consumption in passive and active modes, respectively.

In [107], the authors derive a formula to calculate the energy consumption of a station. They divide the total energy into six different parts: successful transmission,

[4] There are three channel states: successful transmission, collision and idle.

successful reception, unsuccessful transmissions because of collision, overhearing, idle listening and reception of collision. The total energy consumption $J(n)$ by station l, in order to transmit 1 MB of data packet is given by,

$$J(n) = \frac{E[\text{energy consumed by } l \text{ in one slot}]}{E[\text{MB transmimitted by } l \text{ in one slot}]} \tag{2.4}$$

In [107], the authors have assumed that each station is saturated, i.e., the station never enters to the *sleep* or *off* states. The calculation of power consumption thus depends on the *transmit, receive* and *idle* states of the station and does not include the sleep state.

Zheng *et al.* [106] have proposed an analytical study of the IEEE 802.11 in power save mode using the transient analysis techniques to analyzed the delay and power consumption. The analytical model of the ATIM frame transmission is not described by authors. Moreover, they have not analyze the trade-off among throughput, MAC delay and average power conservation of the station in IEEE 802.11 power save mode under different network traffic condition. Nevertheless, according to the standard [2], the data frame transmission depend on the successful transmission of ATIM frame. The effect of power consumption on network throughput and delay is more in unsaturated traffic condition compared to the saturated traffic condition. From the above discussions, the existing models have two major limitations that can be summarized as follows,

1. The analytical models for energy consumption proposed in the literature have assumed that the stations always remain in active mode. To the best of our knowledge, the existing literature do not consider the sleep mode of the station, due to which they have over estimated the power consumption.

2. According to the power save algorithm, as defined by the standard [2], the stations go to sleep mode (power off) to save power. However, all the stations in the network are required to be in active mode (power on) for the duration of the ATIM window. The ATIM and data window concepts have not been explored in the existing literature.

These suggest that a concrete analytical model for IEEE 802.11 IBSS PSM is starkly missing. This thesis fills up the voids by providing an analytical model for IEEE 802.11 DCF PSM in IBSS according to the standard ATIM frame and data frame transmission algorithms. This analytical model is used to evaluate the protocol performance both in a saturated network and an unsaturated network.

2.5 Summary

This chapter briefly discusses the power management in IEEE 802.11 DCF in power save mode for infrastructure BSS and IBSS . From the discussions, it can be inferred that, though several mathematical models are designed for performance analysis of IEEE 802.11 DCF for both saturation and unsaturation traffic conditions, considered the power save mode operation of the wireless stations based on sleep-wake up cycle. This thesis models the standard IEEE 802.11 IBSS PSM in different network conditions to analyze the impact of different design parameters over the performance metrics like network throughput, delay and power consumption.

In the subsequent chapter, we will discuss the performance modeling and evaluation of IEEE 802.11 DCF PSM in IBSS considering the saturated traffic conditions. The saturation analysis shows the impact of network size over the performance metrics and the effect of beacon interval size over the network performance at high traffic load.

Chapter 3

Modeling IEEE 802.11 Power Save Mode in IBSS for Saturated Traffic

As discussed in Chapter 1 power is a critical resource for ad-hoc wireless networks. The design of energy efficient protocols for such networks is an emerging research area. The IEEE 802.11 standard defines power save algorithms for both infrastructure BSS and Independent BSS (as discussed in Chapter 2), where a wireless station goes to the sleep mode when no data communication takes place. However, the power save algorithms for infrastructure BSS and IBSS are different in nature. In infrastructure BSS, the AP acts as the central coordinator and uses polling based functionality to facilitate the wireless stations to go to sleep mode when there is no data communication. In IBSS, as there is no central coordinator, the wireless stations need to be synchronized through beacon messages for sleep-wake up cycles. The synchronization mechanism used in IEEE 802.11 is out of the scope of this thesis. In IEEE 802.11 DCF PSM for IBSS which is discussed in Section 2.2.2, time is divided into beacon intervals (BIs) and each BI is divided into an announcement traffic indication message (ATIM) window and a data window. If a station successfully transmits an ATIM frame in the ATIM window, then it is allowed to transmit a data frame in the data window. Otherwise it goes to sleep mode in the data window. This chapter proposes an analytical model for IEEE 802.11 DCF PSM in

IBSS under saturated traffic condition.

In this chapter we are mostly interested in the performance modeling of IEEE 802.11 Power Save Mode in IBSS under saturation network traffic conditions. The IEEE 802.11 standard [2] defines the PSM scheme to manage power using the ATIM window. However, several MAC protocols have been designed for wireless LANs to further improve the power consumption in IEEE 802.11 IBSS [24, 25]. As discussed in previous chapters, most of the analytical models do not consider the power consumption for IEEE 802.11 DCF with PSM, where the stations goes to the sleep state in the data window if it fails to transmit or receive an ATIM frame in the ATIM window. This motivates us to look into the performance modeling and evaluation of IEEE 802.11 IBSS in PSM. The probability of successful transmission of an ATIM frame has a great impact over the data frame transmission of a node in IBSS PSM. Therefore, the probability of a successful transmission of an ATIM frame is required for the calculation of the throughput for IEEE 802.11 DCF PSM in IBSS. The average MAC delay and the average power consumption depends on the successful transmission of an ATIM frame transmission. Therefore, the model is used to also analyze the MAC delay and average power consumption at saturated network condition.

The rest of this chapter is organized as follows. Section 3.1 presents a brief overview of the IEEE 802.11 PSM in IBSS. A discrete time Markov model is proposed in Section 3.2 to calculate the throughput using the probability that an ATIM frame is transmitted successfully. Sections 3.3 and 3.4 present an analytical model for delay analysis and for power consumption, respectively. In Section 3.5, simulation results are reported to validate the proposed theoretical model. This section also gives a detailed analysis of the performance of IEEE 802.11 DCF in PSM for IBSS. Finally, Section 3.6 concludes the chapter.

3.1 The IEEE 802.11 DCF in Power Save Mode

The IEEE 802.11 standard [2] defines a power save technique for IBSS. It is assumed that all the stations are synchronized and awake at the beginning of each BI. The stations in PSM wake up periodically to listen to the beacon messages and stay awake for a period of time called the ATIM window. The ATIM frame is a control frame which is exchanged by the stations within the ATIM window to determine whether to go for PSM or stay awake for data transmission after the end of the ATIM window. When a station has a data frame to transmit, it transmits an ATIM frame to the corresponding receiver during the ATIM window following the 802.11 CSMA/CA DCF backoff mechanism specified in the IEEE 802.11 standard [2]. The standard does not define the retry limit for ATIM frame transmission in IBSS. However, in the paper [25], the authors have defined the retry limit of three for an ATIM frame transmission within an ATIM window and up to three BIs. This paper assumes that if the ATIM frame is not transmitted successfully the corresponding data frame is rebuffered for the next BI. After the third ATIM window if the ATIM frame is not transmitted successfully then the data frame is dropped. A similar assumption is made in this chapter to model the ATIM frame transmission. The stations that have successfully transmitted an ATIM frame within the ATIM window compete to transmit a data frame in the rest of the BI. It can be noted that the standard does not specify the number of BIs for data frame transmission. According to the paper [106], there is a high probability of delivering a data frame successfully by the end of the first data window. For this reason, it is assumed a single data window.

Algorithm 3.1 shows the transmission of an ATIM frame and data frame in IBSS PSM. In Algorithm 3.1, the variable $\text{BeaconNum}_{\text{ATIM}}$ represents the number of beacon intervals for ATIM frame. A station may be unable to transmit an ATIM frame due to either contention with other stations or reaching the end of the ATIM window at the time of ATIM frame transmission. Similarly, an unsuccessful transmission of data frame can occur either due to contention with other stations or reaching the end of the data window, before the ACK is received successfully. According to Algorithm 3.1, the station sets the value of contention window (CW_{ATIM}) to CW_{min} for ATIM, where CW_{min} is the minimum contention window size. CW_{ATIM} is doubled up to $\text{CW}^{\text{a}}_{\text{max}}$ for an unsuccessful transmission of an ATIM frame, where $\text{CW}^{\text{a}}_{\text{max}}$ is the maximum contention window size for an ATIM frame transmission, $\text{CW}^{\text{a}}_{\text{max}} = 2^2 \times (\text{CW}_{\text{min}})$. An ATIM frame may collide with another ATIM frame. In this case the station will retransmit the ATIM frame with a retry limit of three within one ATIM window. If an ATIM-ACK is not received within the same ATIM window or $CW_{\text{ATIM}} = \text{CW}^{\text{a}}_{\text{max}}$, then the ATIM frame is dropped and the corresponding data is rebuffered for another try in the

Algorithm 3.1 Transmission of a data frame with ATIM frame in power save mode

$\text{BeaconNum}_{\text{ATIM}} \leftarrow 0$
$CW_{ATIM} \leftarrow CW_{\min}$
$W \leftarrow$ random integer from an uniform distribution over the interval $[0, CW_{ATIM} - 1]$
while $W > 0$ **do**
    if Channel = Idle **then**
        $W \leftarrow W - 1$
    end if
end while
Transmit ATIM frame.
if ATIM window ends before ATIM-ACK is received **then**
    $\text{BeaconNum}_{\text{ATIM}} \leftarrow \text{BeaconNum}_{\text{ATIM}} + 1$
    if $\text{BeaconNum}_{\text{ATIM}} \leq 2$ **then**
        GOTO 2
    else
        DROP the ATIM frame.
    end if
else
    if ATIM-ACK is not received successfully **then**
        $CW_{ATIM} \leftarrow 2 \times CW_{ATIM}$
        if $CW_{ATIM} \leq CW^{a}_{\max}$ **then**
            GOTO 3
        else
            $\text{BeaconNum}_{\text{ATIM}} \leftarrow \text{BeaconNum}_{\text{ATIM}} + 1$
            if $\text{BeaconNum}_{\text{ATIM}} \leq 2$ **then**
                GOTO 2
            else
                DROP the ATIM frame.
            end if
        end if
    else
        Use Algorithm 3.2 to transmit the DATA frame
    end if
end if

Algorithm 3.2 Data frame transmission in power save mode

1: $CW_{data} \leftarrow CW_{\min}$
2: $W \leftarrow$ random integer from an uniform distribution over the interval $[0, CW_{data} - 1]$
3: **while** $W > 0$ **do**
4:   **if** Channel = Idle **then**
5:     $W \leftarrow W - 1$
6:   **end if**
7: **end while**
8: Transmit DATA frame.
9: **if** data window ends before ACK is received **then**
10:   DROP the data frame.
11: **else**
12:   **if** ACK is not received after ACK time out **then**
13:     $CW_{data} \leftarrow 2 \times CW_{data}$
14:     **if** $CW_{data} \leq CW^{d}_{\max}$ **then**
15:       **GOTO** 2
16:     **else**
17:       DROP the DATA frame.
18:     **end if**
19:   **else**
20:     Success of data frame transmission
21:     **GOTO** 1
22:   **end if**
23: **end if**

next ATIM window (reset $CW_{\mathrm{ATIM}} = \mathrm{CW}_{\min}$). An attempt is made to transmit the ATIM frame up to three ATIM windows. After three ATIM windows if the ATIM frame is not transmitted successfully then the data frame is dropped.

Algorithm 3.2 is the procedure for data frame transmission after successful transmission of an ATIM frame. Here $\mathrm{CW}^{\mathrm{d}}_{\max}$ is the maximum contention window size for a data frame transmission. Initially, the station sets the value of contention window $\mathrm{CW}_{\mathrm{data}}$ to $\mathrm{CW}_{\min}$[1]. $\mathrm{CW}_{\mathrm{data}}$ is doubled up to $\mathrm{CW}^{\mathrm{d}}_{\max}$ for each unsuccessful transmission of a data frame.

[1]It is assumed that both ATIM and data frame transmissions use the same $\mathrm{CW}_{\min}$

3.2 Modeling and Analysis

In this section, we will present the network assumptions that are required to model the system of IEEE 802.11 DCF in IBSS. A discrete time Markov model is proposed and analyzed to calculate the throughput using the probability that a station transmits an ATIM frame and data frame in a randomly chosen slot.

3.2.1 Network Model Assumptions

To model and analyze the Power Save Mode of IEEE 802.11 DCF in IBSS, the following assumptions have been made. A fixed network size of n stations with basic access mechanism is considered. All stations are considered to be in saturation condition, that is at all times each station has data packets to transmit. The ATIM window size is fixed. If a station A successfully transmits an ATIM frame to station B in an ATIM window, then it cannot transmit another ATIM frame to the same station in the same ATIM window. After a successful transmission of an ATIM frame from station A to station B within the ATIM window in a BI, the station A can transmit multiple data frames to station B within the data window of that BI.

3.2.2 System Model

Consider stochastic processes $s(t)$ representing the backoff stage, $b(t)$ representing the backoff counter and $a(t)$ representing the backoff layer (the beacon interval number counting from 0 to 2) at time t. The backoff stage $s(t)$ counts number of attempts (or retries) to transmit an ATIM or data frame within one beacon interval. In the paper [32], the Markov chain model for IEEE 802.11 DCF takes freezing of the backoff counter into account by a self loop in each state. However for simplicity as in Bianchi's model [1], in this chapter the backoff counter is decremented by one at the beginning of each slot. The backoff layer $a(t)$ represents the number of beacon intervals used to successfully transmit an ATIM frame. A Discrete time Markov model for data frame transmission in PSM is presented in Figure 3.1 with 3-tuple $\{s(t), b(t), a(t)\}$. The following notations are used to represent the transition probabilities, where a single prime and a double prime are used to represent transition probabilities for ATIM and data frame transmission respectively. The

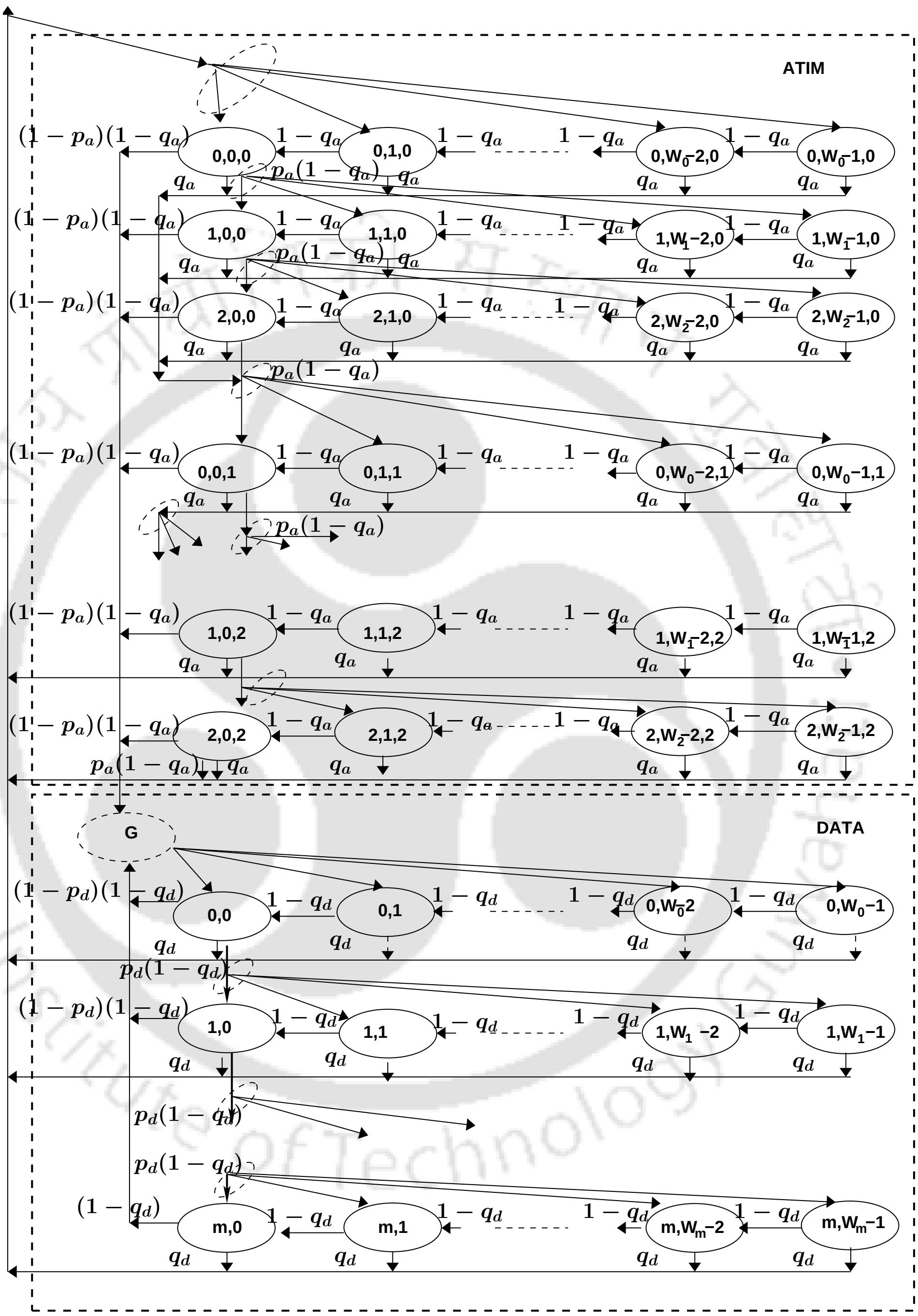

Figure 3.1: Markov model for data frame transmission in power save mode

state G is a dummy state introduced for ease of presentation and does not have any impact on the solution of the Markov chain model. The following notations are used in presenting the Markov model:

$$P\{(i_1, j_1, k_1)^{'}|(i_0, j_0, k_0)^{'}\} = P\{s(t+1) = i_1, b(t+1) = j_1, a(t+1) = k_1|s(t) = i_0, b(t) = j_0, a(t) = k_0\}.$$

and

$$P\{(i_1, j_1)^{''}|(i_0, j_0)^{''}\} = P\{s(t+1) = i_1, b(t+1) = j_1|s(t) = i_0, b(t) = j_0\}.$$

Note that for data frame transmission there is no third component k, as one data window is used for each successful ATIM frame transmission. In Figure 3.1 p_a and p_d are conditional collision probabilities in the ATIM window and data window, respectively, where p_a and p_d are independent of the number of retransmissions and are constant for a fixed network size[2].

Assume that q_a is the probability that the ATIM window ends when a station is attempting to transmit an ATIM frame. Similarly q_d is the probability that the data window ends while transmitting a data frame. The value of q_a depends on the number of competing stations in the ATIM window as well as the ATIM window size. Similarly q_d is proportional to the the number of active stations in the data window. The value of q_d also depends on the data window size. The analysis and estimation of q_a and q_d will be discussed in the Section 3.2.4. The non zero one-step transition probabilities of the Markov chain in Figure 3.1 are shown as set of equations in equation (3.1). W_i is the contention window size at the i^{th} backoff stage and $W_i = 2^i \times W_0$. Here $\mathrm{W_0} = \mathrm{CW_{min}}$, the minimum contention window size.

- The first equation indicates that within the ATIM window, the ATIM frame backoff counter decrements with probability $(1 - q_a)$.

- The second equation indicates that at any backoff stage and for any backoff counter value if the ATIM window ends, the protocol tries to retransmit the ATIM frame with backoff stage 0 in the next ATIM window.

- The third equation presents an unsuccessful transmission of an ATIM frame, when the ATIM window ends at the third beacon interval (indicated by $a(t) = 0$).

[2]the data ACK and ATIM-ACK are avoid because of the ideal channel condition and single hop topology. The collision probability depends only on the transmission probability

$$
\begin{cases}
(1) & P\{(i,j,k)^{'}|(i,j+1,k)^{'}\} = 1-q_a, & i\in[0,2], j\in[0,W_i-1], k\in[0,2];\\
(2) & P\{(0,j,k+1)^{'}|(i,j',k)^{'}\} = \frac{q_a}{W_0}, & i\in[0,2], j\in[0,W_0-1], k\in[0,1], j'\in[0,W_i-1];\\
(3) & P\{(0,j,0)^{'}|(i,j',2)^{'}\} = \frac{q_a}{W_0}, & i\in[0,2] j\in[0,W_0-1], j'\in[0,W_i-1];\\
(4) & P\{G|(i,0,k)^{'}\} = (1-p_a)\times(1-q_a), & i\in[0,2], k\in[0,2],\\
(5) & P\{(0,j,0)^{'}|(2,0,2)^{'}\} = \frac{p_a\times(1-q_a)}{W_0}, & j\in[0,W_0-1];\\
(6) & P\{(0,j,k+1)^{'}|(2,0,k)^{'}\} = \frac{p_a\times(1-q_a)}{W_0}, & j\in[0,W_0-1], k\in[0,1];\\
(7) & P\{(i+1,j,k)^{'}|(i,0,k)^{'}\} = \frac{p_a\times(1-q_a)}{W_i}, & i\in[0,1], j\in[0,W_i-1], k\in[0,2];\\
(8) & P\{(i,j)^{''}|(i,j+1)^{''}\} = 1-q_d, & i\in[0,m], j\in[0,W_i-1];\\
(9) & P\{(0,j,0)^{'}|(i,j_0)^{''}\} = \frac{q_d}{W_0}, & i\in[0,m], j\in[0,W_0-1], j_0\in[0,W_i-1];\\
(10) & P\{(0,j)^{''}|(i,0)^{''}\} = \frac{(1-p_d)\times(1-q_d)}{W_0}, & i\in[0,m], j\in[0,W_0-1];\\
(11) & P\{(i+1,j)^{''}|(i,0)^{''}\} = \frac{p_d\times(1-q_d)}{W_i}, & i\in[0,m], j\in[0,W_i-1];\\
(12) & P\{(0,j)^{''}|(m,0)^{''}\} = \frac{(1-q_d)}{W_0}, & j\in[0,W_0-1]
\end{cases}
\tag{3.1}
$$

- The fourth equation indicates a successful transmission of an ATIM frame.
- The fifth equation indicates that at the third ATIM window and at the last retry limit the frame is either successfully transmitted or discarded.
- The sixth equation indicates that there is a collision at the last try within an ATIM window.
- The seventh equation indicates that the station increases the backoff stage and selects the backoff counter uniformly after an unsuccessful transmission of an ATIM frame.
- The eighth equation indicates that within the data window, the data frame backoff counter decrements with probability $(1-q_d)$.
- The ninth equation indicates the end of data window has been reached at any backoff stage or any backoff counter, resulting in dropping of the data frame.
- The tenth equation models the successful transmission of a data frame.
- The eleventh equation indicates that the station increases the backoff stage and chooses the backoff counter uniformly after an unsuccessful transmission of a data frame within the data window.
- The twelfth equation models the unsuccessful transmission of a data frame at the last backoff stage.

3.2.3 Model Analysis

Let $b'_{i,j,k}$ and $b''_{i,j}$ be the stationary distributions of the Markov chain for the ATIM and data windows, respectively. Here,

$$\begin{aligned} b'_{i,j,k} &= \lim_{t\to\infty} P\{s(t)=i, b(t)=j, a(t)=k\}, \\ & \quad i \in [0,2], j \in [0, W_i - 1], k \in [0,2] \end{aligned}$$

and

$$\begin{aligned} b''_{i,j} &= \lim_{t\to\infty} P\{s(t)=i, b(t)=j\}, \\ & \quad i \in [0,m], j \in [0, W_i - 1] \end{aligned}$$

To obtain a closed-form solutions for the Markov chain presented in Figure 3.1, iterative equation (3.2) and equation (3.3) are used:

$$b'_{i,0,k} = \tfrac{p_a(1-q_a)}{W_i} \textstyle\sum_{l=0}^{W_i-1}(1-q_a)^l b'_{i-1,0,k} \quad 0 < i \le 2 \tag{3.2}$$

$$b''_{i,0} = \tfrac{p_d(1-q_d)}{W_i} \textstyle\sum_{l=0}^{W_i-1}(1-q_d)^l b''_{i-1,0} \quad 0 < i \le m \tag{3.3}$$

The above equation 3.2 and equation 3.3 reflects that the state $b'_{i,0,k}$ and $b''_{i,0}$ can be reached from the state $b'_{0,0,k}$ and $b''_{0,0}$, respectively, $\forall i \in [0,2]$ and $k \in [0,2]$.

$$b'_{i,j,k} = \begin{cases} \frac{1}{W_0}, & i=0, j=W_0-1, k=0; \\ \frac{1}{W_0} \times \sum_{l=0}^{W_0-(j+1)}(1-q_a)^l, & i=0, j\in[0,W_0-2], k=0; \\ M, & i=0, j=W_0-1, k\in[1,2]; \\ M \times \sum_{l=0}^{W_0-(j+1)}(1-q_a)^l, & i=0, j\in[0,W_0-2], k\in[1,2]; \\ \frac{p_a(1-q_a)}{W_i} \times \sum_{l=0}^{W_i-(j+1)}(1-q_a)^l b'_{i-1,0,k}, & i\in[1,2], j\in[0,W_i-1], k\in[0,2] \end{cases} \tag{3.4}$$

$$b''_{i,j} = \begin{cases} N, & i=0, j=W_0-1; \\ N \times \sum_{l=0}^{W_0-(j+1)}(1-q_d)^l, & i=0, j\in[0,W_0-2]; \\ \frac{p_d(1-q_d)}{W_i} \times \sum_{l=0}^{W_i-(j+1)}(1-q_d)^l b''_{i-1,0}, & i\in[1,m], j\in[0,W_i-1], \end{cases} \tag{3.5}$$

The Markov chain presented in Figure 3.1 is a regular chain. So for each $j \in [0, W_i - 1]$ and $k \in [0,2]$, we have equation (3.4) and equation (3.5). The values of M and N are

$$M = \frac{1}{W_0}\Big[p_a(1-q_a)b^{'}_{2,0,k-1} + q_a\sum_{i=0}^{2}\sum_{j=0}^{W_i-1}b^{'}_{i,j,k-1}\Big]$$

$$N = \frac{1}{W_0}\Big[(1-p_d)(1-q_d)\sum_{i=0}^{m-1}b^{''}_{i,0} + (1-q_d)b^{''}_{m,0}\Big]$$

Let τ_a be the probability that a station transmits an ATIM frame in a randomly chosen slot. This can be obtained as

$$\begin{aligned}\tau_a &= \sum_{k=0}^{2}\sum_{i=0}^{2}b^{'}_{i,0,k} \qquad (3.6)\\ &= \sum_{k=0}^{2}\sum_{i=0}^{2}\Big(\frac{C\times p_a}{q_a}\Big)^i\prod_{j=1}^{i}\frac{\{1-C^{W_j}\}}{W_j}b^{'}_{0,0,k},\end{aligned}$$

here, $C = (1-q_a)$. From the equation (3.4), value of the $b^{'}_{0,0,k}$ can be written as

$$\begin{aligned}b^{'}_{0,0,k} &= M\times\sum_{l=0}^{W_0-1}(1-q_a)^l \qquad (3.7)\\ &= \frac{1}{W_0}[p_a(1-q_a)b_{2,0,k-1} + q_a\sum_{i=0}^{2}\sum_{j=0}^{W_i-1}b_{i,j,k-1}]\times\sum_{l=0}^{W_0-1}(1-q_a)^l\end{aligned}$$

The equation (3.7) shows the relation between $b^{'}_{0,0,k}$ and $b^{'}_{0,0,k-1}$ for $k\in[1,2]$. The value of τ_a can be obtained by solving equation (3.2), equation (3.4) and equation (3.7). The relation between p_a and τ_a is[3]

$$p_a = 1-(1-\tau_a)^{(n-1)}. \qquad (3.8)$$

where n is the number of stations in the network. The value of τ_a and p_a can be solved numerically using fixed point iteration. Let P_{as} denotes the probability that an ATIM frame transmission is successful is given by the probability that exactly one

[3]The collision probability p_a depends only on the transmission probability τ_a because of the ideal channel condition and single hop topology

station transmits on the channel, conditioned on the fact that at least one station transmits an ATIM frame. The P_{as} can be calculated as follows:

$$P_{as} = \frac{n\tau_a(1-\tau_a)^{(n-1)}}{1-(1-\tau_a)^n}. \tag{3.9}$$

Similarly, to find out the probability of success for a data frame transmission after successfully transmitting an ATIM frame, let τ_d be the probability that a station transmits a data frame in a randomly chosen slot in the data window. So the value of τ_d depends on the value of τ_a. The former can be represented as:

$$\tau_d = \sum_{i=0}^{m} b''_{i,0} \tag{3.10}$$

From equation (3.3) the value of $b''_{i,0}$ can be expressed in terms of $b''_{0,0}$ as follows:

$$\sum_{i=0}^{m} b''_{i,0} = \sum_{i=0}^{m} \left(\frac{p_d(1-q_d)}{q_d}\right)^i \prod_{j=1}^{i} \frac{\{1-(1-q_d)^{W_j}\}}{W_j} b''_{0,0} \tag{3.11}$$

The value of the $b''_{0,0}$ can be obtained from the normalized condition:

$$1 = \sum_{i=0}^{m} \sum_{j=0}^{W_i-1} b''_{i,j} \tag{3.12}$$

Using the value of $b''_{i,j}$ from equation (3.5), the equation (3.12) can be written as

$$1 = \sum_{i=0}^{m} \sum_{j=0}^{W_i-1} \frac{1-(1-q_d)^{W_i-j}}{1-(1-q_d)^{W_i}} b''_{i,0}$$

From equation (3.3),

$$1 = \sum_{i=0}^{m} \sum_{j=0}^{W_i-1} \frac{p_d(1-q_d)}{W_i} \sum_{l=0}^{W_i-(j+1)} (1-q_d)^l b''_{i-1,0}$$

From the above equation the value of the $b_{0,0}$ can be written as

$$b''_{0,0} = \frac{1}{A} \tag{3.13}$$

where

$$A = \sum_{i=0}^{m} \Big(\frac{p_d(1-q_d)}{q_d}\Big)^i \times \prod_{j=1}^{i} \frac{1-(1-q_d)^{W_j}}{W_j} \Big[\frac{W_i}{1-(1-q_d)^{W_i}} - \frac{(1-q_d)}{q_d}\Big]. \quad (3.14)$$

Now the value of τ_d can be calculated from equation (3.10), equation (3.11) and equation (3.13). The relation between p_d and τ_d is[4]

$$p_d = 1-(1-\tau_d)^{(n'-1)}. \quad (3.15)$$

where $n' = \lceil n \times P_{as} \rceil$ and n is the number of stations in the network. The quantity $\lceil n \times P_{as} \rceil$ denotes the expected number of active communication pairs in the data window after the completion of the ATIM window. However, this quantity is not equal to the number of active stations, as a sender may have multiple receivers. For simplicity, it has been assumed that a sender can send data frames to a single receiver in a data window. Thus the number of active stations in a data window is proportional to n'. So at the beginning of each data window, the network with n' number of stations are in saturation condition. Let P_{tr} be the probability that there is at least one data frame transmission in the considered slot. Let P_{ds} be the joint probability that a data frame is transmitted successfully after the successful transmission of an ATIM frame. The values of P_{tr} and P_{ds} are given by

$$P_{tr} = 1-(1-\tau_d)^{n'} \quad (3.16)$$

$$P_{ds} = \frac{n'\tau_d(1-\tau_d)^{(n'-1)}}{P_{tr}}. \quad (3.17)$$

3.2.4 Analysis and Estimation of q_a and q_d

It has been assumed in the model in Figure 3.1 that q_a is the probability of reaching the end of an ATIM window and q_d is the probability of reaching the end of a data window. The probability q_a depends on the network size as well as ATIM window size. We assume a fixed ATIM window size and that all stations satisfy the saturation condition. For a fixed ATIM window size, the value of q_a is constant. In [24], the authors show that the performance of the network is maximum with

[4]The collision probability p_d depends only on the transmission probability τ_d because of the ideal channel condition and single hop topology

ATIM window size $20ms$. From analysis of simulation results it has been observed that the probability of success in ATIM window with ATIM window size $= 20ms$ agrees with the theoretical model for $q_a = 0.002$. In this chapter, ATIM window size is assumed to be fixed of size $20ms$. Accordingly, in theoretical analysis q_a is assumed as 0.002.

However, the size of the data window is considerably larger than the size of the ATIM window, and the network size has a large impact on the probability of reaching the end of the data window. The probability value q_d is proportional to the number of active stations in the data window and the data window size. From the assumption that a station can send data to a single station only in a particular data window, the quantity n' denotes the expected number of active stations in a data window. So,

$$q_d \propto n' \tag{3.18}$$

This can be written as,

$$q_d = c \times n' \tag{3.19}$$

where c is the proportionality constant. For a fixed ATIM window size, the value of c depends on the size of the data window. The impact of the parameter c on beacon interval is analyzed using simulation results.

3.2.5 Saturation Throughput Analysis

The fraction of time the channel is used to successfully transmit payload bits is called the system throughput [1]. Let S denote the normalized system throughput in the data window. The normalized saturation throughput at the data window is given by

$$S_{\text{DATA}} = \frac{E[\text{payload information transmitted in a slot}]}{E[\text{duration of a slot}]}$$

Let, $E[p]$ be the average packet payload size (in terms of time unit, e.g., μs). $P_{ds}P_{tr}$ is the probability that payload information is transmitted successfully in a slot. The average length of a slot in a data window is computed by considering three mutually exclusive and exhaustive cases. $(1 - P_{tr})$ is the probability that a slot is empty, $P_{ds}P_{tr}$ is the probability of successful transmission of data and $(1 - P_{ds})P_{tr}$ is the collision probability for a data frame. Therefore,

$$S_{\text{DATA}} = \frac{P_{ds}P_{tr}E[p]}{(1-P_{tr})\sigma + P_{ds}P_{tr}T_s + (1-P_{ds})P_{tr}T_c} \tag{3.20}$$

Here T_s and T_c are the average time the channel is sensed busy because of a successful transmission or a collision respectively, and σ is the empty slot time. T_s and T_c can be calculated as follows,

$$\begin{aligned} T_s &= \text{DIFS} + H + E[P] + 2\delta + \text{SIFS} + \text{ACK} \\ T_c &= \text{DIFS} + H + E[P] + \text{SIFS} + \text{ACK}_{\text{TO}} \end{aligned} \tag{3.21}$$

It has been assumed that all packets have the same size, so $E[p] = P$ is the average payload. The ACK timeout (ACK_{TO}) is added in T_c according to the standard [2] specification that a station waits for an EIFS time when the channel is sensed busy because of collision. $\text{EIFS} = \text{SIFS} + \text{ACK}_{\text{TO}} + \text{DIFS}$. Let $H = \text{PHY}_{\text{hdr}} + \text{MAC}_{\text{hdr}}$ be the packet header and δ the propagation delay.

S_{DATA} provides the channel throughput at the data window only. The overall channel throughput has the ATIM overhead included with the data window channel throughput. The overall normalized throughput (S) can be calculated as,

$$S = S_{\text{DATA}} \times \frac{\text{Data Window size}}{\text{Duration of Beacon Interval}} \tag{3.22}$$

This section provided an analytical model to calculate the network throughput in IEEE 802.11 DCF power save mode. The next section provides the theoretical model for delay analysis in IEEE 802.11 DCF PSM using the discrete time Markov Model presented in Figure 3.1.

3.3 Analytical Model for Delay Analysis

A delay for a data frame transmission in MAC layer in PSM depends on the delay in ATIM window to transmit an ATIM frame successfully. Let $\overline{D}$ denote the average MAC delay. Then $\overline{D}$ can be written as:

$$\overline{D} = \overline{D^{(a)}_{\text{succ}}} + \overline{D^{(d)}_{\text{succ}}} \tag{3.23}$$

where $\overline{D_{\text{succ}}^{(a)}}$ denotes the average delay in transmitting an ATIM frame successfully, and $\overline{D_{\text{succ}}^{(d)}}$ denotes the average delay in transmitting the corresponding data frame successfully.

Assume that $D_{\text{succ}}^{(a)}(k)$ be the delay experienced up to the k^{th} ATIM window to transmit an ATIM frame successfully. $\text{ATIM}_{\text{size}}$ represents the ATIM window size, which is fixed. Therefore,

$$D_{\text{succ}}^{(a)}(k) = k \times \text{BI} + \text{ATIM}_{\text{size}} \tag{3.24}$$

Assume that $D_{\text{succ}}^{(d)}(i, b)$ is the delay to transmit a data frame successfully in the i^{th} backoff stage of the data window when the sum of the backoff values up to stage i is b. Assume that b is the average value of the CW. Since $(W_i - 1)$ is the maximum CW size at the i^{th} backoff stage, the average value of b is $\frac{Wi}{2}$. The value of $D_{\text{succ}}^{(d)}(i, b)$ is given by:

$$D_{\text{succ}}^{(d)}(i, b) = b \times T_{\text{avg}} + i \times T_c + T_s \tag{3.25}$$

Here T_s and T_c are the average time the channel is sensed busy because of a successful transmission or a collision, respectively, of the data frame in the data window.

Now, the average delay in transmitting an ATIM frame successfully is equal to the total delay up to the k^{th} ATIM window, given that the ATIM success occurs at the k^{th} ATIM window. Let the probability $P_{\text{succ}}^{(a)'}(i, k)$ be the conditional probability that the backoff process of an ATIM frame transmission ends at the i^{th} stage of the k^{th} ATIM window, given that the ATIM frame is transmitted successfully. Then, the value of $\overline{D_{\text{succ}}^{(a)}}$ is calculated as:

$$\overline{D_{\text{succ}}^{(a)}} = \sum_{k=0}^{2} \sum_{i=0}^{2} P_{\text{succ}}^{(a)'}(i, k) \times D_{\text{succ}}^{(a)}(k) \tag{3.26}$$

Assume that $P_{\text{succ}}^{(a)}(i, k)$ is the probability that an ATIM frame is transmitted successfully at the i^{th} backoff stage of the k^{th} ATIM window, and $P_{\text{drop}}^{(a)}$ denotes the probability that an ATIM frame is dropped because of the retry limit being exceeded in the last ATIM window. Since $D_{\text{succ}}^{(a)}(k)$ represents the delay of an ATIM frame that is successfully transmitted, we should only consider the packets that are successfully transmitted while excluding the packets that are dropped. Therefore, we define the following conditional probability $P^{(a)'}_{\text{succ}}(i,k)$ is calculated as follows:

$$P^{(a)'}_{\text{succ}}(i,k) = \frac{P^{(a)}_{\text{succ}}(i,k)}{1 - P^{(a)}_{\text{drop}}} \tag{3.27}$$

$P^{(a)}_{\text{succ}}(i,k)$ is given by:

$$P^{(a)}_{\text{succ}}(i,k) = X^{i}_{k}(1 - p_a)(1 - q_a) \tag{3.28}$$

where X^i_k is the probability that a station will try to send an ATIM frame in the i^{th} backoff stage of the k^{th} ATIM window. We have

$$X^i_k = \begin{cases} L^i, & k = 0; \\ L^{(3+i)} + q_a \times L^i, & k = 1; \\ L^{(3*2+i)} + 2 \times q_a \times L^{(3+i)} + q_a^2 \times L^i, & k = 2; \end{cases} \tag{3.29}$$

Here, $L = p_a(1 - q_a)$. Consequently, $P^{(a)}_{\text{drop}}$ is calculated as:

$$P^{(a)}_{\text{drop}} = 1 - \sum_{k=0}^{2}\sum_{i=0}^{2} P^{(a)}_{\text{succ}}(i,k) \tag{3.30}$$

From equation (4.32) and equation (4.29), the average delay in transmitting an ATIM frame successfully ($\overline{D^{(a)}_{\text{succ}}}$) is calculated using equation (4.31).

Similarly, the value of the average delay in transmitting a data frame successfully within the data window ($\overline{D^{(d)}_{\text{succ}}}$) is calculated in a similar way. Let, $B(i)$ is the total backoff value up to i^{th} backoff stage, and $B(i)_{\max}$ is the summation of maximum contention window sizes up to the backoff stage i $\left(\sum_{j=0}^{i}(CW_j - 1)\right)$.

Then, $\overline{D^{(d)}_{\text{succ}}}$ is calculated as:

$$\overline{D^{(d)}_{\text{succ}}} = \sum_{i=0}^{m}\sum_{b=0}^{B(i)_{\max}} P^{(d)'}_{\text{succ}}(i,b) \times D^{(d)}_{\text{succ}}(i,b). \tag{3.31}$$

The value $P^{(d)'}_{\text{succ}}(i,b)$ denotes the conditional probability that the backoff process of a data frame transmission ends at the i^{th} stage of the data window, with total backoff value b up to the i^{th} backoff stage, given that the data frame is transmitted successfully. $P^{(d)'}_{\text{succ}}(i,b)$ is given by:

$$P^{(d)'}_{\text{succ}}(i,b) = \frac{P^{(d)}_{\text{succ}}(i,b)}{1 - P^{(d)}_{\text{drop}}} \tag{3.32}$$

Here $P^{(d)}_{\text{drop}}$ is the probability of dropping a data frame that exceeds the retry limit in the data window. $P^{(d)}_{\text{succ}}(i, b)$ is the probability that a data frame is transmitted at the i^{th} stage and b is the the sum of backoff values up to the i^{th} backoff stage. Therefore,

$$P^{d}_{\text{succ}}(i, b) = P^{(d)}_{\text{succ}}(i) Pr(B(i) = b)$$

$$P^{(d)}_{\text{drop}} = 1 - (1 - p_d)(1 - q_d) \sum_{i=0}^{m} \{p_d(1 - q_d)\}^i$$

where m is the maximum retry limit to transmit a data frame in the data window. Assume, $P^{(d)}_{\text{succ}}(i)$ is the probability of transmitting a data frame successfully in the i^{th} backoff stage of the data window, and $p_d(1 - q_d)$ is the probability that there is a collision within the data window. Therefore,

$$P^{(d)}_{\text{succ}}(i) = \{p_d(1 - q_d)\}^i \{(1 - p_d)(1 - q_d)\} \tag{3.33}$$

Let $P^{(d)}_{\text{idle}}$, $P^{(d)}_{\text{col}}$ and $P^{(d)}_{\text{succ}}$ are the probability that a randomly chosen slot in the data window is idle, leads to a collision and results in successful transmission, respectively. Then,

$$\begin{aligned} P^{(d)}_{\text{idle}} &= (1 - \tau_d) \\ P^{(d)}_{\text{succ}} &= n^{'} \tau_d (1 - \tau_d)^{(n^{'}-1)} \\ P^{(d)}_{\text{col}} &= 1 - (1 - \tau_d) - n^{'} \tau_d (1 - \tau_d)^{(n^{'}-1)} \end{aligned}$$

Here τ_d, calculated according to equation (3.10), represents the probability that a station transmits a data frame in the randomly chosen slot in the data window and $n^{'} = \lceil n \times P_{as} \rceil$ is the number of station in active mode in the data window. Then,

$$T_{avg} = P^{(d)}_{\text{idle}} \sigma + P^{(d)}_{\text{succ}} T_s + P^{(d)}_{\text{col}} T_c \tag{3.34}$$

where σ is the empty slot time. From equation (4.37) and equation (4.30) the value of $\overline{D^{(d)}_{succ}}$ is calculated. Therefore, the average delay, calculated using equation (4.28), and is given by:

$$\begin{aligned} \overline{D} = &\sum_{k=0}^{2} \sum_{i=0}^{2} \left(P^{(a)'}_{\text{succ}}(i, k) \times D^{(a)}(k) \right) + \\ &\sum_{i=0}^{m} \sum_{b=0}^{B(j)_{max}} \left(P^{(d)'}_{\text{succ}}(i, b) \times D^{(d)}_{\text{succ}}(i, b) \right) \end{aligned} \tag{3.35}$$

3.3.1 Analytical Model for Standard Deviation of Delay

Let X be a random variable and $E[X]$ denotes the expected value of X. Then the standard deviation (SD) of X is the quantity

$$SD = \sqrt{E[X^2] - E[X]^2}$$

Using equation (4.31), equation (4.36) and equation (3.35), the standard deviation (SD) of the delay to successfully transmit a data frame can be calculated. Therefore

$$SD = \sqrt{\sum_{k=0}^{2}\sum_{i=0}^{2} P_{\text{succ}}^{(a)'}(i,k) \times \left(D^{(a)}(k)\right)^2 + \sum_{i=0}^{m}\sum_{b=0}^{B(j)_{max}} P_{\text{succ}}^{(d)'}(i,b) \times \left(D_{\text{succ}}^{(d)}(i,b)\right)^2 - \left(\overline{D}\right)^2} \tag{3.36}$$

3.4 Analytical Model for Power Consumption

Let $\overline{PW}$ be the average power consumed by a station. The station may be in one of the radio modes viz. transmit, receive, idle and sleep. It is assumed that the same power is consumed in transmit and receive mode. Let PW_{idle}, $\text{PW}_{\text{tx/rx}}$ and PW_{sleep} be the power consumed per unit time in idle, transmit/ receive and sleep modes respectively. $\overline{PW}$ can be written as

$$\overline{PW} = \frac{P}{T}. \tag{3.37}$$

Here P is the total energy consumed in an interval of size T time units which includes transmit/receive time, idle time and sleep time. P can be represented as

$$P = \overline{T_{\text{tx/rx}}} \times PW_{\text{tx/rx}} + \overline{T_{\text{idle}}} \times PW_{\text{idle}} + \overline{T_{\text{sleep}}} \times PW_{\text{sleep}}$$

Similarly T can be represented as

$$T = \overline{T_{\text{tx/rx}}} + \overline{T_{\text{idle}}} + \overline{T_{\text{sleep}}} \tag{3.38}$$

Here $\overline{T_{\text{tx/rx}}}$ is the expected time spent in transmit mode by a station (a station is in transmit mode when it transmits ATIM frame or data frame). $\overline{T_{\text{idle}}}$ and $\overline{T_{\text{sleep}}}$ are the expected time spent in idle and sleep mode respectively.

$\overline{T_{\text{tx/rx}}}$ has following components:

- Average time spent to transmit an ATIM frame in the ATIM window ($\overline{T^{a}_{\text{tx/rx}}}$), and
- Average time spent to transmit data frame in the data window ($\overline{T^{d}_{\text{tx/rx}}}$), after successful transmission of ATIM frame in the ATIM window.

Therefore,

$$\begin{aligned}\overline{T_{\text{tx/rx}}} &= \overline{T^{a}_{\text{tx/rx}}} + \overline{T^{d}_{\text{tx/rx}}} \\ &= \sum_{k=0}^{2}\sum_{i=0}^{2} P^{(a)}_{\text{succ}}(i,k) \times (i \times T_{\text{acol}} + T_{\text{asucc}}) + \\ & \quad \sum_{i=0}^{m} P^{(d)}_{\text{succ}}(i) \times (i \times T_c + T_s)\end{aligned} \tag{3.39}$$

The values of $P^{(a)}_{\text{succ}}(i,k)$ and $P^{(d)}_{\text{succ}}(i)$ are presented in equations (4.33) and equation (4.38) respectively[5]. The value of T_c and T_S are presented in equation (3.21). T_{asucc} and T_{acol} are the average time for which the channel is sensed busy because of a successful transmission and a collision of an ATIM frame respectively. Therefore,

$$\begin{aligned}T_{\text{asucc}} &= \text{ATIM}_{\text{framesize}} + \delta + \text{SIFS} + \text{ATIMACK}_{\text{TO}} + \delta. \\ T_{\text{acol}} &= \text{ATIM}_{\text{framesize}} + \text{SIFS} + \text{ATIMACK}_{\text{TO}}.\end{aligned}$$

Here $\text{ATIM}_{\text{framesize}}$ is the size of an ATIM frame and $\text{ATIMACK}_{\text{TO}}$ is the timeout interval for ATIMACK .

A station can be in idle mode either in the ATIM window or in the data window. So $\overline{T_{\text{idle}}}$ can be calculated as,

$$\overline{T_{\text{idle}}} = \overline{T^{a}_{\text{idle}}} + \overline{T^{d}_{\text{idle}}} \tag{3.40}$$

In the i^{th} backoff stage the station chooses a uniformly distributed backoff counter W, where $W \in \{0, W_i - 1\}$. The station waits for W time units before sending a frame and decrements the backoff counter after each slot time (assuming that each slot is an empty slot). The station transmits the frame when the backoff counter

[5] I did not use the conditional probability because this represents that the backoff process of an ATIM/data frame transmission ends at a particular backoff stage, given that the ATIM frame is transmitted successfully.

reaches zero. When a station chooses W as the backoff counter in the i^{th} backoff stage then the idle period in that stage is W. As W is uniformly distributed in $\{0, W_i - 1\}$ the station spends $\frac{W_i}{2}$ slots in idle mode in the i^{th} backoff stage on an average. After a successful transmission of ATIM frame the station will remain in the idle mode for the rest of the ATIM window. Therefore, $\overline{T^a_{\text{idle}}}$ can be written as

$$\overline{T^a_{\text{idle}}} = \sum_{k=0}^{2}\sum_{i=0}^{2} P^{(a)}_{\text{succ}}(i,k) \times \left(\frac{W_i}{2} \times \sigma\right) + \sum_{k=0}^{2}\sum_{i=0}^{2} P^{(a)}_{\text{succ}}(i,k) \times (\text{ATIM}_{\text{size}} - (i \times T_{\text{acol}} + T_{\text{asucc}})) \tag{3.41}$$

Here $\text{ATIM}_{\text{size}}$ is the time duration of an ATIM window and σ is the duration of one slot time.

For the data window, the idle time can be calculated as,

$$\overline{T^d_{\text{idle}}} = \sum_{i=0}^{2} P^{(d)}_{\text{succ}}(i) \times \left(\frac{W_i}{2} \times \sigma\right) \tag{3.42}$$

According to the PSM algorithm given in the IEEE 802.11 standard [2], a station can send multiple data frames in the data window. So after one successful data transmission the station may be in transmit mode to transmit the remaining data frames to the same receiver in that data window.

If a station fails to transmit the ATIM frame in the ATIM window then it goes to the sleep mode in the following data window. Then

$$\overline{T_{\text{sleep}}} = \sum_{k=0}^{2}\sum_{i=0}^{2} k \times \text{DATA}_{\text{size}} \times (1 - P^{(a)}_{succ}(i,k)) \tag{3.43}$$

Here, $\text{DATA}_{\text{size}}$ represents the time duration of the data window. From equation (3.37), equation (3.39), equation (3.40) and equation (3.43) the average power consumed by a station per unit time can be calculated.

3.5 Model Validation and Performance Evaluation

The proposed theoretical model is validated using simulation results obtained from the Qualnet 5.0.1 network simulator [44]. In the analytical model, it is assumed that channel is ideal and a all stations are within the communication range (single-hop network). To satisfy this condition, the simulation parameters are, transmit power 15dBm, receive sensitivity $-87dBm$, antenna gain 15dB, noise factor 10dB, communication range 100ft (approx), interference range 250ft (approx). For simulation in IBSS power save mode, the size of the ATIM window is taken to be 20ms. The beacon interval size is varied in simulation to study the behavior of the model. The throughput for the basic access in power save mode is calculated under the DSSS physical layer [2]. The power consumption in different states are taken from the data-sheet of CISCO Aironet 350 Series Client Adapters [109]. The system parameters used in the calculation are listed in Table 3.1. CW_{min} is the minimum contention window, CW^{a}_{max} and CW^{d}_{max} are maximum contention window for ATIM and data window respectively. The simulation is done for 10 different cases with randomly generated seed values and the average is plotted.

Table 3.1: Parameters used in the simulation

Parameter	**value**
Payload size	1024 bytes
ATIM	28 bytes + PHY header
ACK	14 bytes + PHY header
PHY header	192μs
MAC header	28 bytes
Basic rate	1Mbps
Data rate	2Mbps
Slot time	20μs
SIFS	10μs
DIFS	50μs
CW_{min}	32
CW^{a}_{max}	128
CW^{d}_{max}	1024
$PW_{\text{tx/rx}}$	2.25W (Watt)
PW_{idle}	1.35W (Watt)
PW_{sleep}	0.07W (Watt)

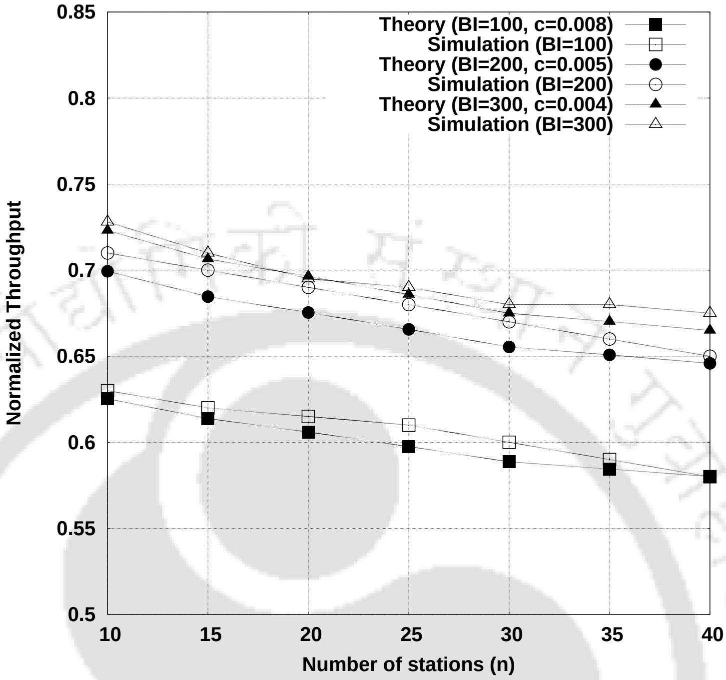

Figure 3.2: Overall Normalized Throughput (DATA window + ATIM Overhead)

3.5.1 Analysis of the Proportional Constant c

It has been discussed in Subsection 3.2.4 that for a fixed ATIM window size, the value of the parameter c depends on the size of the data window. Figure 3.2 shows the overall normalized throughput calculated for different c values using the theoretical analysis presented in this chapter. The figure also shows the overall normalized throughput obtained from simulations for different beacon interval sizes with ATIM window fixed at $20ms$. It can be observed from the figure that for a particular beacon interval size in simulation and different values for c are tried in order to find the value that provides the best matches between the theoretical results and the simulation results. For $c = 0.008$, the theoretical result matches with the simulation result for beacon interval size $100ms$. Similarly, for $c = 0.005$, the theoretical result matches with the simulation result for beacon interval size $200ms$, and for $c = 0.004$, the theoretical result matches with the simulation result for beacon interval size $300ms$.

Recall that q_d is the probability that the data window ends while transmitting a data frame. For a fixed number of stations and for a fixed ATIM window size, q_d should decrease with the increase of data window size. Furthermore, for a fixed

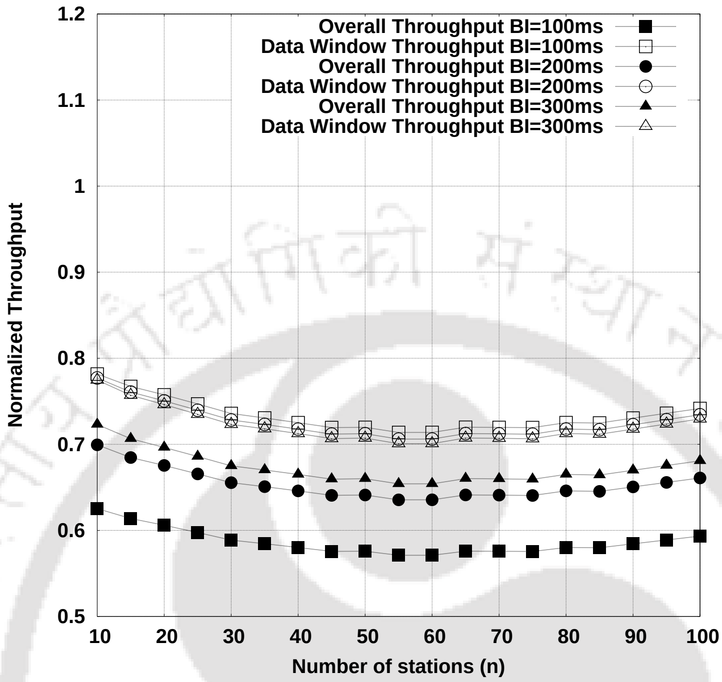

Figure 3.3: Normalized Throughput in the Data Window vs Overall Throughput (According to Theory)

ATIM window size, the number of nodes that compete in the data window for data frame transmission, i.e., $\lceil n \times P_{as} \rceil$, is independent of data window size. So the value of c should decrease with the increase of data window size. This is also reflected in Figure 3.2. For a fixed ATIM window size of $20ms$, the values of c are 0.008, 0.005 and 0.004 for beacon interval sizes $100ms$, $200ms$ and $300ms$, respectively. This is consistent with equation (3.19).

Unless stated otherwise, the value of c is taken to be 0.005 for the rest of the analysis in this chapter. This c value is equivalent to ATIM window size of $20ms$ and data window size of $180ms$.

3.5.2 Saturation Throughput

Figure 3.3 shows the normalized data window throughput and overall throughput[6] for different beacon interval sizes, calculated using different c values as stated in the previous subsection. The ATIM window size is kept fixed at $20ms$. Two important

[6]The results obtained from the analytical model (not simulation)

observations can be drawn out from this figure. First, the overall throughput is less than the data window throughput because of ATIM overhead. For BI=200ms and ATIM window size=20ms, there is an ATIM overhead that reduces overall throughput by 10%. The second observation is that the data window throughput is almost the same for different beacon interval sizes. If the ATIM window size is fixed, the number of stations competing for channel access in the data window, given by $\lceil n \times P_{as} \rceil$, is almost constant, and so the data window throughput remain close to each other for all the beacon interval sizes. However, as the beacon interval size increases, the overall throughput tends to increase. With the increase of beacon interval size, the ATIM overhead decreases (since the ATIM window size is kept fixed). The overall throughput reduction for BI=100ms is 20%, whereas with BI=300ms, the throughput reduction due to ATIM overhead is 6.67%.

3.5.3 Delay Analysis

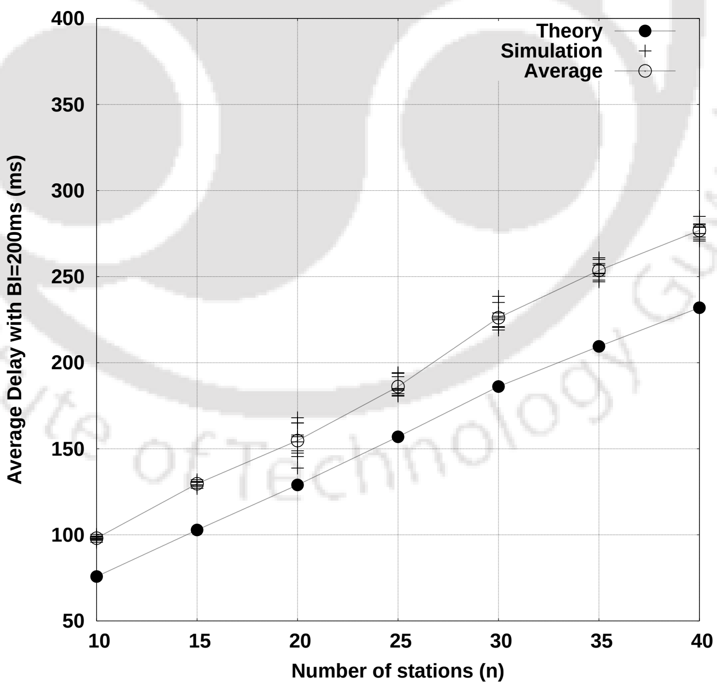

Figure 3.4: Average Delay for Data Frame Transmission

Figure 3.4 presents average delay against different network sizes. The figure shows that the theoretical and simulation results are close. Figure 3.5 shows the

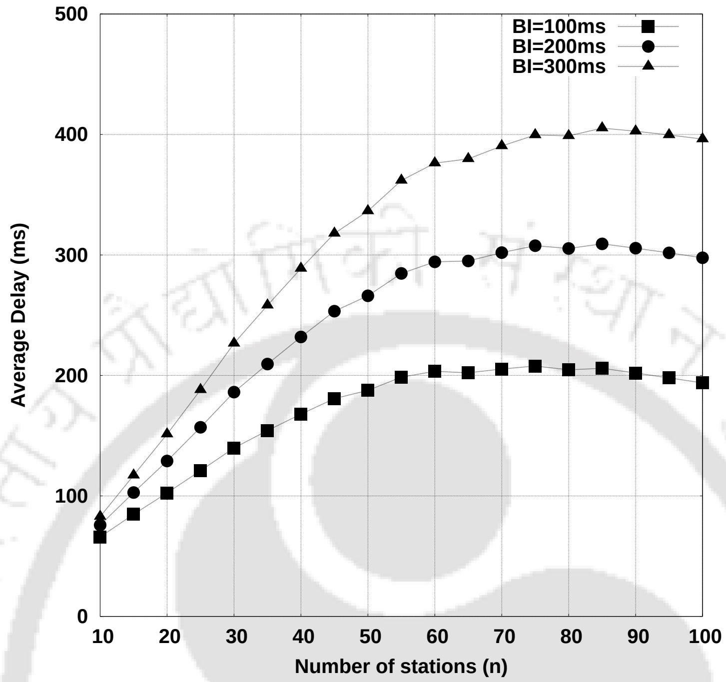

Figure 3.5: Average Delay for Different Beacon Intervals (According to Theory)

impact of the beacon interval size on the average delay for different network sizes. As the beacon interval size increases, the average delay increases. The MAC delay is the time period between the instant that the frame is at the head of the queue to the instant when it is successfully transmitted[7]. The waiting time is due to the backoff mechanism and size of the beacon interval.

The stations that fail to transmit an ATIM frame successfully in the ATIM window have to wait for the rest of the beacon interval to get the next chance to transmit another ATIM frame in the next ATIM interval. This increases the average waiting time to get a chance to transmit data frames. As the beacon interval size increases, the average waiting time also increases. For this reason, the average delay increases with the increase of beacon interval size.

Figure 3.6 presents the standard deviation of the delay to successfully transmit a data frame as calculated from the analytical model for delay analysis. From Figure 3.6, it can be observed that the standard deviation is very high. For example for a network size of 30 and BI=200ms, the average delay is 186ms and standard

[7]There is no consideration of queuing delay.

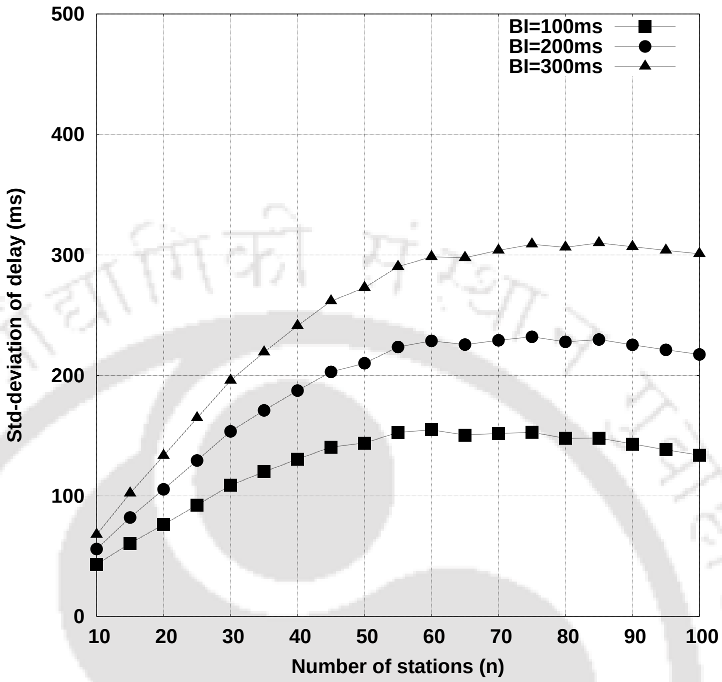

Figure 3.6: Standard Deviation for Delay (According to Theory)

deviation is 153ms. To verify the above result, the simulation result in Figure 3.7 presents the observed delay to transmit a data frame for (BI=200ms) with 30 wireless stations. From Figure 3.7, it can be concluded that there is unfairness in data frame transmission and the delay distribution is not a uniform distribution. This results in a very high value for the standard deviation of the delay.

It is worth mentioning that the average delay and jitter (i.e., standard deviation of delay) increase with increase in duration of the beacon interval. For example, with BI=300ms and network size of 30 nodes, delay and jitter are 226.6ms and 200ms respectively. Obviously, they will be significantly high for larger BI duration, which is impractical from an application point-of-view. Considering this, the simulation and theoretical results up to BI=300ms are reported in this chapter.

3.5.4 Power Consumption

Figure 3.8 shows the average power consumption with respect to the number of stations in IEEE 802.11 IBSS power save mode. The result obtained from the analytical model for power consumption in Section 3.4 has been verified through

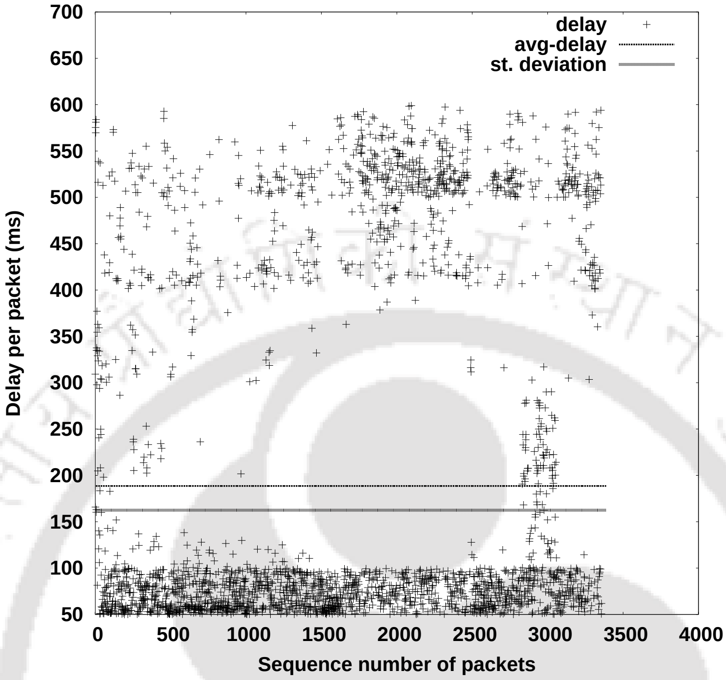

Figure 3.7: Delay per Packet (ms), Simulation Results for Number of Wireless Stations = 30

simulation. Figure 3.9 gives a comparison of the average power consumption for packet transmission for different beacon intervals as obtained from the analytical model. It can be seen from the figure that as the size of beacon interval increases, average power consumption decreases. This is because, with a large beacon interval the stations remain in sleep mode for large amounts of time, and thus save power.

Furthermore, the figure shows that the average power consumption for a network of size 10 is more than the average power consumption for a network of size 20. This is because for small network sizes, contention is less, and so most of the stations are in transmit or receive state, leading to higher power consumption. However, as the network size increases, contention becomes high, and on average $n - n'$ stations go to sleep mode in the data window. This reduces the average power consumption.

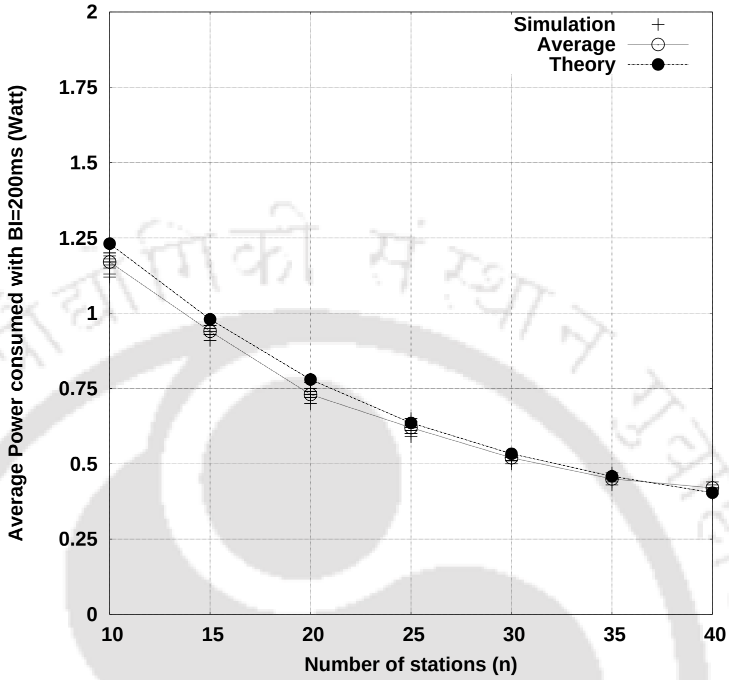

Figure 3.8: Average power consumed for data frame transmission

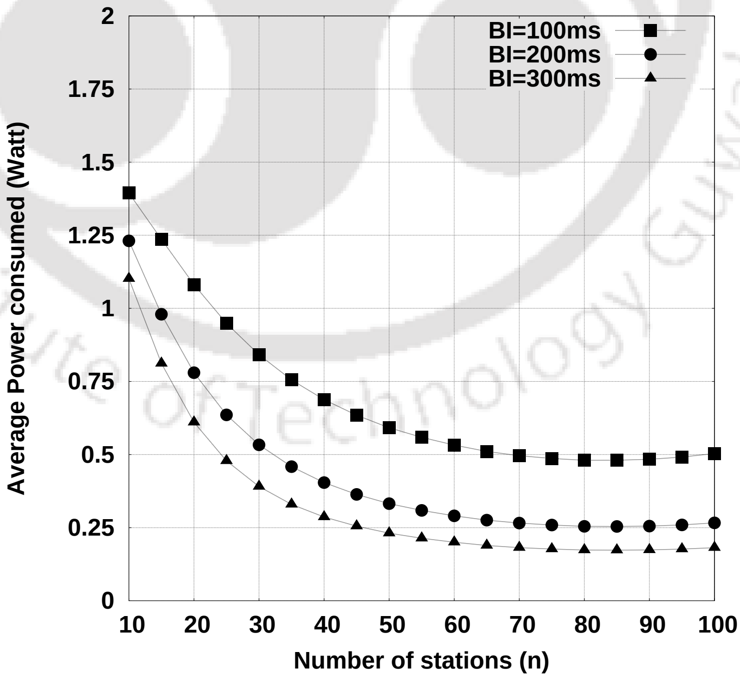

Figure 3.9: Average power consumed for different beacon intervals

3.5.5 Comparison between DCF with and without Power Save Mode

A comparison between IEEE 802.11 DCF with Power Save Mode (PSM) and without Power Save Mode (WPSM) is given in Table 3.2. The performance for IEEE 802.11 DCF without PSM is obtained from the models given in [53], [90], [105] which are generalizations of Bianchi's model [1]. For WPSM, the values do not depend on BI. However, for the ease of presentation these values are given in the table.

It can be noted from the table that the overall throughput obtained for the proposed model for power save mode (PSM) is marginally less than the one obtained for WPSM, whereas in PSM the data window throughput is very high. The loss in overall throughput is because of the ATIM window overhead. On the other hand, the contention is less in the data window as some of the nodes that fail to transmit ATIM frame successfully in the ATIM window, go to sleep mode in the data window. This makes the data window throughput marginally higher. However, the ATIM transmission imposes an extra control message overhead that reduces overall channel throughput.

From Table 3.2, it can also be observed that the average delay is more in case of PSM compared to WPSM. The delay is more because of the extra time introduced due to ATIM frame transmission. If a station fails to transmit an ATIM frame in the ATIM window, then it has to wait for rest of the beacon interval to get the next chance to transmit another ATIM frame. That is why, as the size of the beacon interval increases (with a fixed ATIM window size), the average delay increases, as shown in Table 3.2 and Figure 3.5.

Table 3.2 shows that the average power consumption is less in PSM compared to WPSM. For PSM, the average power consumption is calculated for different beacon interval, with fixed ATIM window size of $20ms$. From the table, it can be observed, that with BI=$100ms$ at PSM, average power consumption is 60.71% of average power consumption at WPSM. With BI=$300ms$ at PSM, average power consumption is 27.14% of average power consumption at WPSM.

The above analysis shows that in IEEE 802.11 PSM, power saving comes at the cost of network throughput and delay. The network throughput for IEEE 802.11 DCF in PSM is marginally less than the throughput obtained in IEEE 802.11

Table 3.2: Comparison between WPSM and PSM with 30 Nodes

Data Window Throughput		
	WPSM	**PSM**
BI=100ms	0.712	0.73583
BI=200ms	0.712	0.72822
BI=300ms	0.712	0.72315
Overall Normalized Throughput		
	WPSM	**PSM**
BI=100ms	0.712	0.58867
BI=200ms	0.712	0.65540
BI=300ms	0.712	0.67494
Average Delay		
	WPSM	**PSM**
BI=100ms	140 ms	139.845 ms
BI=200ms	140 ms	186.165 ms
BI=300ms	140 ms	226.612 ms
Average Power Consumption		
	WPSM	**PSM**
BI=100ms	1.4 Watt	0.84139 Watt
BI=200ms	1.4 Watt	0.53326 Watt
BI=300ms	1.4 Watt	0.39072 Watt

DCF. For a fixed ATIM window size with saturation condition, as the size of the BI increases, the network throughput increases and power consumption decreases. However, the network delay increases considerably. Therefore, it can be said that by tuning the size of beacon interval based on the number of active stations in the data window, the network lifetime can be increased while keeping the network performance at par without power save mode.

3.6 Summary

In this chapter a discrete time Markov chain model is presented for the transmission of ATIM and data frames in IEEE 802.11 DCF power save mode. The model is used to calculate the probability of successful packet transmissions, the data window throughput as well as the overall network throughput. The model for throughput calculation is validated using the simulation results. The analytical model shows the impact of the network size over the overall network throughput at saturated traffic conditions. Further, the model is used to calculate the average MAC delay and power consumption. An analysis is done between IEEE 802.11 DCF with PSM and without PSM for different performance metrics, with respect to the beacon interval size. This analysis indicates a trade-off among throughput, delay and power consumptions at different beacon interval sizes.

The saturation analysis gives a performance overview of the IEEE 802.11 DCF PSM algorithm at one extreme traffic condition, when every node have data to send, and all node contends with each other to gain access to the channel. As all the nodes participate in contention at the ATIM window when the network is saturated, this analysis gives a clear idea of the protocol behavior with the increase in the network size. However, as discussed in Chapter 1 and Chapter 2, the performance of a communication protocol may vary significantly in the unsaturated network conditions, when different stations transmit traffic at different data rates. The next chapter provides a discrete time Markov model of the IEEE 802.11 DCF in PSM for unsaturated traffic condition.

Chapter 4

Modeling IEEE 802.11 IBSS Power Save Mode for Unsaturated Traffic

As discussed in the previous chapter, the saturation modeling gives an overview of the protocol performance at extreme traffic conditions. However, these models do not reflect the actual performance of public wireless networks due to their restriction to saturated traffic conditions. Traffic in public wireless LANs follow self-similar characteristics [68] where data frames from users come in a burst. Therefore, only the stations that have frames to transmit contend for the channel access. Thus *network unsaturation* is common for practical wireless channel access scenarios. This chapter analyzes network throughput, delay and power consumption for IEEE 802.11 DCF PSM considering an unsaturated network. The proposed analysis is based on a Markov chain model, which is an extension of the model presented in Chapter 3 for the ATIM window along with the data window.

This chapter contains the following sections. Section 4.1 presents a discrete time Markov model of the IEEE 802.11 DCF in PSM for unsaturated traffic and the analytical model for network throughput is presented. Section 4.2 presents an analytical model for average MAC delay and Section 4.3 presents an analytical model for power consumption. In Section 4.4, the proposed theoretical model is validated through simulation results. This section also gives a detailed analysis of the performance of IEEE 802.11 DCF in PSM for IBSS for unsaturated traffic. Section 4.5 concludes the chapter.

4.1 Modeling and Analysis of IEEE 802.11 PSM for Unsaturated Traffic

In this section we will present the assumptions on the network architecture for the modeling of a discrete time Markov model of the IEEE 802.11 DCF in PSM for unsaturated traffic condition. The given model is analyzed and calculated the network throughput.

4.1.1 Network Model Assumption

The following assumptions are made to model and analyze the performance of IEEE 802.11 PSM having unsaturated traffic.

1. The network consists of n stations with basic access mechanism enabled for data frame communication.

2. Every station generates data traffic (per time slot) with probability α $(0 < \alpha \leq 1)$. The value of α is derived from the frame generation rate at the application layer.

3. The retry limit for an ATIM frame is *three within one beacon interval.* [25]

4. A station can try at most *three beacon intervals* for successful transmission of one ATIM frame [25].

5. One data window is sufficient to successfully transmit a data frame, after transmitting an ATIM frame successfully in the ATIM window [110].

6. There is no higher layer buffering of data frames. When a data frame is generated, it is forwarded to the MAC layer. This point is assumed to isolate the higher layer effects over the MAC layer modeling.

4.1.2 Modeling and Analysis

Assume that the random process $s(t)$ counts the number of attempts (retries) to transmit an ATIM or a data frame within one BI. The second random process $b(t)$ is used to represent the backoff counter. Assume that the backoff counter is decremented by one at the beginning of each slot. The value of $b(t)$ depends on the backoff stage $s(t)$. In the i^{th} backoff stage ($s(t) = i$), the backoff counter value is within $[0, W_i - 1]$ where $W_i = 2^i W_0$ and W_0 is the initial CW ($CW_{\min}$). From the assumption (point 3) in Subsection 4.1.1, the value of the backoff stage $s(t)$ is within $\{0, 1, 2\}$. The third random process $a(t)$ represents the backoff layer. From the assumption in Subsection 4.1.1 (point 4), the value of the backoff layer $a(t)$ is within $\{0, 1, 2\}$ at time t. The number of active stations that participate in the channel access during the data window are effected based on the probability of the successful transmission of an ATIM frame. This phenomenon is modeled using two discrete time Markov models, one for the ATIM frame transmission and another for the data frame transmission, as shown in Figure 4.1, where the state G is a dummy state to connect between the two models. Another state I is introduced in the combined model to represent the unsaturated traffic conditions at a station. State I considers the following two situations;

- After a successful frame transmission, there is another frame in the buffer, with probability α,

- The buffer is empty, and the station waits for the next frame at state I with probability $1 - \alpha$.

Let p_a denote the conditional collision probability in the ATIM window and p_d the same for the data window. The quantities q_a and q_d are the probabilities that the ATIM and data window end, when a station is attempting to transmit an ATIM frame and a data frame respectively. The one-step non zero transition probabilities of the Markov chain in Figure 4.1 are presented in equation (4.1), where a single prime ($'$) represents the transition probabilities in the ATIM window and a double prime ($''$) represents transition probabilities in the data window. These transition probabilities are summarized as follows;

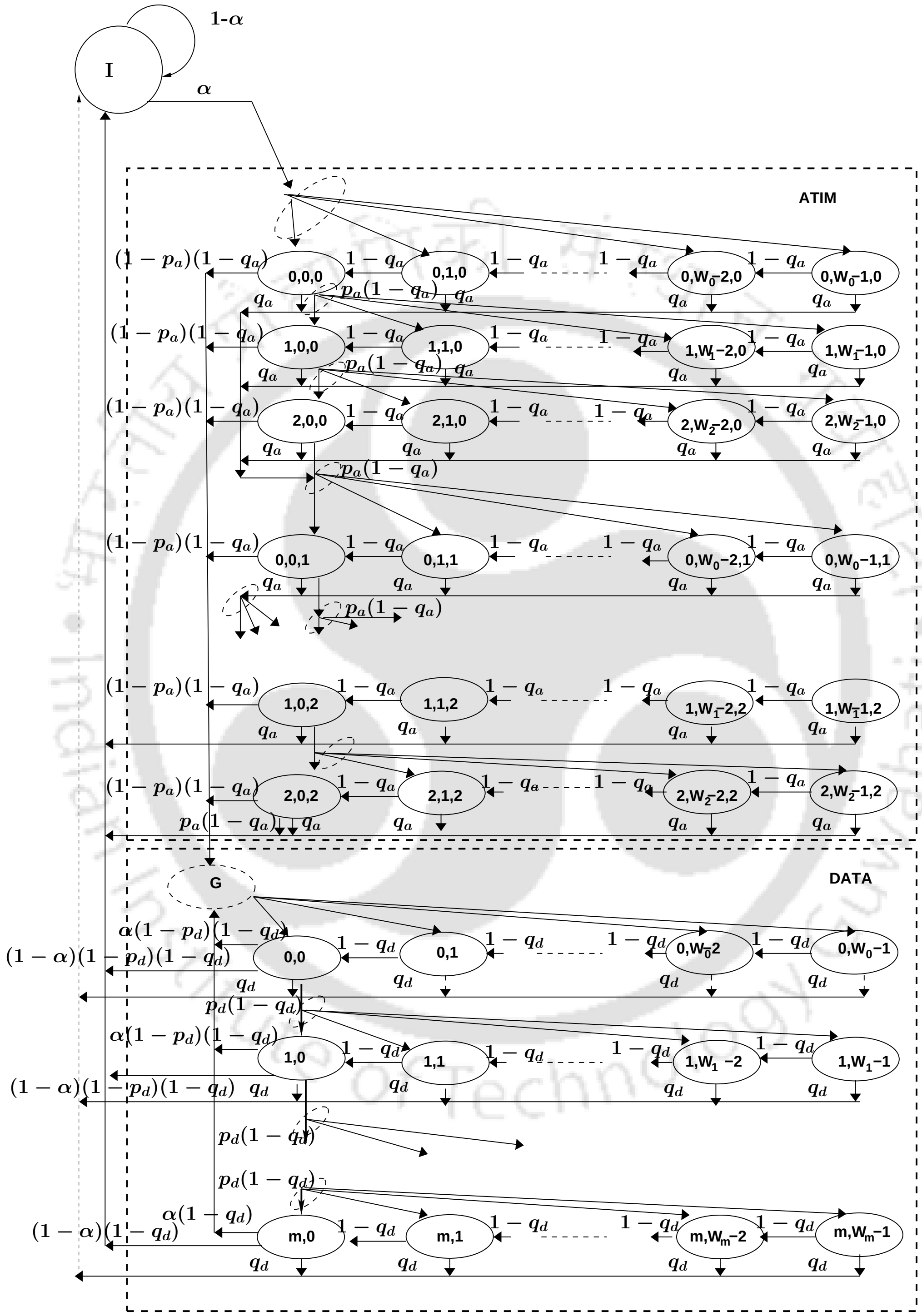

Figure 4.1: Markov model for IEEE 802.11 IBSS PSM with unsaturated traffic

$$
\begin{cases}
(1) & P\{I|I\} = 1-\alpha & \\
(2) & P\{(0,j,0)^{'}|I\} = \frac{\alpha}{W_0}, & j \in [0, W_0-1]; \\
(3) & P\{(i,j,k)^{'}|(i,j+1,k)^{'}\} = 1-q_a, & i \in [0,2], j \in [0, W_i-1], k \in [0,2]; \\
(4) & P\{(0,j,k+1)^{'}|(i,j',k)^{'}\} = \frac{q_a}{W_0}, & i \in [0,2], j \in [0, W_0-1], k \in [0,1], j' \in [0, W_i-1]; \\
(5) & P\{I|(i,j,2)^{'}\} = q_a, & i \in [0,2], j \in [0, W_i-1]; \\
(6) & P\{I|(2,0,2)^{'}\} = p_a \times (1-q_a), & \\
(7) & P\{(0,j,k+1)^{'}|(2,0,k)^{'}\} = \frac{p_a \times (1-q_a)}{W_0}, & j \in [0, W_0-1], k \in [0,1]; \\
(8) & P\{(i+1,j,k)^{'}|(i,0,k)^{'}\} = \frac{p_a \times (1-q_a)}{W_i}, & i \in [0,1], j \in [0, W_i-1], k \in [0,2]; \\
(9) & P\{(i,j)^{''}|(i,j+1)^{''}\} = 1-q_d, & i \in [0,m], j \in [0, W_i-1]; \\
(10) & P\{I|(i,j)^{''}\} = q_d, & i \in [0,m], j \in [0, W_i-1]; \\
(11) & P\{(0,j)^{''}|(i,0)^{''}\} = \frac{\alpha(1-p_d)(1-q_d)}{W_0}, & i \in [0,m], j \in [0, W_0-1]; \\
(12) & P\{I|(i,0)^{''}\} = (1-\alpha)(1-p_d)(1-q_d), & i \in [0,m]; \\
(13) & P\{(i+1,j)^{''}|(i,0)^{''}\} = \frac{p_d \times (1-q_d)}{W_i}, & i \in [0,m], j \in [0, W_i-1]; \\
(14) & P\{(0,j)^{''}|(m,0)^{''}\} = \frac{\alpha(1-q_d)}{W_0}, & j \in [0, W_0-1]; \\
(15) & P\{I|(m,0)^{''}\} = (1-\alpha)(1-q_d), &
\end{cases}
\tag{4.1}
$$

$$
b^{'}_{i,j,k} = \begin{cases}
\frac{\alpha}{W_0} b_I, & i=0, j=W_0-1, k=0; \\
\frac{\alpha}{W_0} b_I \times \sum_{l=0}^{W_0-(j+1)} (1-q_a)^l, & i=0, j \in [0, W_0-2], k=0; \\
M, & i=0, j=W_0-1, k \in [1,2]
\end{cases}
\tag{4.2}
$$

$$
b^{''}_{i,j} = \begin{cases}
N, & i=0, j=W_0-1; \\
N \times \sum_{l=0}^{W_0-(j+1)} (1-q_d)^l, & i=0, j \in [0, W_0-2]
\end{cases}
\tag{4.3}
$$

1. The first equation indicates the probability that the station has no frame in the buffer to transmit, $(1-\alpha)$.

2. The second equation shows probability α that a station has a data frame in the buffer to transmit.

3. The third equation indicates that within the ATIM window, the ATIM frame back-off counter decrements with probability $(1-q_a)$.

4. The fourth equation indicates that at any back-off stage and for any back-off counter value, if the ATIM window ends, the system tries to retransmit the ATIM frame with back-off stage 0 in the next ATIM window.

5. The fifth equation presents an unsuccessful transmission of an ATIM frame, when the ATIM window ends at the third BI (indicated by $a(t) = 2$).

6. The sixth equation indicates that at the third ATIM window and at the last retry limit, the ATIM frame is discarded, and check the buffer for new data frame.

7. The seventh equation indicates that there is a collision at the last attempt within an ATIM window.

8. The eighth equation indicates that the station increases the back-off stage, and selects the back-off counter uniformly after an unsuccessful transmission of an ATIM frame.

9. The ninth equation indicates that within the data window, the data frame back-off counter decrements with probability $(1 - q_d)$.

10. The tenth equation indicates the end of data window has been reached at any back-off stage or any back-off counter, resulting in dropping of the data frame.

11. The eleventh equation models the successful transmission of a data frame, and the station has a next frame in the buffer to transmit with probability α.

12. The twelfth equation indicates that after a successful transmission of data frame the station goes to the idle state with probability $(1 - \alpha)$.

13. The thirteenth equation indicates that the station increases the back-off stage and chooses the back-off counter uniformly after an unsuccessful transmission of a data frame within the data window.

14. The fourteenth equation models that there may be a successful or an unsuccessful transmission of a data frame at the last back-off stage, and the station has another frame in the buffer to be send.

15. The fifteenth equation indicates that at the last back-off stage, it may be a successful or an unsuccessful transmission of a data frame and the buffer is empty. So the station goes to the idle state.

4.1.3 Model Analysis

Let $b^{'}_{i,j,k}$ and $b^{''}_{i,j}$ be the stationary distributions of the Markov chain for the ATIM and the data windows, respectively. Here,

$$\begin{aligned} b^{'}_{i,j,k} &= \lim_{t\to\infty} P\{s(t)=i, b(t)=j, a(t)=k\}, \\ &\quad i\in[0,2], j\in[0,W_i-1], k\in[0,2] \end{aligned}$$

and

$$b^{''}_{i,j} = \lim_{t\to\infty} P\{s(t)=i, b(t)=j\}, i\in[0,m], j\in[0,W_i-1]$$

To obtain a closed-form solutions for the Markov chain presented in Fig. 4.1, iterative equation (4.4) and equation (4.5) are used:

$$b^{'}_{i,0,k} = \tfrac{p_a(1-q_a)}{W_i} \textstyle\sum_{l=0}^{W_i-1}(1-q_a)^l b^{'}_{i-1,0,k} \quad 0<i\leq 2 \tag{4.4}$$

$$b^{''}_{i,0} = \tfrac{p_d(1-q_d)}{W_i} \textstyle\sum_{l=0}^{W_i-1}(1-q_d)^l b^{''}_{i-1,0} \quad 0<i\leq m \tag{4.5}$$

The stationary probabilities for each state of the Markov models presented in Fig. 4.1 are derived in equation (4.6) and equation (4.7).

$$b^{'}_{i,j,k} = \begin{cases} \frac{\alpha}{W_0} b_I, & i=0, j=W_0-1, k=0; \\ M_1, & i=0, j\in[0,W_0-2], k=0; \\ M_2, & i=0, j=W_0-1, k\in[1,2] \end{cases} \tag{4.6}$$

$$b^{''}_{i,j} = \begin{cases} N_1, & i=0, j=W_0-1; \\ N_\times N_2, & i=0, j\in[0,W_0-2] \end{cases} \tag{4.7}$$

The values of M_1, M_2, N_1 and N_2 are

$$M_1 = \frac{\alpha}{W_0} b_I \times \sum_{l=0}^{W_0-(j+1)} (1-q_a)^l$$

$$M_2 = \frac{1}{W_0}\left[p_a(1-q_a)b^{'}_{2,0,k-1} + q_a \sum_{i=0}^{2}\sum_{j=0}^{W_i-1} b^{'}_{i,j,k-1}\right]$$

$$N_1 = \frac{P_{as}}{W_0}\left[1+\alpha\Big((1-p_d)(1-q_d) \sum_{i=0}^{m-1} b^{''}_{i,0} + (1-q_d)b^{''}_{m,0}\Big)\right]$$

$$N_2 = \sum_{l=0}^{W_0-(j+1)} (1-q_d)^l$$

Let P_{as} be the probability of successful transmission of an ATIM frame. The derivation of P_{as} will be discussed later in the section. The stationary probability in the state I is,

$$\begin{aligned} b_I &= b^{'}_{2,0,2} + q_a \textstyle\sum_{j=1}^{W_2-1} b^{'}_{2,j,2} + \sum_{i=0}^{1}\sum_{j=0}^{W_i-1} b^{'}_{i,j,2} \\ &\quad +(1-\alpha)b_I \\ &= \tfrac{1}{\alpha}\left[(1-q_a)b^{'}_{2,0,2} + q_a \textstyle\sum_{i=0}^{2}\sum_{j=0}^{W_i-1} b^{'}_{i,j,2}\right] \end{aligned} \quad (4.8)$$

A normalization condition is required to compute the value of $b^{'}_{0,0,0}$. It can be noted that the normalization condition for the ATIM frame transmission is independent of the data frame model. The normalization equation is represented as,

$$1 = \textstyle\sum_{k=0}^{2}\sum_{i=0}^{m}\sum_{j=0}^{W_i-1} b^{'}_{i,j,k} + b_I \quad (4.9)$$

From equation (4.4), equation (4.5), equation (4.8) and equation (4.9) the value of $b^{'}_{0,0,0}$ is written as,

$$b^{'}_{0,0,0} = \tfrac{1}{X(1+Y+Y^2L)} \quad (4.10)$$

where,

$$
\begin{aligned}
X =& \sum_{i=0}^{2} \sum_{j=0}^{W_i-1} A \\
Y =& \frac{1}{W_0} \left[C + q_a X\right] \sum_{l=0}^{W_0-1} (1-q_a)^l \\
L =& X + \frac{1}{\alpha}\left((1-q_a)B + q_a X\right) \\
C =& B \times p_a(1-q_a) \\
B =& \frac{((1-q_a)p_a)^2}{q_a} \prod_{j-1}^{2} \left(\frac{1-(1-q_a)^{W_j}}{W_j}\right) \\
A =& \left(\frac{(1-q_a)p_a{}^2}{q_a}\right) \times \frac{1}{W_i} \times \left(1-(1-q_a)^{(W_i-j)}\right) \times \\
& \prod_{j=1}^{i-1} \left(\frac{1-(1-q)^{W_j}}{W_j}\right)
\end{aligned}
$$

Let τ_a be the probability that a station transmits an ATIM frame in a randomly chosen slot. Hence,

$$
\tau_a = \sum_{k=0}^{2} \sum_{i=0}^{2} b'_{i,0,k} \tag{4.11}
$$

The value of τ_a is obtained by solving equation (4.4), equation (4.6) and equation (4.10). The relation between p_a and τ_a is,

$$
p_a = 1 - (1-\tau_a)^{n'-1}. \tag{4.12}
$$

where n' is the number of active stations participating in the contention at the ATIM window. As ATIM frames are generated instantaneously at the MAC layer in the ATIM window, if a station has a data frame to transmit, n' can be approximated as, $n' = \lceil n\alpha \rceil$ where n is the total number of stations in a network. The values of τ_a and p_a are solved numerically using fixed point iteration. P_{as} is the probability of successful transmission of an ATIM frame. P_{as} is calculated as follows:

$$
P_{as} = \frac{n'\tau_a(1-\tau_a)^{(n'-1)}}{1-(1-\tau_a)^{n'}}. \tag{4.13}
$$

Similarly, we find out the probability of success for a data frame transmission after successfully transmitting an ATIM frame. Let τ_d be the probability that a station transmits a data frame in a randomly chosen slot in the data window. So the value of τ_d depends on the value of τ_a. The τ_d is represented as:

$$\tau_d = \sum_{i=0}^{m} b''_{i,0} \tag{4.14}$$

From equation (4.5), the value of $b''_{i,0}$ is expressed in terms of $b''_{0,0}$ as follows:

$$\sum_{i=0}^{m} b''_{i,0} = \sum_{i=0}^{m} F_i b''_{0,0} \tag{4.15}$$

where,

$$F_i = \left(\frac{p_d(1-q_d)}{q_d}\right)^i \prod_{j=1}^{i} \left(\frac{\{1-(1-q_d)^{W_j}\}}{W^j}\right)$$

Similarly, from equation (4.7), $b''_{0,0} = \frac{1}{R}$ where,

$$R = \frac{W_0 q_d}{\alpha(1-(1-q_d)^{W_0})} - \{(1-p_d)(1-q_d)\sum_{i=0}^{m-1} F_i + (1-q_d)F_m\} \tag{4.16}$$

The relation between p_d and τ_d is

$$p_d = 1-(1-\tau_d)^{(n''-1)}. \tag{4.17}$$

where n'' is the number of active stations participating in the contention at the data window. For simplicity, we assume that a sender can send multiple data frames only to a single receiver in a data window. Further according to assumption (6) as stated earlier, there is no higher layer buffering of data packets, and therefore n'' can be approximated as, $n'' = \lceil (n\alpha \times P_{as}) \rceil$ where n is the total number of stations in the network. Let P_{tr} be the probability that there is at least one data frame transmission in the considered slot. Let P_{ds} be the joint probability that a data frame is transmitted successfully after the successful transmission of an ATIM frame. The values of P_{tr} and P_{ds} are given by,

$$P_{tr} = 1-(1-\tau_d)^{n''} \tag{4.18}$$

$$P_{ds} = \frac{n''\tau_d(1-\tau_d)^{n''-1}}{P_{tr}}. \tag{4.19}$$

4.1.4 Estimation of probability α, $\mathrm{q_a}$, $\mathrm{q_d}$

Let λ be the frame arrival rate of a source that follows a Poisson distribution with parameter λ. Assuming the data traffic is generated according to a Poisson distribution[1], the probability α that a station has a data frame to send, is computed as;

$$\alpha = 1 - \mathrm{e}^{-\lambda \mathrm{E}[\mathrm{s_d}]} \tag{4.20}$$

Here $\mathrm{s_d}$ is the duration of a slot and $\mathrm{E}[\mathrm{s_d}]$ is the expected slot time in the data window. $\mathrm{E}[\mathrm{s_d}]$ is governed by the Markov model discussed earlier, and can be computed as follows. The average length of a slot in a data window is computed by considering three mutually exclusive and exhaustive cases. $(1-P_{tr})$ is the probability that a slot is empty, $P_{ds}P_{tr}$ is the probability of successful transmission of data, and $(1-P_{ds})P_{tr}$ is the collision probability for a data frame. Therefore,

$$\mathrm{E}[\mathrm{s_d}] = (1-P_{tr})\sigma + P_{ds}P_{tr}T_s + (1-P_{ds})P_{tr}T_c \tag{4.21}$$

Here T_s and T_c are the average time the channel is sensed busy because of a successful transmission or a collision in the data window, respectively and σ is the empty slot time. T_s and T_c are calculated as follows,

$$\begin{aligned} T_s &= \mathrm{DIFS} + H + E[P] + 2\delta + \mathrm{SIFS} + \mathrm{ACK} \\ T_c &= \mathrm{DIFS} + H + E[P] + \mathrm{SIFS} + \mathrm{ACK_{TO}} \end{aligned} \tag{4.22}$$

According to the assumption in Subsection 4.1.1 (point 1), every station accesses the channel using the basic access mechanism. Here DIFS and SIFS denote DCF inter-frame space time (in slots), and short interface space time (SIFS) respectively. ACK is the acknowledgement duration in slots. It has been assumed that all packets have the same size, so $E[P] = P$ is the average payload. The ACK timeout ($\mathrm{ACK_{TO}}$) is included in $\mathrm{T_c}$ according to the standard [2] specification, and a station

[1]The Poisson assumption of traffic generation is only a representative case used in this thesis for modeling the effect of the traffic arrival on the MAC layer performance. Any other traffic distributions can be used depending on the specific scenarios, and the probability α, q_a and q_d can be calculated according to that distribution, following a similar procedure. The objective of this analysis is to analyze the MAC layer protocol performance with different data generation rates, and therefore, the assumption for a specific distribution of data generation suffices for the purpose.

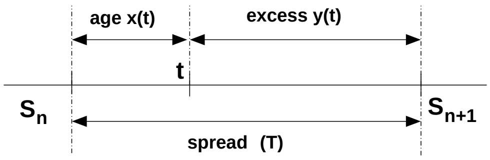

Figure 4.2: The age and excess time of a renewal process [4]

waits for an EIFS time when the channel is sensed busy because of collision. Let $\text{EIFS} = \text{SIFS} + \text{ACK}_{\text{TO}} + \text{DIFS}$. $H = \text{PHY}_{\text{hdr}} + \text{MAC}_{\text{hdr}}$ be the packet header, and δ the propagation delay.

Let $Z(t)$ be a renewal process. The *spread* T, of a renewal process, is defined as the time interval after which the renewal occurs. The *age* of a renewal process, $x(t)$, is defined as the time interval since the last renewal. The *excess* (or residual time) of a renewal process, $y(t)$, is the time to the next renewal after t [4]. The spread, age and excess of a renewal process are shown in Fig. 4.2. Let S_i denote the time of the i^{th} renewal. It can be noted that $x(t)$ and $y(t)$ are independently distributed. As the traffic arrival is assumed to be Poisson, the time from t to the next renewal is exponentially distributed, and independent of all previously occurred renewals [111]. Therefore, $\{Z(t), t \geq 0, t \leq T\}$ be a Poisson process with rate λ. Hence,

$$P\{y(t) \leq s | t \leq T\} = 1 - e^{-\lambda s/T} \quad \forall s \geq 0 \tag{4.23}$$

where s is a generic slot time (either in the ATIM or in the data window).

As discussed earlier, q_a and q_d denote the probability of the end of ATIM window and the data window respectively. The size of the ATIM window and data window is assumed to be fixed as mentioned in Section 4.1.1. The probabilities q_a and q_d depends on λ which is the packet arrival rate. That means they depend on network load. It is obvious that if the number of packets increases, the probability of q_a and q_d should increase. Let $Z_a(t)$ denote the number of transmissions within an ATIM window, and $Z_d(t)$ the number of transmissions within a data window. Then $Z_a(t)$ and $Z_d(t)$ are two counting processes with inter-arrival time s_a and s_d respectively, where s_a and s_d are the duration of an ATIM slot and a data slot, respectively. The counting process of each state eventually reaches its steady state. Let $e_a(t)$ be the excess time in an ATIM window. In the ATIM window, every station waits for SIFS interval before accessing the channel. Then for an ATIM window, the probability of the ATIM window end is expressed as the probability that excess time is less than the SIFS interval plus the mean slot duration in the ATIM window. Let T_{ATIM} be the size of the ATIM window. From equation (4.23),

$$\begin{aligned} q_a &= P(e_a(t) \leq \mathrm{SIFS} + E[s_a] | t \leq T_{\mathrm{ATIM}}) \\ &= 1 - e^{-\lambda\, (\mathrm{SIFS}+E[s_a])/T_{\mathrm{ATIM}}} \end{aligned} \quad (4.24)$$

where $E[s_a]$ is the expected slot duration in an ATIM window, calculated in a similar way as of equation (4.21) using the success and failure probabilities of the ATIM window, the average channel busy time and the average collision time for an ATIM frame transmission. Similarly let $e_d(t)$ be the excess time for the data window. In a data window, every station waits for the DIFS interval for accessing the channel. Then for a data window, the probability that the data window ends can be expressed as the probability that the excess time is less than the DIFS interval plus the mean slot duration in the data window. Let T_{DATA} be the size of the DATA window. So,

$$\begin{aligned} q_d &= P(e_d(t) \leq \mathrm{DIFS} + E[s_d] | t \leq T_{\mathrm{DATA}}) \\ &= 1 - e^{-\lambda\, (\mathrm{DIFS}+E[s_d])/T_{\mathrm{DATA}}} \end{aligned} \quad (4.25)$$

With the value of α, q_a and q_d in hand, the data window throughput and overall normalized throughput is derived, as presented in the next section.

4.1.5 Throughput Analysis

Let S_{DATA} denote the normalized system throughput in the data window for a network with unsaturated traffic.

$$S_{\mathrm{DATA}} = \frac{E[\text{payload information transmitted in a slot}]}{E[\text{duration of a slot}]}$$

Let, $E[p]$ be the average frame payload size (in terms of time unit, e.g., μs). Therefore,

$$S_{\mathrm{DATA}} = \frac{P_{ds} P_{tr} E[p]}{E[s]} \quad (4.26)$$

S_{DATA} provides the channel throughput at the data window only and the value of $E[s]$ is presented in equation (4.21). The overall channel throughput has the

ATIM overhead included with the data window throughput. The overall normalized throughput, S, is calculated as,

$$S = S_{\text{DATA}} \times \frac{\text{Data Window size}}{\text{Duration of BI}} \tag{4.27}$$

4.2 Analytical model for Average MAC Delay

The MAC layer channel access delay is an important parameter to analyze the performance of IEEE 802.11 IBSS. The average MAC delay is defined as the time between the arrival of a frame at the interface queue and the time it is delivered successfully. Let $\overline{D}$ denote the average MAC delay. Then $\overline{D}$ can be written as:

$$\overline{D} = \overline{D^{(a)}_{\text{succ}}} + \overline{D^{(d)}_{\text{succ}}} \tag{4.28}$$

where $\overline{D^{(a)}_{\text{succ}}}$ denotes the average delay in transmitting an ATIM frame successfully, and $\overline{D^{(d)}_{\text{succ}}}$ denotes the average delay in transmitting the corresponding data frame successfully.

Let $D^{(a)}_{\text{succ}}(k)$ be the delay experienced up to the k^{th} ATIM window to transmit an ATIM frame successfully. $\text{ATIM}_{\text{size}}$ represents the fixed ATIM window size. Therefore,

$$D^{(a)}_{\text{succ}}(k) = k \times \text{BI} + \text{ATIM}_{\text{size}} \tag{4.29}$$

Assume that $D^{(d)}_{\text{succ}}(i, b)$ is the delay to transmit a data frame successfully in the i^{th} backoff stage of the data window. The sum of the backoff values up to stage i is b. Assume that b is the average value of the CW. Since $(W_i - 1)$ is the maximum CW size at the i^{th} backoff stage, the average value of b is $\frac{Wi}{2}$. The value of $D^{(d)}_{\text{succ}}(i, b)$ is given by:

$$D^{(d)}_{\text{succ}}(i, b) = b \times T_{\text{avg}} + i \times T_c + T_s \tag{4.30}$$

Here T_s and T_c are the average time the channel is sensed busy because of a successful transmission or a collision, respectively, of the data frame in the data window.

Now, the average delay in transmitting an ATIM frame successfully is equal to the total delay upto the k^{th} ATIM window, given that the ATIM success occurs at the k^{th} ATIM window. Let the probability $P^{(a)'}_{\text{succ}}(i, k)$ be the conditional probability that the backoff process of an ATIM frame transmission ends at the i^{th} stage of the

k^{th} ATIM window, given that the ATIM frame is transmitted successfully. Then, the value of $\overline{D^{(a)}_{\text{succ}}}$ is calculated as:

$$\overline{D^{(a)}_{\text{succ}}} = \sum_{k=0}^{2}\sum_{i=0}^{2} P^{(a)\prime}_{\text{succ}}(i,k) \times D^{(a)}_{\text{succ}}(k) \tag{4.31}$$

Assume that $P^{(a)}_{\text{succ}}(i,k)$ is the probability that an ATIM frame is transmitted successfully at the i^{th} backoff stage of the k^{th} ATIM window, and $P^{(a)}_{\text{drop}}$ denotes the probability that an ATIM frame is dropped because of the retry limit being exceeded in the last ATIM window. $P^{(a)\prime}_{\text{succ}}(i,k)$ is calculated as follows:

$$P^{(a)\prime}_{\text{succ}}(i,k) = \frac{P^{(a)}_{\text{succ}}(i,k)}{1 - P^{(a)}_{\text{drop}}} \tag{4.32}$$

$P^{(a)}_{\text{succ}}(i,k)$ is given by:

$$P^{(a)}_{\text{succ}}(i,k) = X^i_k(1-p_a)(1-q_a) \tag{4.33}$$

where X^i_k is the probability that a station is unsuccessful in transmitting an ATIM frame till the $(i-1)^{th}$ backoff stage of the k^{th} ATIM window, and is given by:

$$X^i_k = \begin{cases} L^i, & k=0; \\ L^{(3+i)} + q_a \times L^i, & k=1; \\ L^{(3*2+i)} + 2\times q_a \times L^{(3+i)} + q_a^2 \times L^i, & k=2; \end{cases} \tag{4.34}$$

Here, $L = p_a(1-q_a)$. Consequently, $P^{(a)}_{\text{drop}}$ is calculated as:

$$P^{(a)}_{\text{drop}} = 1 - \sum_{k=0}^{2}\sum_{i=0}^{2} P^{(a)}_{\text{succ}}(i,k) \tag{4.35}$$

From equation (4.32) and equation (4.29), the average delay in transmitting an ATIM frame successfully ($\overline{D^{(a)}_{\text{succ}}}$) is calculated using equation (4.31).

Similarly, the value of the average delay in transmitting a data frame successfully within the data window ($\overline{D^{(d)}_{\text{succ}}}$) is calculated in a similar way. Let, $B(i)$ is the total backoff value up to i^{th} backoff stage, and $B(i)_{\max}$ is the summation of maximum contention window sizes up to the backoff stage i $\left(\sum_{j=0}^{i}(CW_j - 1)\right)$.

Then, $\overline{D^{(d)}_{\text{succ}}}$ is calculated as:

$$\overline{D^{(d)}_{\text{succ}}} = \sum_{i=0}^{m} \sum_{b=0}^{B(i)_{\max}} P^{(d)'}_{\text{succ}}(i,b) \times D^{(d)}_{\text{succ}}(i,b). \tag{4.36}$$

The value $P^{(d)'}_{\text{succ}}(i,b)$ denotes the conditional probability that the backoff process of a data frame transmission ends at the i^{th} stage of the data window, with total backoff value b up to the i^{th} backoff stage, given that the data frame is transmitted successfully. $P^{(d)'}_{\text{succ}}(i,b)$ is given by:

$$P^{(d)'}_{\text{succ}}(i,b) = \frac{P^{(d)}_{\text{succ}}(i,b)}{1 - P^{(d)}_{\text{drop}}} \tag{4.37}$$

Here $P^{(d)}_{\text{drop}}$ is the probability of dropping a data frame that exceeds the retry limit in the data window. $P^{(d)}_{\text{succ}}(i,b)$ is the probability that a data frame is transmitted at the i^{th} stage and b is the the sum of backoff values up to the i^{th} backoff stage. Therefore,

$$P^{d}_{\text{succ}}(i,b) = P^{(d)}_{\text{succ}}(i) Pr(B(i) = b)$$

$$P^{(d)}_{\text{drop}} = 1 - (1-p_d)(1-q_d) \sum_{i=0}^{m} \{p_d(1-q_d)\}^i$$

where m is the maximum retry limit to transmit a data frame in the data window. Assume, $P^{(d)}_{\text{succ}}(i)$ is the probability of transmitting a data frame successfully in the i^{th} backoff stage of the data window, and $p_d(1-q_d)$ is the probability that there is a collision within the data window. Therefore,

$$P^{(d)}_{\text{succ}}(i) = \{p_d(1-q_d)\}^i \{(1-p_d)(1-q_d)\} \tag{4.38}$$

Let $P^{(d)}_{\text{idle}}$, $P^{(d)}_{\text{col}}$ and $P^{(d)}_{\text{succ}}$ are the probability that a randomly chosen slot in the data window is idle, leads to a collision and results in successful transmission, respectively. Then,

$$\begin{aligned} P^{(d)}_{\text{idle}} &= (1-\tau_d) \\ P^{(d)}_{\text{succ}} &= n^{''}\tau_d(1-\tau_d)^{(n^{''}-1)} \\ P^{(d)}_{\text{col}} &= 1-(1-\tau_d) - n^{''}\tau_d(1-\tau_d)^{(n^{''}-1)} \end{aligned}$$

Here τ_d, calculated according to equation (4.14), represents the probability that a station transmits a data frame in the randomly chosen slot in the data window and n'' is the number of station in active mode in the data window. Then,

$$T_{avg} = P^{(d)}_{\text{idle}}\sigma + P^{(d)}_{\text{succ}}T_s + P^{(d)}_{\text{col}}T_c \tag{4.39}$$

where σ is the empty slot time. From equation (4.37) and equation (4.30) the value of $\overline{D^{(d)}_{succ}}$ is calculated. Therefore, the average delay, calculated using equation (4.28), and is given by:

$$\overline{D} = \sum_{k=0}^{2}\sum_{i=0}^{2}\left(P^{(a)'}_{\text{succ}}(i,k) \times D^{(a)}(k)\right) + \sum_{i=0}^{m}\sum_{b=0}^{B(j)_{max}}\left(P^{(d)'}_{\text{succ}}(i,b) \times D^{(d)}_{\text{succ}}(i,b)\right)$$

4.3 Analytical Model for Average Power Consumption

In IEEE 802.11 IBSS PSM, the stations save critical battery power by going to the sleep mode whenever they do not have data to transmit as well as receive. Let PW_{tx}, PW_{rx}, PW_{idle} and PW_{sleep} denote the power consumed for data frame transmission, data frame reception, channel sensing and station in sleep mode respectively. $E[T_{\text{tx}}]$, $E[T_{\text{rx}}]$, $E[T_{\text{idle}}]$ and $E[T_{\text{sleep}}]$ are the expected time spent in transmit mode, receive mode, idle mode and sleep mode for per data frame transmission, respectively. The power consumed at a station can be classified into the following cases:

- **Transmit Power:** If a station is a transmitter then the expected energy consumption in successful data frame transmission ($\overline{\xi_{tx}}$) is given by:

$$\overline{\xi_{tx}} = E[T_{\text{tx}}] \times PW_{tx} \tag{4.40}$$

Here,

$$E[T_{\text{tx}}] = \sum_{k=0}^{2}\sum_{i=0}^{2}\left(P_{\text{succ}}^{(a)}(i,k) \times (i \times T_{\text{acol}} + T_{\text{asucc}})\right) + \sum_{i=0}^{m}\left(P_{\text{succ}}^{(d)}(i) \times (i \times T_c + T_s)\right) \tag{4.41}$$

Let $P_{\text{succ}}^{(a)}(i,k)$ be the probability that an ATIM frame is transmitted successfully at the i^{th} backoff stage of the k^{th} ATIM window. Similarly, let $P_{\text{succ}}^{(d)}(i)$ denote the probability of transmitting a data frame successfully in the i^{th} backoff stage of the data window. The values of $P_{\text{succ}}^{(a)}(i,k)$ and $P_{\text{succ}}^{(d)}(i)$ are presented in equations (4.33) and equation (4.38) respectively.

T_{asucc} and T_{acol} are the average time for which the channel is sensed busy because of a successful transmission and a collision of an ATIM frame respectively. Therefore,

$$T_{\text{asucc}} = \text{ATIM}_{\text{framesize}} + \delta + \text{SIFS} + \text{ATIMACK}_{\text{TO}} + \delta$$
$$T_{\text{acol}} = \text{ATIM}_{\text{framesize}} + \text{SIFS} + \text{ATIMACK}_{\text{TO}}$$

Here $\text{ATIM}_{\text{framesize}}$ is the size of an ATIM frame in number of slots and $\text{ATIMACK}_{\text{TO}}$ is the timeout interval for ATIM acknowledgement. The value of T_c and T_s are presented in equation (4.22).

- **Receive Power:** If a station does not have any data frame to transmit or has not successfully transmitted an ATIM frame, then there are two possibilities - if the station has successfully received an ATIM frame, then it acts as the receiver, otherwise it goes into sleep mode. Let the expected energy consumption in successful frame reception be $\overline{\xi_{rx}}$. Then,

$$\overline{\xi_{rx}} = E[T_{\text{rx}}] \times PW_{rx} \tag{4.42}$$

It can be noted that the duration of reception of a packet is equivalent to the duration of successful transmission of a packet (in case of collision, the receiver remains in the idle state). Therefore,

$$E[T_{\text{rx}}] = \sum_{k=0}^{2}\sum_{i=0}^{2}\left(P_{\text{succ}}^{(a)}(i,k) \times T_{\text{asucc}}\right) + \sum_{i=0}^{m}\left(P_{\text{succ}}^{(d)}(i) \times T_s\right) \tag{4.43}$$

Idle Power: A station remains in idle mode for two reasons;

1. The station is in the back-off stage, and so it remains idle for the back-off period.
2. The station has transmitted an ATIM frame successfully, and so it has to remain awake in the data window according to the standard. However it does not have sufficient data in its interface buffer, and it has transmitted all frames queued in its interface buffer before the data window ends. So, it has to remain in idle state either for the rest of the data window, or for the time before the next data arrives in its interface buffer, whichever is earlier.

Let the expected energy consumption in idle state be $\overline{\xi_{idle}}$. Then,

$$\overline{\xi_{\text{idle}}} = E[T_{\text{idle}}] \times PW_{idle} \tag{4.44}$$

Here,

$$E[T_{\text{idle}}] = E[T_{\text{idle}}^{a}] + E[T_{\text{idle}}^{d}] \tag{4.45}$$

According to the standard, if a station transmits one ATIM frame successfully, then it cannot send another ATIM frame in the same ATIM window. However, the station has to remain awake for the entire ATIM window. Thus the idle time in ATIM window has two components - expected idle time during back-off period at the ATIM window ($E[T_{\text{back-off}}^{a}]$) and expected idle time after transmitting one ATIM frame successfully, for the rest of the ATIM interval ($E[T_{\text{idle}_{\text{nd}}}^{a}]$). Thus,

$$E[T_{\text{idle}}^{a}] = E[T_{\text{back-off}}^{a}] + E[T_{\text{idle}_{\text{nd}}}^{a}] \tag{4.46}$$

$E[T^a_{\text{back-off}}]$ is given by:

$$E[T^a_{\text{back-off}}] = \sum_{k=0}^{2}\sum_{i=0}^{2}\left(P^{(a)}_{\text{succ}}(i,k) \times \left(\frac{W_i}{2} \times \sigma\right)\right)$$

In an IBSS, the transceiver of an station that is in awake state, remains idle only when it neither transmits nor receives a packet. Further, the transceiver remains in the receive state for all the ongoing communication in the network, may it be intended for that station or an overheard communication. In the ATIM window, on average $n\alpha$ stations transmit ATIM frames, and therefore every station receives $n\alpha$ ATIM frames on average. Consequently, $E[T^a_{\text{idle}_{\text{nd}}}]$ is computed as,

$$E[T^a_{\text{idle}_{\text{nd}}}] = \sum_{k=0}^{2}\sum_{i=0}^{2}\Big(P^{(a)}_{\text{succ}}(i,k) \times \\ (\mathrm{T}_{\text{ATIM}} - (i \times T_{\text{acol}} + (1+n\alpha)T_{\text{asucc}}))\Big)$$

In the above equation, the quality $(1 + n\alpha)T_{\text{asucc}}$ denotes time for one ATIM frame transmission and $n\alpha$ ATIM frames reception, the transmission and the reception times being equal as discussed earlier. As mentioned earlier, T_{ATIM} represents the time duration of an ATIM window and σ is the duration of one slot time.

For the data window, the idle time is calculated as,

$$E[T^d_{\text{idle}}] = E[T^d_{\text{back-off}}] + E[T^d_{\text{idle}_{\text{nd}}}] \tag{4.47}$$

where $E[T^d_{\text{back-off}}]$ denotes the expected idle time in back-off period in data window and $E[T^d_{\text{idle}_{\text{nd}}}]$ denotes the expected idle time. $E[T^d_{\text{back-off}}]$ is given by:

$$E[T^d_{\text{back-off}}] = \sum_{i=0}^{m} P^{(d)}_{\text{succ}}(i) \times \left(\frac{W_i}{2} \times \sigma\right)$$

In the DATA window, a station remains in the idle state after a successful transmission if all of these conditions hold;

(i) The station is not a transmitter: This indicates that the station does not have any data transmit. The probability for this is $(1 - \alpha)$.

(ii) The station is not a receiver: In the DATA window, a station is not a receiver, when neither of the $n \times P_{\text{as}}$ stations, that are in the awake state, have a data frame to transmit. The probability of this event is $(1-\alpha)^{n \times P_{\text{as}}}$.

Therefore, after a successful data transmission, the average idle time is computed as

$$E[T^{d}_{\text{idle}_{\text{nd}}}] = (1-\alpha)^{(1+n \times P_{\text{as}})} \times T_{\text{DATA}}$$

Here T_{DATA} represents the time duration of an data window. It can be noted that in the DATA window, there are $n\alpha P_{\text{as}}$ number of data frame reception with respect to a single data frame transmission, as $n\alpha P_{\text{as}}$ numbers of nodes are in the awake state. The quality $(1 + n\alpha P_{\text{as}})T_{\text{asucc}}$ denotes time for one DATA frame transmission and $n\alpha P_{\text{as}}$ DATA frame reception, the transmission and the reception times being equal as discussed earlier.

- **Sleep Power:** A station can go into the sleep mode if it neither transmits nor receives an ATIM frame in the ATIM window. Let $\overline{\xi_{sleep}}$ be the expected energy consumption during sleep mode. Then,

$$\overline{\xi_{sleep}} = E[T_{\text{sleep}}] \times PW_{sleep} \tag{4.48}$$

where $E[T_{\text{sleep}}]$ is the expected time duration of the sleep mode, which is given by:

$$\begin{aligned} E[T_{\text{sleep}}] = \sum_{k=0}^{2} \left(1 - \sum_{i=0}^{2} P^{(a)}_{\text{succ}}(i,k)\right) \times k \\ \times \left(1 - \frac{P_{as}}{n'}\right) \times DATA_{size} \end{aligned} \tag{4.49}$$

Here P_{as} is the probability of successful transmission of ATIM frame.

Let $\overline{PW}$ be the average power consumed by a station. Therefore,

$$\overline{PW} = \frac{\overline{\xi_{\text{tx}}} + \overline{\xi_{\text{rx}}} + \overline{\xi_{\text{idle}}} + \overline{\xi_{\text{sleep}}}}{E[T_{\text{tx}}] + E[T_{\text{rx}}] + E[T_{\text{idle}}] + E[T_{\text{sleep}}]} \tag{4.50}$$

$\overline{PW}$ shows the average power consumption by all the stations in a network. However, it does not reflect the distribution of power consumption among the stations. To analyze the power distribution among the stations, the standard deviation of power consumption is required along with the average power consumption which is presented in the next subsection.

4.3.1 Standard Deviation of Power Consumption

The standard deviation is the square root of variance. Assume that V is the variance in power consumption. V_{tx}, V_{rx}, V_{idle}, V_{sleep} are variances of power consumption in transmit mode, receive mode, idle mode and sleep mode respectively. Then,

$$V = V_{\text{tx}} + V_{\text{rx}} + V_{\text{idle}} + V_{\text{sleep}} \tag{4.51}$$

The V_{tx}, V_{rx}, V_{idle}, and V_{sleep} are given by:

- The variance of power consumption in transmit mode (V_{tx}) is expressed as [2];

$$V_{\text{tx}} = \frac{\left(E[T_{\text{tx}}^2] \times PW_{tx} - \left(\overline{\xi_{tx}}\right)^2\right)}{(E[T_{\text{tx}}])^2} \tag{4.52}$$

  Here, T_{tx} represents the time spent in transmit mode. The value of $E[T_{\text{tx}}]$ and $E[T_{\text{tx}}^2]$ are calculated using an approach similar to equation (4.41). The quantity $\overline{\xi_{tx}}$ is the expected energy consumption in successful frame transmission.

- The variance of energy consumption in receive mode (V_{rx}) is given by:

$$V_{\text{rx}} = \frac{\left(E[T_{\text{rx}}^2] \times PW_{rx} - \left(\overline{\xi_{rx}}\right)^2\right)}{(E[T_{\text{rx}}])^2} \tag{4.53}$$

  Here, $E[T_{\text{rx}}]$ and $E[T_{\text{rx}}^2]$ are calculated using using an approach similar to equation (4.43). $\overline{\xi_{rx}}$ is the expected energy consumption in successful frame reception.

- The variance of energy consumption in idle mode (V_{idle}) is expressed as;

$$V_{\text{idle}} = \frac{\left(E[T_{\text{idle}}^2] \times PW_{\text{idle}} - \left(\overline{\xi_{\text{idle}}}\right)^2\right)}{(E[T_{\text{idle}}])^2} \tag{4.54}$$

[2] Let $Y = \frac{X}{T}$, X is a random variable and T is a constant. $Var(Y) = Var(\frac{X}{T}) = \frac{Var(X)}{T^2}$.

Here, $E[T_{\text{idle}}]$ and $E[T^2_{\text{idle}}]$ are calculated using using an approach similar to equation (4.45). The quantity $\overline{\xi_{rx}}$ is the expected energy consumption in idle state.

- The variance of energy consumption in sleep mode (V_{sleep}) is given by:

$$V_{\text{sleep}} = \frac{\left(E[T^2_{\text{sleep}}] \times PW_{\text{sleep}} - \left(\overline{\xi_{\text{sleep}}}\right)^2\right)}{(E[T_{\text{sleep}}])^2} \tag{4.55}$$

Here, $E[T_{\text{sleep}}]$ and $E[T^2_{\text{sleep}}]$ are calculated using using an approach similar to equation (4.49). The quantity $\overline{\xi_{rx}}$ is the expected energy consumption during sleep mode.

All the theoretical estimations presented till now have been validated using simulation results. The validation of the theoretical model along with the analysis of network performance in IEEE 802.11 IBSS PSM in terms of throughput, MAC delay and average power consumption are presented in the next section.

4.4 Model Validation and Performance Evaluation

The proposed analytical model has been validated using the network simulator Qualnet 5.0.1 [44]. The system parameters are listed in Table 4.1. CW_{min} is the minimum CW, CW^a_{max} and CW^d_{max} are maximum CW for the ATIM and the data window respectively. The power consumption in different states are taken from the data-sheet of CISCO Aironet 350 Series Client Adapters [109]. In the analytical model, it is assumed that channel is ideal and a all stations are within the communication range (single-hop network). To satisfy this condition, the simulation parameters are, transmit power $15dBm$, receive sensitivity $-87dBm$, antenna gain $15dB$, noise factor $10dB$, communication range $100ft$ (approx), interference range $250ft$ (approx). For simulation in IBSS power save mode, the size of the ATIM window is taken to be $20ms$. The beacon interval size is varied in simulation to study the behavior of the model. The simulation is executed for 10 different cases with randomly generated seed values, and the average values are plotted.

Table 4.1: Parameters used in the simulation

Parameter	**value**
Payload size	1024 bytes
ATIM	28 bytes + PHY header
ACK	14 bytes + PHY header
PHY header	$192\mu s$
MAC header	28 bytes
Basic rate	1Mbps
Data rate	2Mbps
Slot time	$20\mu s$
SIFS	$10\mu s$
DIFS	$50\mu s$
$CW_{\min}$	32
$CW^a_{\max}$	128
$CW^d_{\max}$	1024
$PW_{\text{tx/rx}}$	2.25W (Watt)
PW_{idle}	1.35W (Watt)
PW_{sleep}	0.07W (Watt)

Figure 4.3 presents the normalized throughput against different arrival rates having a fixed network with $n = 20$ and BI $= 200ms$ (with fixed ATIM window at 20 ms). The figure shows that there is a good agreement between the theoretical and the simulation results. For the unsaturation case, Figure 4.4 and Figure 4.5 (results obtained from analytical model) show how the normalized throughput depends on network size and the size of the BI. The observations from Figure 4.3, Figure 4.4 and Figure 4.5 are summarized as follows.

- In the unsaturation case, the throughput increases at an exponential rate where data arrival rate varies from 1 frames/second to 10 frames/second. After 10 frames/seconds, the network becomes saturated. For frame arrival rate 10 frames/second to 40 frames/second, throughput decreases in a linear fashion. During this period, the network throughput decreases because of the increasing contention among stations in the saturated network.

- The network throughput stabilizes when the data arrival rate is more than 40

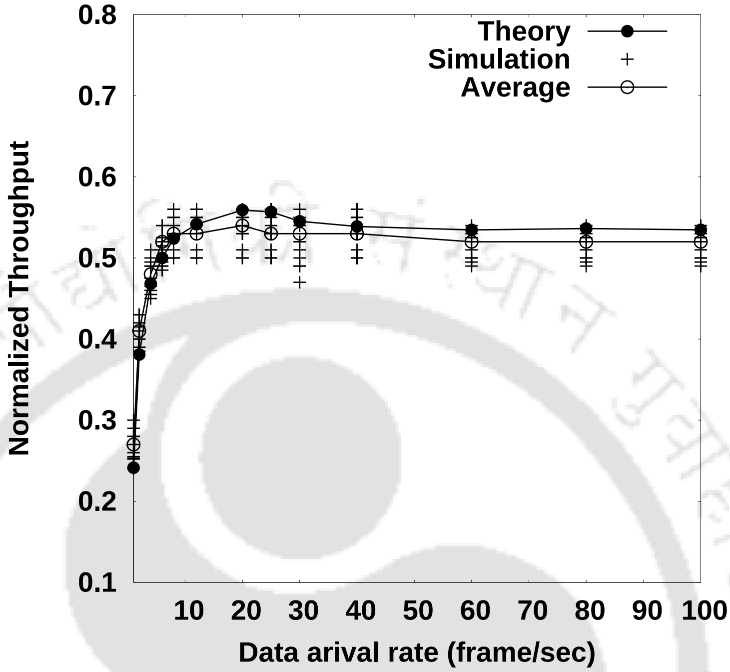

Figure 4.3: Overall Throughput (S) for $n = 20$

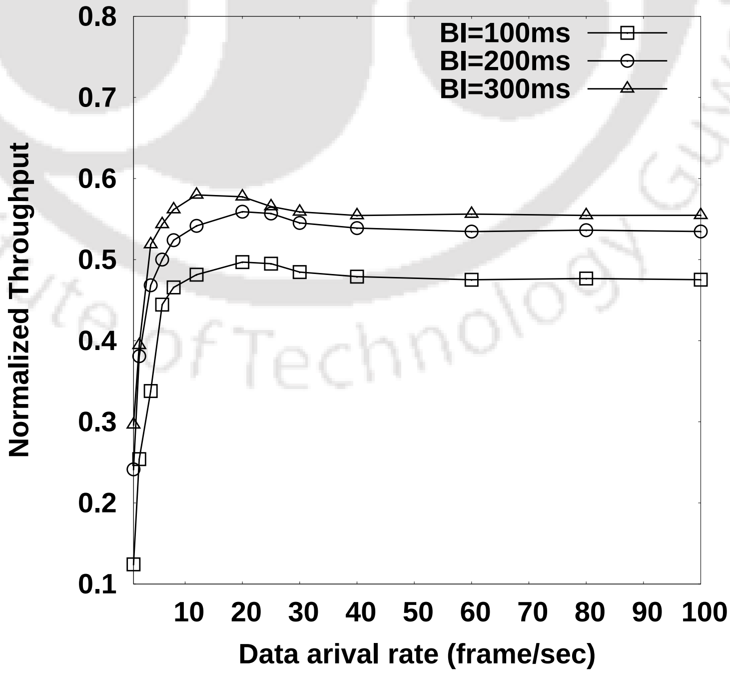

Figure 4.4: Overall Throughput (S) for $n = 20$

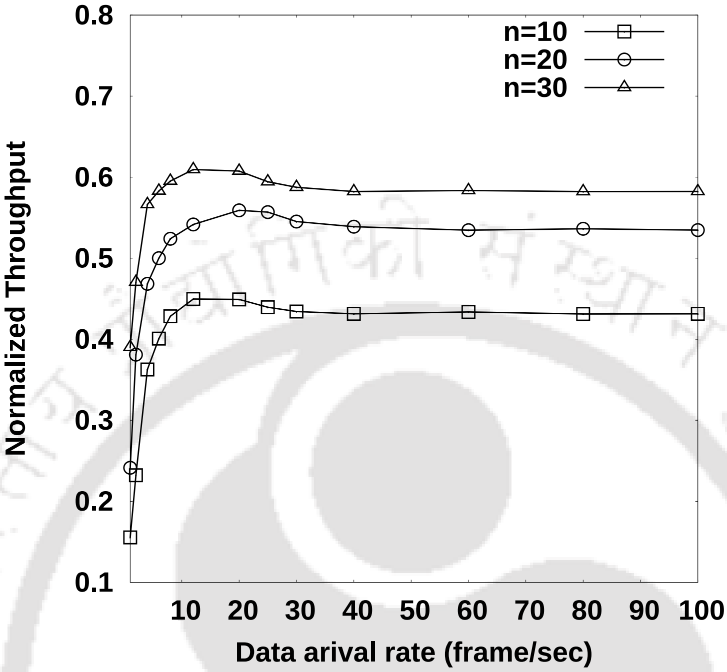

Figure 4.5: Overall Throughput (S) for $BI = 200ms$

frames/second. Normalized throughput remains almost fixed when the data arrival rate is beyond 40 frames/second (network size $n = 20$).

- It can be seen from Figure 4.4 that as the size of the BI increases with a fixed ATIM window at 20 ms, the normalized network throughput increases. The reason behind this is that, for a fixed ATIM window size at 20 ms, the size of the data window increases with the increase of the BI. Thus the ATIM overhead becomes low which increases the overall network throughput.

- Figure 4.5 shows the effect of the number of stations over the network throughput for fixed BI size at 200 ms. The ATIM window size is also fixed at 20 ms. As the number of stations increases, the overall throughput also increases.

Figure 4.6 shows the average MAC delay against the frame arrival rate. Though both the curves follow similar trends, there is a slight gap between the theoretical and the simulation results (simulation result is approximately 30% more than the theoretical result). The difference between the theoretical result and simulation

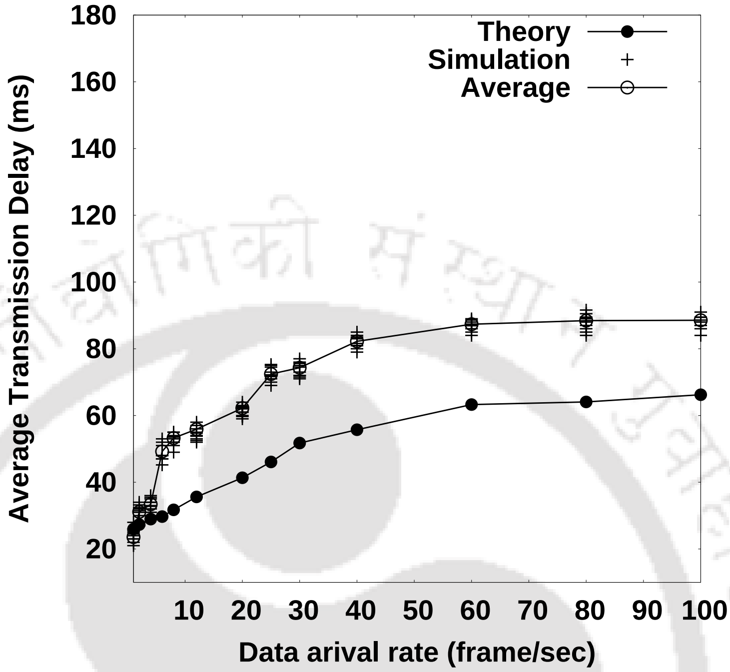

Figure 4.6: $\overline{D}$ for $n = 20$

result is because of the practical wireless channel properties such as: channel quality, fading, queue size and distance between stations, which significantly affects the MAC layer channel access delay, although less impact over the throughput and the power. It can be noted that these properties vary with time and are difficult to incorporate in the present model.

However, the present model gives a good approximation of the MAC delay that can be used effectively for comparison purpose, as described next. All the results presented in Figure 4.7 and Figure 4.8 are obtained from the analytical model. Figure 4.7 presents the impact of the BI size (with fixed ATIM window at 20 ms) on the average MAC delay for different frame arrival rate. Average MAC delay is the sum of two components - the channel access time, plus the average waiting time in a BI. The stations that fail to transmit an ATIM frame successfully in the ATIM window, have to wait for the rest of the BI to get next chance in the next ATIM window. This increases the average waiting time to get a chance to transmit data frames. For this reason, average delay increases with the increase of BI size. Figure 4.8 shows the impact of the network size over the MAC delay for different

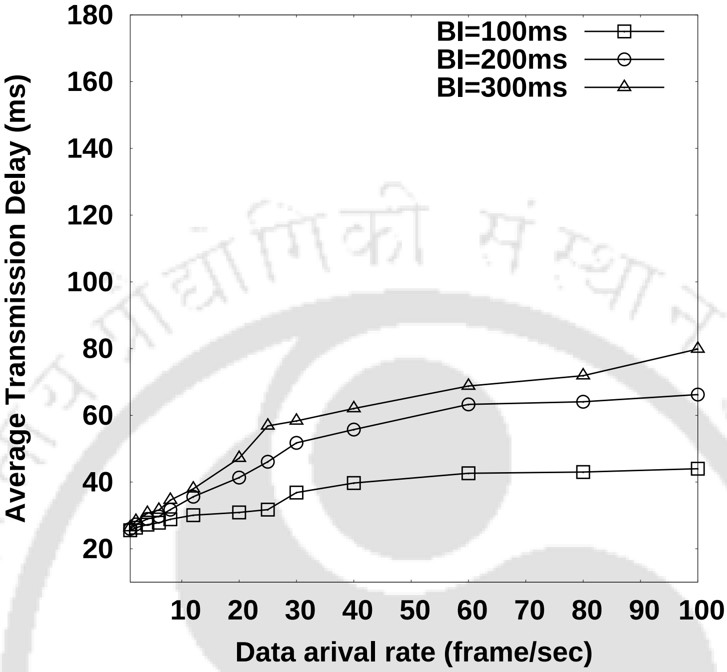

Figure 4.7: $\overline{D}$ for $n = 20$

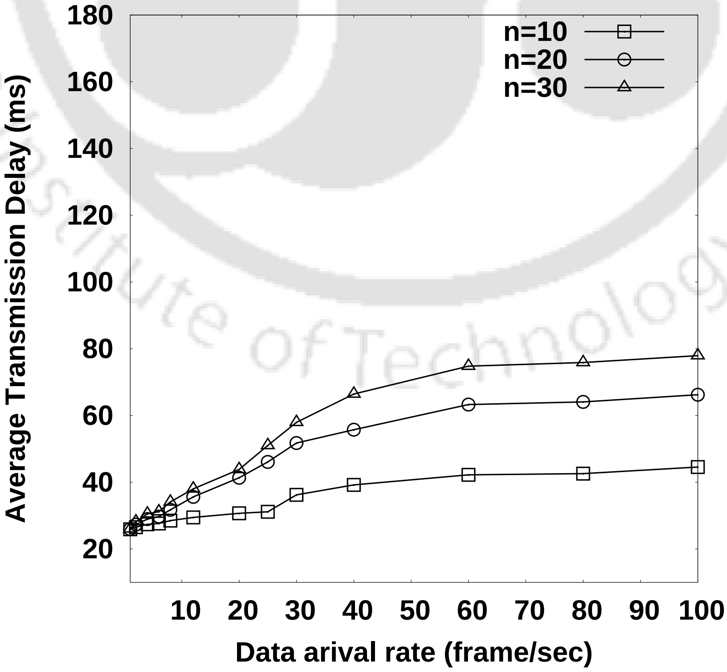

Figure 4.8: $\overline{D}$ for $BI = 200ms$

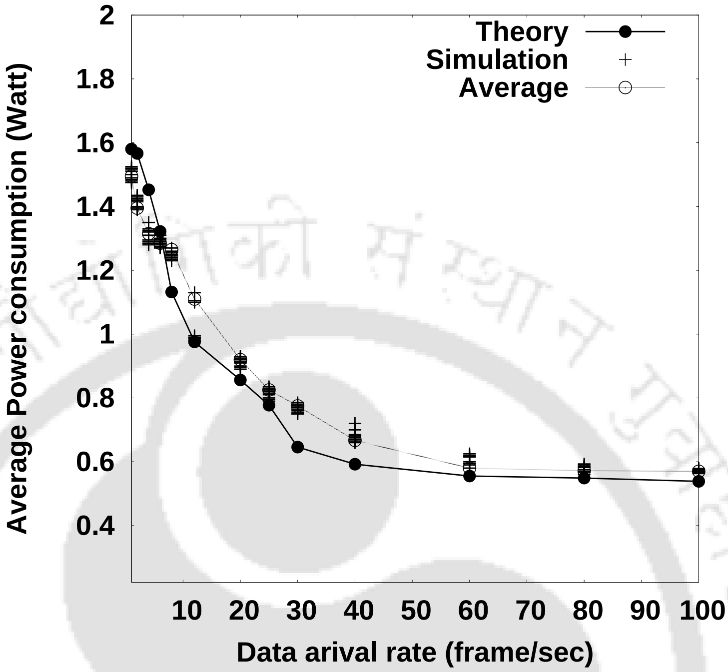

Figure 4.9: $\overline{PW}$ for $n = 20$

data arrival rates. When data arrival rate is low and the network is unsaturated, the end to end MAC delay does not differ too much for different network sizes. For higher data arrival rates, the MAC delay increases as the network size increases. Further, increasing the data arrival rate also prolongs the MAC delay. Therefore, the MAC delay mainly depends on the network contention. During unsaturation, traffic in the network is low and so increasing the network size does not have an impact on the network contention and the MAC delay. In a saturated network, the contention among stations increases as the network size increases. The network contention increases even further as the data arrival rate increases. Thus the MAC delay increases significantly with the increase in the network size and the data arrival rate.

Figure 4.9 shows the average power consumption with respect to data arrival rate for beacon interval (BI) size $200ms$. The result obtained from the analytical model for power consumption in Section 4.3 has been verified through simulation. Figure 4.9 shows that the simulation result matches with the theoretical analysis.

The impact of the network size and the BI size on the power consumption is

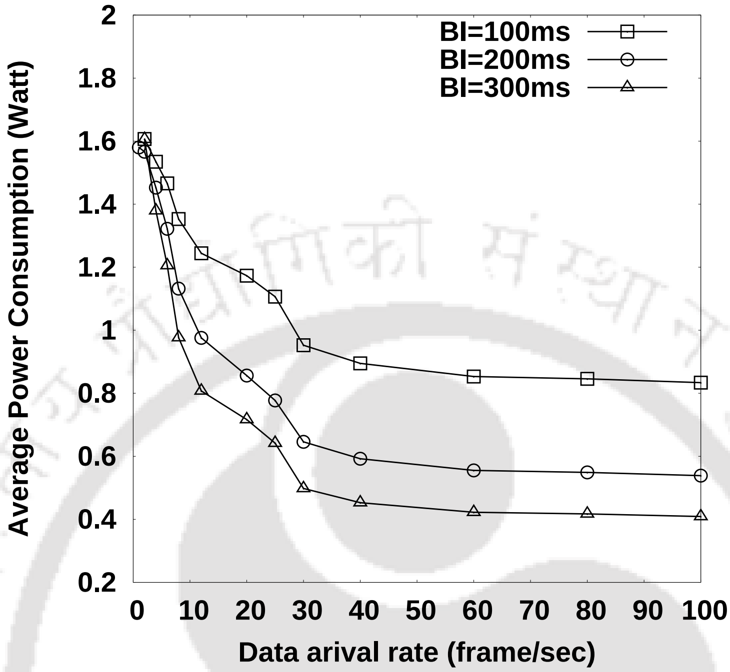

Figure 4.10: $\overline{PW}$ for $n = 20$

presented in Figure 4.10 and Figure 4.11. Figure 4.10 gives a comparison of average power consumption for different BI (for fixed ATIM window) against the data arrival rate. It can be observed from the figure that as the size of the BI increases, the average power consumption decreases. A station that neither transmits an ATIM frame successfully nor receives an ATIM frame remains in sleep mode for a long time when the BI is large. It is also observed that as the data arrival rate increases, the amount of power consumption decreases. A higher data arrival rate implies more number of stations contend at the ATIM window for successfully transmitting ATIM frames. This increased contention reduces the percentage of stations that get a chance to participate in the data communication. The remaining stations go to the sleep state in the data window. Thus the average power consumption decreases. During unsaturation, the average power consumption decreases linearly and then becomes constant at the saturation state. Figure 4.11 presents the average power consumption for different network sizes. It can be observed from the figure that the average power consumption for a network of size 10 is more than the average power consumption for a network of size 20. This is because contention is less for small

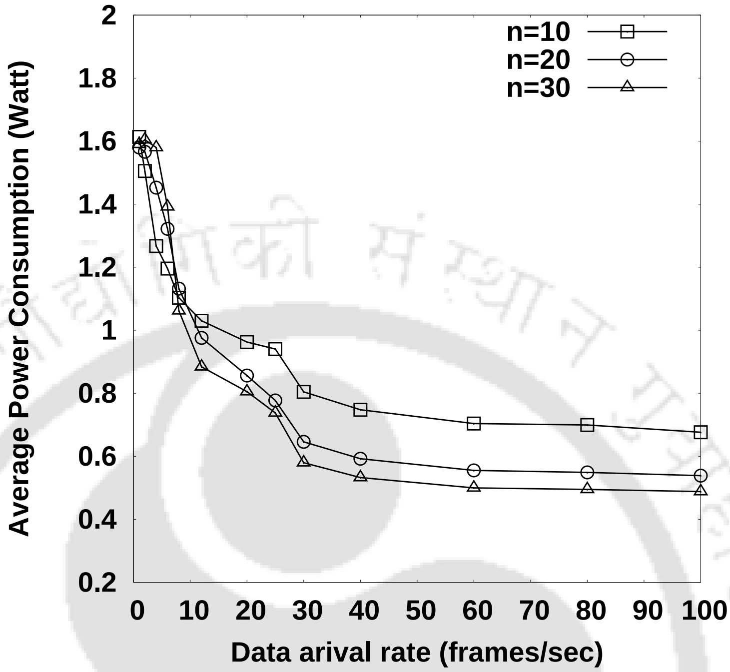

Figure 4.11: $\overline{PW}$ for $BI = 200ms$

network size, and so, most of the stations are in transmit or receive state, leading to higher power consumption. Figure 4.9 to Figure 4.11 show that IEEE 802.11 PSM saves significant amount of power by letting stations go to the sleep mode when there is no data to transmit or receive.

However, the power consumption is not local for a set of stations, rather it is evenly distributed in the network, as shown through the standard deviation of power in the network. The theoretical model for the standard deviation of power consumption is first validated through simulation. Figure 4.12 compares the theoretical model for standard deviation of power with simulation results, for 20 number of nodes. The standard deviation of the power distribution among the stations is shown in Fig. 4.13, as derived from the theoretical model presented in this thesis. It can be seen from the figure that the value of the standard deviation is very low. The deviation of power among the stations is less than 10%. This indicates that the power consumption is uniformly distributed among all the stations in the network. Henceforth, no station in the network dissipates considerably high power compared to others, which in turn increases the network lifetime.

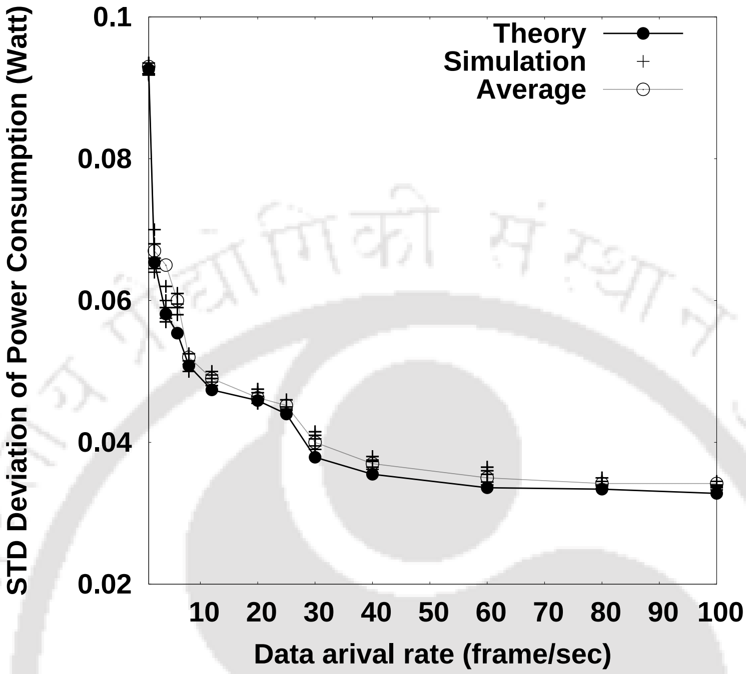

Figure 4.12: Standard Deviation $\overline{PW}$ for $n = 20$

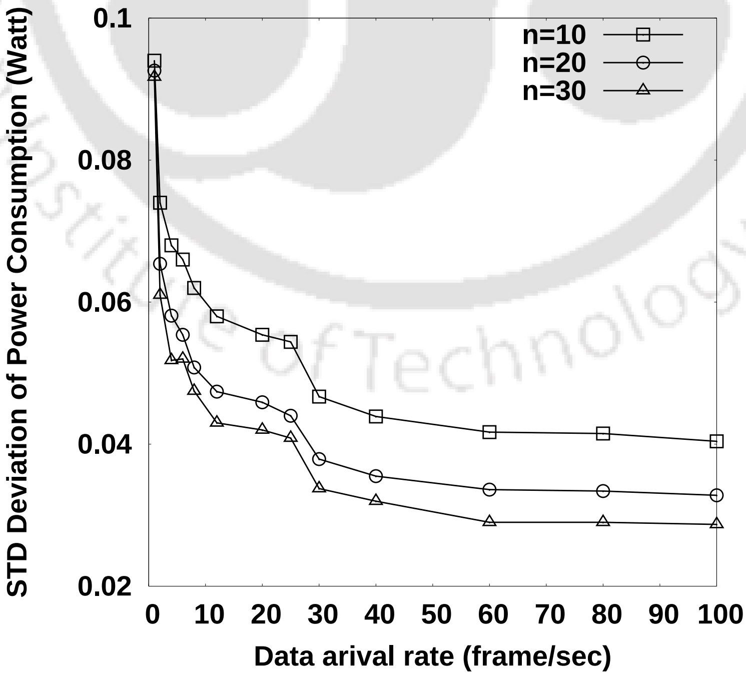

Figure 4.13: Standard Deviation of $\overline{PW}$

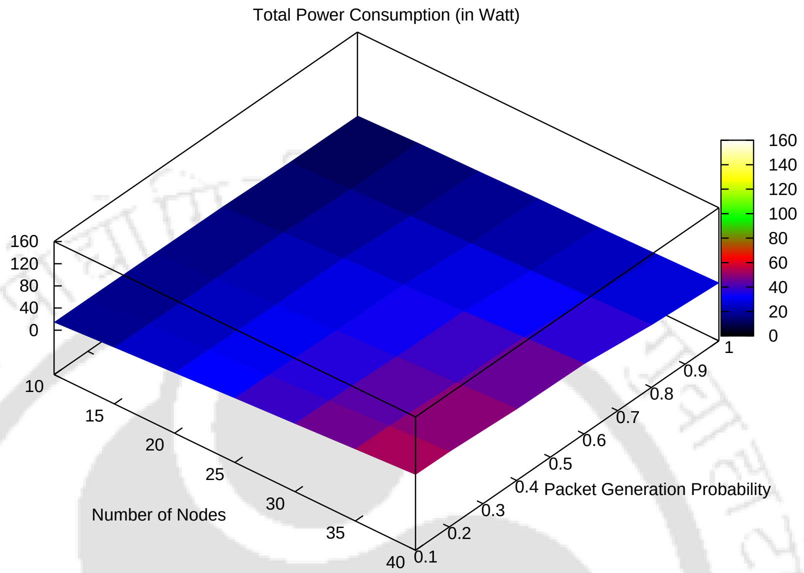

Figure 4.14: Total Power Consumption in PSM

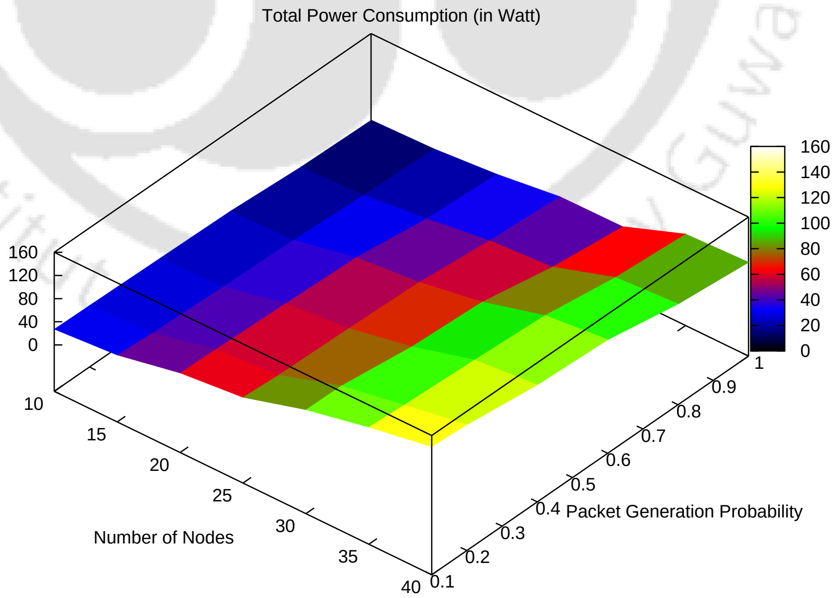

Figure 4.15: Total Power Consumption in without PSM

Figure 4.14 to Figure 4.17 give a comparative study of the power consumption between IEEE 802.11 with and without power save mode. The results for IEEE 802.11 DCF without PSM analysis is obtained from simulation with similar parameters as shown in Table 4.1. The packet generation probability is calculated from the traffic generation rate according to equation (4.20). Figure 4.14 shows the total power consumption in IEEE 802.11 PSM with respect to the number of stations and the packet generation probability. Figure 4.15 shows the same for IEEE 802.11 running without PSM enabled. These two figures clearly indicate that total power consumption in PSM is significantly less compared to IEEE 802.11 without PSM. Further in PSM (as well as without PSM) total power consumption increases as the packet generation probability decreases. This is because, in PSM a station needs to remain in the power on mode if it successfully transmits an ATIM frame in the ATIM window. Thus at a low data rate, even if the station does not have data to transmit, it needs to remain in the power on mode in the entire data window, after transmitting the data from its interface buffer.

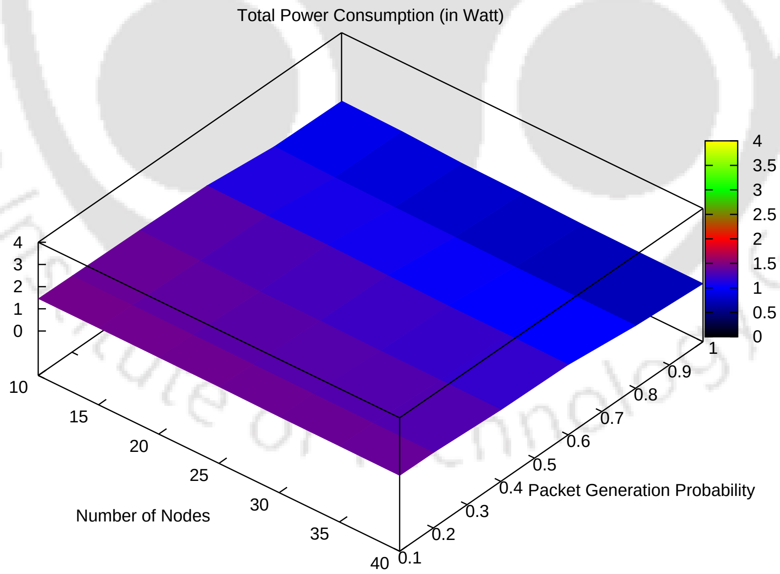

Figure 4.16: Average Power Consumption in PSM

Figure 4.16 and Figure 4.17 show the comparison of average power consumption per station in PSM and without PSM. It can be seen from the figures, that as the number of station increases, the average power consumption decreases in

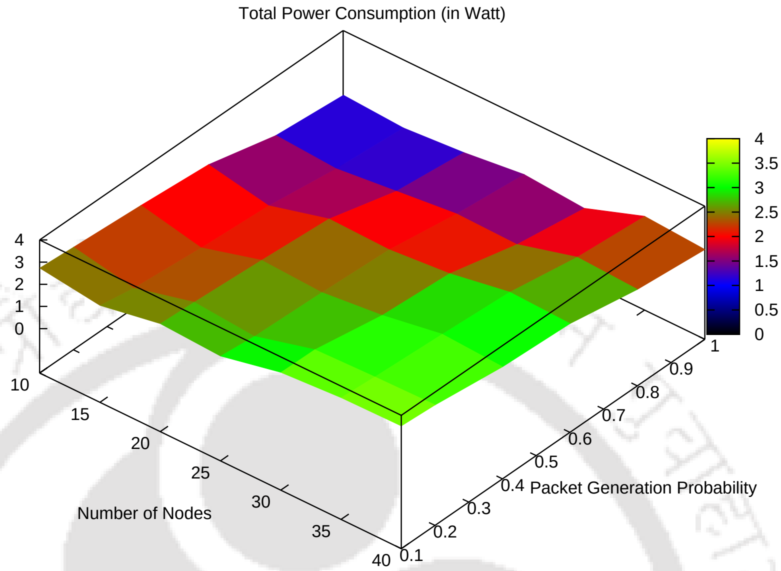

Figure 4.17: Average Power Consumption in without PSM

PSM, whereas, the average power consumption increases without PSM. In PSM, the stations that do not have any data to transmit go to the sleep state to save power. Thus with a large number of stations, the stations that can not transmit or receive an ATIM frame successfully, go to the sleep mode. This reduces average power consumption with a large number of nodes. Again with a higher data rate, contention among stations increases, and thus the stations that fail to transmit or receive an ATIM frame, go to the sleep mode. This further reduces average power consumption.

4.5 Summary

This chapter proposes an analytical model for IEEE 802.11 IBSS PSM with unsaturated traffic. The data frame transmission along with the corresponding ATIM frame transmission is modeled using a discrete time Markov chain. The network performance parameters, such as overall normalized throughput, average MAC delay and average power consumption is calculated from the Markov chain model. The proposed theoretical model is validated using simulation results. The performance of IEEE 802.11 IBSS PSM is also analyzed and compared with standard IEEE 802.11 IBSS without PSM. The analysis shows that there is a trade-off among throughput, MAC delay and average power consumption. A dynamic and adaptive BI can provide better power saving with little compromise in delay and throughput, that can open several directions for future research.

Chapter 5

Conclusions and scope of Future Work

This thesis provides analytical models to aid in the performance analysis and evaluation of the standard IEEE 802.11 IBSS in Power Save Mode. These analytical models are designed based on discrete time Markov chains for both saturated and unsaturated traffic conditions in wireless ad hoc networks. This chapter sums up the major contributions of this thesis along with the future directions of research.

5.1 Summary of Contributions

The modeling and analysis of the throughput, delay and power consumption in IEEE 802.11 DCF PSM for IBSS networks is very challenging because of the unique characteristics of data frame transmission along with the corresponding ATIM frame transmission. Hence in this thesis, our focus is on the analytical modeling and performance evaluation of IEEE 802.11 IBSS PSM. A novel analytical model with saturated traffic condition has been developed to provide an overview of the protocol performance at extreme traffic scenarios. The model is used to establish the relationship of the impact of network size and beacon interval size on the performance. The saturation model is further extended for unsaturated traffic conditions that represents real world traffic scenarios. The main research contributions of this thesis can be summarized as follows:

- **Performance Modeling of IEEE 802.11 PSM in IBSS for Saturated Traffic:** In Chapter 3, we have proposed a discrete time Markov chain model for the transmission of ATIM and data frame in IEEE 802.11 IBSS power save mode for saturated traffic. Thereafter, analytical models for normalized network throughput, average MAC delay and average power consumption in the IEEE 802.11 IBSS PSM are presented. Using the proposed model, an extensive and insightful performance evaluation of IEEE 802.11 IBSS in power save mode system parameters is carried out. Our results show the dependance of the throughput, delay, and power consumption on system parameters such as network size and beacon interval size. The conclusive result of our analysis establishes the fact that in IEEE 802.11 PSM, power can be saved at the cost of network throughput and delay. It has also been found that the dynamic tuning of the system parameters have great impact in achieving optimal performance in IEEE 802.11 IBSS in power save mode. Moreover, the analysis reveals that there exists a trade-off among overall network throughput, MAC delay and average power consumption, that can be explored to design a beacon window tuning mechanism for efficient usage of the power save option in an IEEE 802.11 IBSS network.

- **Performance Modeling of IEEE 802.11 PSM in IBSS for Unsaturated Traffic:** In practice, wireless networks do not operate in saturated traffic conditions. The characteristics of such networks get altered according to the application in use, such as web browsing, e-mail, voice over internet protocols (VoIP) etc. To capture the network performances in such unsaturated traffic conditions, it becomes imperative to design a more rigorous and generalized model that includes the details of traffic arrival with 802.11 MAC operation in power save mode. Chapter 4 elucidates a discrete time Markov chain model of IEEE 802.11 IBSS PSM for unsaturated traffic along with analytical models to compute the throughput, expected delay and expected power consumption. The impact of data arrival rate, network size and the Beacon Interval size on the performance of the IEEE 802.11 DCF in PSM is also analyzed. The analytical results are validated using simulation studies. Several important observations that are gathered from our analysis are as follows:

- An increase in the size of the beacon interval and network size enhances the network throughput while decreasing the average power consumption. This also results in an increase in average MAC delay due to the longer waiting times. However, for delay sensitive applications, beacon interval should be chosen based on the requirements of the application.
- As the number of stations increases in the network, it results the increment of the network throughput and the decrement of the average power consumption, while the MAC delay increases.
- According to IEEE 802.11 DCF PSM , the stations transit to the sleep mode to save the battery power. From our observations, we have learned that the transitions to sleep mode occur due to the higher contention in the ATIM window for transmitting or receiving the ATIM frames. This leads to the reduction of average power consumption as well as contention in the data window.

The modeling and analysis of IEEE 802.11 DCF power save mode in IBSS provides fruitful insights to set up an optimized wireless ad hoc network in power save mode. This thesis facilitates the system designer to take into account the trade-off among the throughput, delay and power consumption according to different network sizes and beacon interval sizes. Though the saturated traffic model is targeted towards specific application scenarios, the unsaturated traffic model inherently captures a broader category of network applications. In the succeeding section, we will point out the plausible areas of research to further the present work.

5.2 Scope of Future Work

This thesis gives a theoretical analysis of impact on the design parameters on the performance metrics in a IEEE 802.11 DCF PSM in IBSS network. The contributions of this thesis can be extended in several ways to analyze the impact of power save options on different network types as well as considering various network dynamics. We outline some of the possible future research works in this field of research.

- The model can be extended to analyze the performance of M-group heterogeneous IEEE 802.11 DCF PSM in IBSS with distinct arrival rates, network sizes and beacon interval sizes in each group. Fairness can be measured in terms of throughput, delay and power consumption with respect to the number of stations and offer load in each group.
- The model can be further extended to develop an analytical model of IEEE 802.11 DCF power save mode under saturated and unsaturated traffic conditions in multi-hop ad hoc networks. In a multi-hop ad hoc network the behavior of a station not only depends on it's neighbor's behavior but also the behavior of other hidden stations, thus increasing the complexity of the performance analysis of such networks. The problems that can arise in the IEEE 802.11 DCF power save mode when operating in a multi-hop ad hoc network in the presence of hidden nodes can be investigated. The performance of the IEEE 802.11 DCF in multi-hop ad hoc networks for different traffic loads, packet sizes and carrier sense ranges can be analyzed.
- An analytical model of IEEE 802.11 DCF power save mode in multi-hop ad hoc networks based on queuing theory can be designed to study the average throughput share among the different priority classes. By modeling each node as a discrete time $G/G/1$ queue, the throughput, end-to-end delay and power consumption for different circumstances can be derived.

References

[1] G.Bianchi, "Performance analysis of the IEEE 802.11 distributed coordination function," *IEEE Journal on Selected Areas in Communications*, vol. 18, no. 3, pp. 535–547, March 2000.

[2] *IEEE Std 802.11-2007, Part 11: Wireless LAN Medium Access Control (MAC) and Physical Layer (PHY) Specifications, Edition 2007*, IEEE.

[3] F. Daneshgran, M. Laddomada, and M. Mondin, "A Model of the IEEE 802.11 DCF in Presence of Non Ideal Transmission Channel and Capture Effects ," in *Proceedings of the Global Telecommunications Conference.* IEEE, 2007, pp. 5112–5116.

[4] M. Cao, W. Ma, Q. Zhang, X. Wang, and W. Zhu, "Modelling and performance analysis of the distributed scheduler in IEEE 802.16 mesh mode," in *Proceedings of the 6th International symposium on Mobile ad hoc networking and computing.* ACM, 2005, pp. 78–89.

[5] H. Schaffers, N. Komninos, M. Pallot, B. Trousse, M. Nilsson, and A. Oliveira, "Smart Cities and the Future Internet: Towards Cooperation Frameworks for Open Innovation," in *Proceedings of the Future Internet.* Springer, 2011, pp. 431–446.

[6] W. Lehr and L. W. McKnight, "Wireless Internet access: 3G vs. WiFi?" *Telecommunications Policy*, vol. 27, no. 5, pp. 351–370, 2003.

[7] "The WiFi Alliance." [Online]. Available: http://www.wi-fi.org/

[8] D. Vassis, G. Kormentzas, A. Rouskas, and I. Maglogiannis, "The IEEE 802.11g standard for high data rate WLANs," *IEEE Network.*, vol. 19, no. 3, pp. 21–26, 2005.

[9] H. Zhu, M. Li, I. Chlamtac, and B. Prabhakaran, "A survey of quality of service in IEEE 802.11 networks," *IEEE Wireless Communications.*, vol. 11, no. 4, pp. 6–14, 2004.

[10] Q. Ni, L. Romdhani, and T. Turletti, "A survey of qos enhancements for IEEE 802.11 wireless LAN," *Wireless Communications and Mobile Computing*, vol. 4, no. 5, pp. 547–566, 2004.

[11] Y. Peng, H. Wu, S. Cheng, and K. Long, "A new self-adapt DCF algorithm," in *Proceedings of the Global Communication Conference*, vol. 1. IEEE, 2002, pp. 87–91.

[12] N.-O. Song, B.-J. Kwak, J. Song, and M. Miller, "Enhancement of IEEE 802.11 distributed coordination function with exponential increase exponential decrease backoff algorithm," in *Proceedings of the Vehicular Technology Conference*, vol. 4. IEEE, 2003, pp. 2775–2778.

[13] A. Adya, P. Bahl, R. Chandra, and L. Qiu, "Architecture and techniques for diagnosing faults in IEEE 802.11 infrastructure networks," in *Proceedings of the 10th Annual International Conference on Mobile Computing and Networking.* ACM, 2004, pp. 30–44.

[14] B. P. Crow, I. Widjaja, L. Kim, and P. T. Sakai, "IEEE 802.11 wireless Local Area Networks," *IEEE Communications Magazine.*, vol. 35, no. 9, pp. 116–126, 1997.

[15] S. Kurkowski, T. Camp, and M. Colagrosso, "MANET simulation studies: the incredibles," *ACM SIGMOBILE Mobile Computing and Communications Review*, vol. 9, no. 4, pp. 50–61, 2005.

[16] I. F. Akyildiz, W. Su, Y. Sankarasubramaniam, and E. Cayirci, "Wireless sensor networks: a survey," *Computer networks*, vol. 38, no. 4, pp. 393–422, 2002.

[17] H. Hartenstein and K. P. Laberteaux, "A tutorial survey on vehicular ad hoc networks," *IEEE Communications Magazine*, vol. 46, no. 6, pp. 164–171, 2008.

[18] C. E. Jones, K. M. Sivalingam, P. Agrawal, and J. C. Chen, "A survey of energy efficient network protocols for wireless networks," *wireless networks*, vol. 7, no. 4, pp. 343–358, 2001.

[19] W. Ye, J. Heidemann, and D. Estrin, "An energy-efficient MAC protocol for wireless sensor networks," in *Proceedings of the International Conference on Computer Communications*, vol. 3. IEEE, 2002, pp. 1567–1576.

[20] H. Hartenstein and K. P. Laberteaux, "A tutorial survey on vehicular ad hoc networks," *IEEE Communications Magazine.*, vol. 46, no. 6, pp. 164–171, 2008.

[21] L. M. Feeney and M. Nilsson, "Investigating the energy consumption of a wireless network interface in an ad hoc networking environment," in *Proceedings of the Twentieth Annual Joint Conference of the IEEE Computer and Communications Societies*, vol. 3. IEEE, 2001, pp. 1548–1557.

[22] I. Ramani and S. Savage, "SyncScan: practical fast handoff for 802.11 infrastructure networks," in *Proceedings of the 24th Annual Joint Conference of the IEEE Computer and Communications Societies.*, vol. 1. IEEE, 2005, pp. 675–684.

[23] K.-Y. Jang, S. Hao, A. Sheth, and R. Govindan, "Snooze: Energy management in 802.11 n WLANs," in *Proceedings of the Seventh Conference on emerging Networking Eperiments and Technologies.* ACM, 2011.

[24] M. J. Miller and N. H. Vaidya, "Improving power saving protocols using carrier sensing for dynamic advertisement windows," in *Proceedings of the International Conference on Mobile Adhoc and Sensor Systems Conference.* IEEE, 2005, pp. 1–13.

[25] E. S. Jung and N. H. Vaidya, "Energy efficient MAC protocol for wireless LANs," in *Proceedings of the Twenty-First Annual Joint Conference of the*

IEEE Computer and Communications Societies, vol. 3. IEEE, 2002, pp. 1756–1764.

[26] Y.-C. Tseng, C.-S. Hsu, and T.-Y. Hsieh, "Power-saving protocols for IEEE 802.11-based multi-hop ad hoc networks," *Computer Networks*, vol. 43, no. 3, pp. 317–337, 2003.

[27] L. Gannoune, S. Robert, N. Tomar, and T. Agarwal, "Dynamic tuning of the maximum contention window (CWmax) for enhanced service differentiation in IEEE 802.11 wireless ad-hoc networks," in *Proceedings of the Vehicular Technology Conference*, vol. 4. IEEE, 2004, pp. 2956–2961.

[28] L. Gannoune, "A Non-linear Dynamic Tuning of the Minimum Contention Window for Enhanced Service Differentiation in IEEE 802.11 ad-hoc Networks," in *Proceedings of the Vehicular Technology Conference*, vol. 3. IEEE, 2006, pp. 1266–1271.

[29] J. Lv, X. Zhang, X. Han, and Y. Fu, "A novel adaptively dynamic tuning of the contention window (CW) for distributed coordination function in IEEE 802.11 ad hoc networks," in *Proceedings of the International Conference on Convergence Information Technology.* IEEE, 2007, pp. 290–294.

[30] A. Nafaa, A. Ksentini, A. Mehaoua, B. Ishibashi, Y. Iraqi, and R. Boutaba, "Sliding Contention Window (SCW): towards backoff range-based service differentiation over IEEE 802.11 wireless LAN networks," *IEEE Network*, vol. 19, no. 4, pp. 45–51, 2005.

[31] D.-J. Deng, C.-H. Ke, H.-H. Chen, and Y.-M. Huang, "Contention window optimization for IEEE 802.11 DCF access control," *IEEE Transactions on Wireless Communications.*, vol. 7, no. 12, pp. 5129–5135, 2008.

[32] M. Ergen and P. Varaiya, "Throughput Analysis and Admission Control for IEEE 802.11a," *Mobile networks and Applications*, vol. 10, no. 5, pp. 705–716, 2005.

[33] A. Alshanyour and A. Agarwal, "Three-Dimensional Markov Chain Model for Performance Analysis of the IEEE 802.11 Distributed Coordination Function,"

in *Proceedings of the Global Telecommunications Conference.* IEEE, 2009, pp. 1–7.

[34] T. C. Hou, L. F. Tsac, and H. C. Lia, "Throughput analysis of the IEEE 802.11 DCF in multihop ad hoc networks," in *Proceedings of the International Conference on Wireless Networks.* IEEE, June 2003, pp. 653–659.

[35] V. M. Vishnevsky and A. I. Lyakhov, "IEEE 802.11 LANs: Saturation Throughput in the Presence of Noise," in *Proceedings of the NETWORKING 2002: Networking Technologies, Services, and Protocols.* Springer, 2006, pp. 1008–1019.

[36] G. A. Safdar and W. G. Scanlon, "Performance analysis of an improved power-saving medium access protocol for IEEE 802.11 point coordination function WLAN," *IEEE proceedings Communication*, vol. 153, no. 5, 2006.

[37] X. Chu and Y. Yan, "Performance Evaluation of IEEE 802.11 Infrastructure Mode with Intra-Cell UDP Traffic," in *Proceedings of the Second International Conference on Communications and Networking in China.* IEEE, 2007, pp. 893–898.

[38] H. Lei and A. A. Nilsson, "Queuing Analysis of Power Management in the IEEE 802.11 Based Wireless LANs," *IEEE Transactions on Wireless Communications*, no. 4, pp. 1286–1294, 2007.

[39] S. Baek and B. D. Choi, "Performance Analysis of Power Save Mode in IEEE 802.11 Infrastructure WLAN," in *Proceedings of the International Conference on Telecommunications.* IEEE, 2008, pp. 1–4.

[40] N. Blefari-Melazzi, A. Detti, I. Habib, A. Ordine, and S. Salsano, "TCP Fairness Issues in IEEE 802.11 Networks: Problem Analysis and Solutions Based on Rate Control," *IEEE Transactions on Wireless Communications*, vol. 6, no. 4, pp. 1346–1355, 2007.

[41] W. Lee, C. Wang, and K. Sohraby, "On use of traditional M/G/1 model for IEEE 802.11 DCF in unsaturated traffic conditions," in *Proceedings of the*

Wireless Communications and Networking Conference, vol. 4. IEEE, 2006, pp. 1933–1937.

[42] A. Alshanyour and A. Agarwal, "Performance of IEEE 802.11 RTS/CTS with Finite Buffer and Load in Imperfect Channels: Modeling and Analysis," in *Proceedings of the Conference on Global Telecommunications*. IEEE, 2010, pp. 1–6.

[43] F. Daneshgaran, M. Laddomada, and M. Mondin, "Unsaturated Throughput Analysis of IEEE 802.11 DCF in the Presence of Non Ideal Transmission Channel and Capture Effects," *IEEE Transaction on wireless communications*, vol. 7, pp. 1276–1286, APRIL 2008.

[44] "Qualnet 5.0.1 Network Simulator, http://www.scalable-networks.com/products/qualnet/."

[45] F. Tobagi and L. Kleinrock, "Packet Switching in Radio Channels: Part II–The Hidden Terminal Problem in Carrier Sense Multiple-Access and the Busy-Tone Solution," *Communications, IEEE Transactions on*, vol. 23, no. 12, pp. 1417–1433, 1975.

[46] Y. Xiao and Y. R. X. Shan, "Game theory models for IEEE 802.11 DCF in wireless ad hoc networks," *IEEE Communication magazine.*, vol. 43, pp. S22 – S26, 2005.

[47] A. Kumar, E. Altman, D. Miorandi, and M. Goyal, "New insights from a fixed-point analysis of single cell IEEE 802.11 WLANs," *IEEE/ACM Transaction on Network*, vol. 15, no. 3, pp. 588–601, 2007.

[48] P. Rathod, O. Dabeer, A. Karandikar, and A. Sahoo, "Characterizing the exit process of a non-saturated IEEE 802.11 wireless network," in *Proceedings of the International Symposium on Mobile Ad Hoc Networking and Computing*. ACM, 2009, pp. 249–258.

[49] O. Tickoo and B. Sikdar, "A queueing model for finite load IEEE 802.11 random access MAC," in *Proceedings of the International Conference on Communications*, vol. 1. IEEE, 2004, pp. 175–179.

[50] N. Bisnik and A. A. Abouzeid, "Queuing network models for delay analysis of multihop wireless ad hoc networks," *Ad Hoc Networks*, vol. 7, no. 1, pp. 79–97, 2009.

[51] R. P. Liu, G. J. Sutton, and I. B. Collings, "A new queueing model for QoS analysis of IEEE 802.11 DCF with finite buffer and load," *Transactions on Wireless Communications*, vol. 9, no. 8, pp. 2664–2675, 2010.

[52] H. Zhai, Y. Kwon, and Y. Fang, "Performance analysis of IEEE 802.11 MAC protocols in wireless LANs," *Wireless Communications and Mobile Computing*, vol. 4, no. 8, pp. 917–931, 2004.

[53] H. Wu, Y. Peng, K. Long, S. Cheng, and J. Ma, "Performance of reliable transport protocol over IEEE 802.11 wireless LAN: analysis and enhancement," in *Proceedings of the Twenty-First Annual Joint Conference of the IEEE Computer and Communications Societies.*, vol. 2. IEEE, 2002, pp. 599–607.

[54] E. Ziouva and T. Antonakopoulos, "CSMA/CA performance under high traffic conditions: throughput and delay analysis," *Computer Communications*, vol. 25, no. 3, pp. 313–321, 2002.

[55] I. Tinnirello, G. Bianchi, and Y. Xiao, "Refinements on IEEE 802.11 Distributed Coordination Function Modeling Approaches," *IEEE Transaction on VEHICULAR TECHNOLOGY*, vol. 59, no. 3, March 2010.

[56] R. Wang, j. Zhang, and X. Zou, "Performance Analysis and Optimization of IEEE 802.11 DCF with Constant Contention Window," in *Proceedings of the International Colloquium on Computing, Communication, Control, and Management*, vol. 2. IEEE, 2008, pp. 407–411.

[57] Q. Ni, I. Aad, C. Barakat, and T. Turletti, "Modeling and analysis of slow CW decrease IEEE 802.11 WLAN," in *Proceedings of the Personal, Indoor and Mobile Radio Communications*, vol. 2. IEEE, 2003, pp. 1717–1721.

[58] Y. Xiao, "Performance analysis of priority schemes for IEEE 802.11 and IEEE 802.11e wireless LANs," *IEEE Transactions on Wireless Communications*, vol. 4, no. 4, pp. 1506–1515, 2005.

[59] H. Chen and Y. Li, "Performance model of IEEE 802.11 DCF with variable packet length," *Communications Letters*, vol. 8, no. 3, pp. 186–188, 2004.

[60] A. N. Zaki and M. El-Hadidi, "Throughput analysis of IEEE 802.11 DCF under finite load traffic," in *Proceedings of the First International Symposium on Control, Communications and Signal Processing.* IEEE, 2004, pp. 535–538.

[61] Y. S. Liaw, A. Dadej, and A. Jayasuriya, "Performance analysis of IEEE 802.11 DCF under limited load," in *Proceedings of the Asia-Pacific Conference on Communications.* IEEE, 2005, pp. 759–763.

[62] G. R. Cantieni, Q. Ni, C. Barakat, and T. Turletti, "Performance analysis under finite load and improvements for multirate 802.11," *Computer Communications*, vol. 28, no. 10, pp. 1095–1109, 2005.

[63] Q. Zhao, D. H. Tsang, and T. Sakurai, "Modeling Nonsaturated IEEE 802.11 DCF Networks Utilizing an Arbitrary Buffer Size," *Transactions on Mobile Computing*, vol. 10, no. 9, pp. 1248–1263, 2011.

[64] B. Kwak and N. Song, "Analysis of the Probabilities of Collision in the IEEE 802.11 DCF," in *Proceedings of the Conference on Global Telecommunications.* IEEE, 2007, pp. 5128–5132.

[65] H. Chen and Y. Li, "Performance model of IEEE 802.11 DCF with variable packet length," *IEEE Communications Letters*, vol. 8, no. 3, pp. 186–188, 2004.

[66] L. Xiong and G. Mao, "Performance Analysis of IEEE 802.11 DCF with Data Rate Switching," *IEEE Communications Letters*, vol. 11, no. 9, pp. 759–761, 2007.

[67] F. J. Simó-Reigadas, A. Martínez-Fernández, F. Ramos-Lopez, and J. S. Pascual, "Modeling and Optimizing IEEE 802.11 DCF for Long-Distance Links," *IEEE Transactions on Mobile Computing*, vol. 9, no. 6, pp. 881–896, 2010.

[68] A. Balachandran, G. M. Voelker, P. Bahl, and P. V. Rangan, "Characterizing user behavior and network performance in a public wireless LAN," *SIGMETRICS Performance Evaluation Review*, vol. 30, no. 1, pp. 195–205, Jun. 2002.

[69] F. Hung and I. Marsic, "Performance analysis of the IEEE 802.11 DCF in the presence of the hidden stations," *Computer Network*, vol. 54, no. 15, pp. 2674–2687, 2010.

[70] T.-C. Hou, L.-F. Tsao, and H.-C. Liu, "Analyzing the throughput of IEEE 802.11 DCF scheme with hidden nodes," in *Proceedings of the Vehicular Technology Conference*, vol. 5. IEEE, 2003, pp. 2870–2874.

[71] R. P. Liu, G. Sutton, X. Yang, and I. B. Collings, "Modelling QoS Performance of IEEE 802.11 DCF under Practical Channel Fading Conditions," in *Proceedings of the International Conference on Communications.* IEEE, 2011, pp. 1–6.

[72] Z. Hadzi-Velkov and B. Spasenovski, "Saturation throughput-delay analysis of IEEE 802.11 DCF in fading channel," in *Proceedings of the International Conference on Communications*, vol. 1. IEEE, 2003, pp. 121–126.

[73] ——, "Saturation Throughput, Delay Analysis of IEEE 802.11 DCF in Fading Channel," in *Proceedings of the International Conference on Communications*, vol. 1. IEEE, 2003, pp. 121–126.

[74] P. Raptis, V. Vitsas, A. Banchs, and K. Paparrizos, "Delay Distribution Analysis of IEEE 802.11 with Variable Packet Length," in *Proceedings of the Vehicular Technology Conference.* IEEE, 2007, pp. 830–834.

[75] T. Joshi, A. Mukherjee, and D. P. Agrawal, "Analytical Modeling of the Link Delay Characteristics for IEEE 802.11 DCF Multi-Rate WLANs," in *Proceedings of the Canadian Conference on Electrical and Computer Engineering.* IEEE, 2006, pp. 2164–2167.

[76] C. Liu, Y. Shu, W. Yang, and O. W. W. Yang, "Throughput Modeling and Analysis of IEEE 802.11 DCF with Selfish Node," in *Proceedings of the Conference on Global Telecommunications.* IEEE, 2008, pp. 1283–1287.

[77] X. J. Dong and P. Varaiya, “Saturation throughput analysis of IEEE 802.11 wireless LANs for a lossy channel,” *Communications Letters*, vol. 9, no. 2, pp. 100–102, 2005.

[78] Q. Ni, T. Li, T. Turletti, and Y. Xiao, “Saturation throughput analysis of error-prone 802.11 wireless networks,” *Wireless Communications and Mobile Computing*, vol. 5, no. 8, pp. 945–956, 2005.

[79] Z. Tao and S. Panwar, “Throughput and delay analysis for the IEEE 802.11e enhanced distributed channel access,” *Communications, IEEE Transactions on*, vol. 54, no. 4, pp. 596–603, 2006.

[80] H. Chen, “Revisit of the Markov Model of IEEE 802.11 DCF for an Error-Prone Channel,” *IEEE Communications Letters*, vol. 15, no. 12, pp. 1278–1280, 2011.

[81] Q. Zhao, D. H. Tsang, and T. Sakurai, “A Simple and Approximate Model for Nonsaturated IEEE 802.11 DCF,” *Transactions on Mobile Computing*, vol. 8, no. 11, pp. 1539–1553, 2009.

[82] Z. Cao, R. P. Liu, X. Yang, and Y. Xiao, “Modeling IEEE 802.11 DCF System Dynamics,” in *Proceedings of the Wireless Communications and Networking Conference*. IEEE, 2010, pp. 1–5.

[83] L. Yun, L. Ke-Ping, Z. Wei-Liang, and W. Chong-Gang, “Analyzing the channel access delay of IEEE 802.11 DCF,” in *Proceedings of the Conference on Global Telecommunications*, vol. 5. IEEE, 2005, pp. 2997–3001.

[84] H. L. Vu and T. Sakurai, “Accurate delay distribution for IEEE 802.11 DCF,” *IEEE Communications Letters*, vol. 10, no. 4, pp. 317–319, 2006.

[85] G. Sun and B. Hu, “Delay Analysis of IEEE 802.11 DCF with Back-off Suspension,” in *Proceedings of the Future Generation Communication and Networking*, vol. 1. IEEE, 2007, pp. 148–151.

[86] T. Sakurai and H. L. Vu, “MAC access delay of IEEE 802.11 DCF,” *IEEE Transactions on Wireless Communications*, vol. 6, no. 5, pp. 1702–1710, 2007.

[87] O. Tickoo and B. Sikdar, "Modeling queueing and channel access delay in unsaturated IEEE 802.11 random access MAC based wireless networks," *IEEE/ACM Transactions on Networking*, vol. 16, no. 4, pp. 878–891, 2008.

[88] P. Chatzimisios, A. C. Boucouvalas, and V. Vitsas, "IEEE 802.11 packet delay-a finite retry limit analysis," in *Proceedings of the Conference on Global Telecommunications*. IEEE, 2003, pp. 950–954.

[89] M. M. Carvalho and J. J. Garcia-Luna-Aceves, "Delay Analysis of IEEE 802.11 in Single-Hop Networks," in *Proceedings of the 11th IEEE International Conference on Network Protocols*. IEEE, 2003, pp. 146–155.

[90] Z. Li, A. Das, A. K. Gupta, and S. Nandi, "Performance Analysis of IEEE DCF: Throughput, Delay, and Fairness, http://www.iitg.ernet.in/sukumar/analysisof80211.pdf."

[91] Y. D. Barowski, S. Biaz, and P. Agrawal, "Towards the performance analysis of IEEE 802.11 in multi-hop ad-hoc networks," in *Proceedings of the Wireless Communications and Networking Conference*, vol. 1. IEEE, 2005, pp. 100–106.

[92] J. He and H. K. Pung, "Performance modelling and evaluation of IEEE 802.11 distributed coordination function in multihop wireless networks," *Computer Communications*, vol. 29, no. 9, pp. 1300–1308, 2006.

[93] X. Liu and T. N. Saadawi, "Throughput analysis of IEEE 802.11 multihop ad hoc wireless networks under saturation condition," in *Proceedings of the Symposium on Computers and Communications*. IEEE, 2010, pp. 245–248.

[94] F. Alizadeh-Shabdiz and S. Subramaniam, "Analytical models for single-hop and multi-hop ad hoc networks," *Mobile Networks and Applications*, vol. 11, no. 1, pp. 75–90, 2006.

[95] A. Tsertou and D. I. Laurenson, "Revisiting the hidden terminal problem in a CSMA/CA wireless network," *IEEE Transactions on Mobile Computing*, vol. 7, no. 7, pp. 817–831, 2008.

[96] P. C. Ng and S. C. Liew, "Throughput analysis of IEEE 802.11 multi-hop ad hoc networks," *IEEE/ACM Transactions on Networking*, vol. 15, no. 2, pp. 309–322, Apr 2007.

[97] P. Li and Y. Fang, "Saturation throughput of IEEE 802.11 DCF in multi-hop ad hoc networks," in *Proceedings of the Military Communications Conference.* IEEE, 2008, pp. 1–7.

[98] K. Ghaboosi, M. L., Y. Xiao, and B. H. Khalaj, "Modeling IEEE 802.11 DCF Using Parallel Space-Time Markov Chain: Multi-Hop Ad Hoc Networks," in *Proceedings of the Conference on Global Telecommunications.* IEEE, 2009, pp. 1–7.

[99] Y. Xiao and X. Yin, "Performance Modeling and Analysis of IEEE 802.11 MAC Protocol in Multihop Ad Hoc Networks," in *Proceedings of the 6th International Conference on Wireless Communications Networking and Mobile Computing.* IEEE, 2010, pp. 1–5.

[100] L. Xie, G. Wei, H. Wang, and Z. Xie, "Performance Analysis of IEEE 802.11 DCF in Multi-hop Ad Hoc Networks," in *Proceedings of the Eighth IEEE/ACIS International Conference on Computer and Information Science.* IEEE, 2009, pp. 222–227.

[101] Z. Li, S. Nandi, and A. K. Gupta, "Modeling the short-term unfairness of IEEE 802.11 in presence of hidden terminals," *Performance Evaluation*, vol. 63, no. 4, pp. 441–462, 2006.

[102] C. Aydogdu and E. Karasan, "An Analysis of IEEE 802.11 DCF and Its Application to Energy-Efficient Relaying in Multihop Wireless Networks," *IEEE Transactions on Mobile Computing*, vol. 10, no. 10, pp. 1361–1373, 2011.

[103] W. K. Kuo, "Energy efficiency modeling for IEEE 802.11 DCF system without retry limits," *Computer communications*, vol. 30, no. 4, pp. 856–862, 2007.

[104] L. Ning, "A power-consumption analysis for 802.11 DCF," in *Proceedings of the Wireless Communication, Networking and Mobile Computing.* IEEE, 2006, pp. 1–4.

[105] M. M. Carvalho, C. B. Margi, K. Obraczka, and J. J. Garcia-Luna-Aceves, "Modeling energy consumption in single-hop IEEE 802.11 ad hoc networks," in *Proceedings of the 13th International Conference on Computer Communications and Networks.* IEEE, 2004, pp. 367–372.

[106] R. Zheng, J. C. Hou, and L.Sha, "Performance analysis of the ieee 802.11 power saving mode," *Urbana*, vol. 51, p. 61801, 2004.

[107] M. Ergen and P. Varaiya, "Decomposition of Energy Consumption in IEEE 802.11," in *Proceedings of the International Conference on Communications.* IEEE, 2007, pp. 403–408.

[108] M. H. Ye, C. T. Lau, and A. B. Premkumar, "A modified power saving mode in IEEE 802.11 distributed coordinator function," *Computer Communications*, vol. 28, pp. 1214–1224, June 2005.

[109] "Cisco Aironet 350 Series Client Adapters, http://www.cisco.com/en/US/prod/collateral/wireless/ps6442/ps4555/ps448/product_data_sheet09186a0080088828.html."

[110] Y. Zheng, K. lu, D. Wu, and Y. Fang, "Performance Analysis of IEEE 802.11 DCF in Imperfect Channels," *IEEE Transaction on Vehicular Technology*, vol. 55, pp. 1648–1656, Sep. 2006.

[111] S. M. Ross, *Introduction to Probability Models*, 10th ed. Academic Press, 2009.

Publications Related to Thesis

Journals

- **P. Swain**, S. Chakraborty, S. Nandi and P. Bhaduri, Performance Modeling and Evaluation of IEEE 802.11 IBSS Power Save Mode. Ad Hoc Networks, Elsevier, vol. 13, pp. 336–350, 2014..

- **P. Swain**, S. Chakraborty, S. Nandi and P. Bhaduri, Performance Modeling and Evaluation of IEEE 802.11 IBSS Power Save Mode in Unsaturated Traffic Condition, IEEE Transaction on Mobile Computing, 2013. (Submitted after third revision).

Conference Proceedings

- **P. Swain**, S. Chakraborty, S. Nandi, and P. Bhaduri, Performance Analysis of IEEE 802.11 IBSS Power Save Mode using a Discrete-Time Markov Model. 27th ACM Symposium on Applied Computing (SAC) 2012, .

- **P. Swain**, S. Chakraborty, S. Nandi, and P. Bhaduri, Throughput Analysis of the IEEE 802.11 Power Save Mode in Single Hop Ad hoc Networks, 10th International Conference on Wireless Networks, ICWN'11 (July 18-21, 2011, USA).

Other Publications of the Author

1. Sandip Chakraborty, **Pravati Swain**, Sukumar Nandi, "Proportional Fairness in MAC Layer Channel Access of IEEE 802.11s EDCA based Wireless Mesh Networks" Ad Hoc Networks, Elsevier, Volume 11, Issue 1, January 2013, Pages 570-584

2. **P. Swain**, P. Bhaduri and S. Nandi, Performance Analysis of IEEE 802.11 IBSS Power Save Mode via Model Checking. Int. Journal of Wireless Mobile Computing, 2014. (Accepted).

Brief Biography of the Author

The author is born in Jajpur, Orissa, India on 6th June, 1984. After completing her schooling in Jajpur, she has completed the 12th and B.A.(Math) degree from the *S. B. Women's College, Cuttack*, Orissa, India in the year 2001 and 2004, respectively. She has completed her Master in Mathematics from *Utakal University, Bhubaneswar, Orissa, India.* She completed her M. Tech in 2008 from the same university. She has received the Junior Research Fellowship (JRF) and Senior Research Fellowship (SRF) from MHRD, India, for pursuing her PhD programme from *Indian Institute of Technology Guwahati (IITG), India.* She has received Senior Research fellowship (SRF) from Council of Scientific and Industrial Research (CSIR), Human Resource Development Group, 2013. Her research interests include Performance Analysis, Network Optimization, Stochastic Process, Wireless Networks, Algorithms and Formal System of Verification etc.

Department of Computer Science and Engineering

Indian Institute of Technology Guwahati

Guwahati 781039, India